RESEARCH CONTRACT ANTAR/II/05

CARBON AND NITROGEN CYCLING THROUGH THE MICROBIAL NETWORK OF THE MARGINAL ICE ZONE OF THE SOUTHERN OCEAN WITH PARTICULAR EMPHASIS ON THE NORTHWESTERN WEDDELL SEA

Ch. Lancelot, S. Mathot,
S. Becquevort, J.-M. Dandois
and G. Billen

GROUPE DE MICROBIOLOGIE DES
MILIEUX AQUATIQUES

Université Libre de Bruxelles
Campus de la Plaine CP 221,
Bd du Triomphe
B-1050 Brussels, Belgium

TABLE OF CONTENTS

ABSTRACT

Detailed biological measurements (phyto– and bacterioplankton biomass and activity and counting of two classes of protozooplankton) were carried out in the marginal ice zone of the northwestern Weddell Sea during sea ice retreat 1988 (EPOS expedition, Leg 2). These measurements clearly showed enhanced phyto–, bacterio– and protozooplankton production in the marginal ice zone, as compared to ajacent open sea and permanently ice–covered areas.

The combined analysis of available physical, chemical and biological observations indicated that the initiation of the phytoplankton bloom – dominated by nanoplanktonic species – was determined by physical processes operating in the marginal zone at the time of ice melting. The additional effects of grazing pressure by protozoa and deep mixing appeared responsible for a rather moderate phytoplankton biomass (4 μg Chl *a* l^{-1}) with a relatively narrow geographical extent (100–150 km). The role of trace metals, in particular iron, was minor.

On the basis of these data, as well as of physical measurements related to the hydrodynamical stability of the water column, a coupled hydrodynamical–biological model describing the microbial network developing at the receding ice–edge of the circumpolar marginal ice zone of the Southern Ocean has been established. This model takes into account the various physical and biological controls exerted on phytoplankton development, and allows calculation of carbon and nitrogen circulation through the lower trophic levels of the pelagic ecosystem.

Carbon budget calculation thus reveals the quantitative importance of heterotrophic microorganisms in the fate of primary production : 88% of net primary production is assimilated by the microbial loop composed of bacteria, bactivorous and herbivorous protozoa. These latter, ingesting as high as 61% of the primary production play a key role, both by linking krill and other mesozooplankton to microorganisms, and by regenerating ammonium. Total net microbial food web secondary production contributes 66% of the food resources available to krill and other mesozooplankton at the receding ice–edge. Ammonium released through the metabolic activity induces a shift from a nitrate–based primary production system in the ice–covered area to an ammonium–based one in the ice–free area. Similar budget calculated for the adjacent permanently open sea area magnifies the key role of protozoa, constituting as much as 88% of resource available to krill and other mesozooplankton.

Extrapolation of these calculations to the entire Southern Ocean area (bordered at the Antarctic Convergence), taking into account the seasonal variations of the sea ice cover, yields a value of 1.85 GT C for annual net primary production, increasing by a factor 3 the previous estimate proposed by El–Sayed (1984).

1. INTRODUCTION

Recognition of the important role played by the ocean in atmospheric cycles prompted closer examination of the role of organisms in these processes. A significant amount of atmospheric carbon dioxide is indeed susceptible to be fixed by surface waters and exported to the deep ocean after incorporation into the food–web, giving support to the concept of the biological pump. The efficiency of this pump depends on the complex functioning of the phytoplankton–based pelagic ecosystem. It is driven by solar irradiance and fueled by the supply of inorganic nutrients (nitrate, phosphate, silicate) originated from the deep ocean. In most marine areas, inorganic nutrients are exhausted by phytoplankton uptake during the growing season; the transport of carbon to deep waters is then controlled by the flux of inorganic nutrients to surface waters. In this case, the pump works at its maximum efficiency. In the Southern Ocean, however, relatively high concentrations of nitrate, phosphate and silicate are found in surface waters throughout the year. Yet phytoplankton biomass and primary production are lower than would be expected from inorganic nutrients availability. The pump therefore does not function at its maximal capacity. The Southern Ocean is thus a leading concern in oceanographic research not only as it relates to global biogeochemical cycles, but also as a potential site for intentional artificial enhancement of CO_2 flux into the ocean. Of particular interest within this context, is the identification of the factors controlling phytoplankton development and of the importance of the microbial loop in the surface layer. Indeed the timescale for the retention of photo–assimilated carbon in surface waters is dependent on biological and chemical transformations occurring in upper waters. Microbial activity produces dissolved organic carbon and returns inorganic carbon and nutrients through respiration and mineralisation whilst aggregate formation, faecal pellets production and vertical migration of large zooplankton speed up transfer of carbon to deep waters. In this regard, the concept of regenerated and new production is important as it introduces a distinction between the part of primary production which is recycled in the surface waters through rapid metabolism of heterotrophic microorganisms (grazers and bacteria) versus the part which escapes this rapid cycling and reaches the deep oceanic circulation and the benthos (Eppley & Peterson, 1979). New production is characteristically fueled by the winter standing stock of nitrates and sets up upper limits to export rates of organic matter from the surface layer; ammonium supports regenerated production that makes a negligible contribution to export to the deep ocean.

Several hypothesis have tempted to explain the paradox of high nutrients and low primary production in the Southern Ocean. To date, none has emerged as a widely admitted explanation.

The major role played by ice cover and the turbulence of the water column in controlling available light to phytoplankton and hence its development has been evidenced by numerous field data. It is now admitted that deep–mixed, ice–free areas are not exceptionally productive despite of very high nutrient concentrations, and are dominated by nanoplanktonic communities (El–Sayed, 1984; Smetacek *et al.*, 1990). On the other hand, many evidences (Smith & Nelson, 1986; Sullivan *et al.*, 1988; Comiso *et al.*, 1990) indicate that the circumpolar marginal ice zone is a region of enhanced primary production owing to the formation, at the time of ice melting, of a shallow vertically stable upper layer as a result of the production of meltwater and the subsequent seeding by actively growing sea ice microbes (Garrison *et al.*, 1987).

Yet phytoplantkton biomass in these hydrodynamically stable areas remains generally low and surface nutrients, especially nitrate, remains well above depletion throughout the growing season (Hayes *et al.*, 1984). As alternatives, trace metals deficiency, in particular iron (Martin *et al.*, 1990), as well as grazing pressure by krill and other mesoplankton (Stretch *et al.*, 1988, Smetacek *et al.*, 1990) or protozoa (Hewes *et al.*, 1990) have been mentioned as potential chemical and biological factors controlling phytoplankton development in this area. These hypothesis are however not mutually exclusive and their importance may vary with location, time and environmental conditions.

As a matter of fact, ice–edge blooms exhibit consistently higher f ratio (the ratio of nitrate uptake to total inorganic nitrogen uptake) than ice–free communities (Smith & Nelson, 1990) suggesting that marginal ice zones are regions of greater export production. Contradictory, however, Hewes *et al.* (1985, 1990) and Garrison & Buck (1989) indicate that the pelagic food web of the marginal zone of the Weddell Sea is dominated by pico–, and nano–producers and micrograzers, suggesting that an important part of organic carbon and nitrogen is mineralised in the surface layer.

The control of phytoplankton ice–edge bloom development and the quantitative importance of the microbial loop were the main questions we addressed during the EPOS expedition (Leg 2), in the marginal ice zone of the northwestern Weddell Sea in spring 1988.

These objectives were approached through a detailed study of (i) the chemical, physical and biological processes associated with sea ice retreat and their controlling

factors; and (ii) the trophic relationships between dominant microorganisms, characterized by their size (pico–, nano–, micro–) and their trophic mode (auto–, heterotrophic).

A comprehensive analysis of the data collected during the EPOS expedition is presented here in order to (i) delineate the most important factors controlling phytoplankton ice–edge bloom development, (ii) evaluate the contribution of microbial secondary production and (iii) identify key organisms in regenerating inorganic nitrogen in upper surface waters of the investigated area. On this basis a predictive mathematical model of carbon and nitrogen circulation through the microbial network of the Antarctic food web is described and validated. By application to the marginal ice zone of the northwestern Weddell Sea, it makes possible to calculate a coherent budget of carbon and nitrogen cycling through the microbial network of the Antarctic food–web during the ice retreat period. This calculation provides an estimation of new production, of the quality of food available for krill ingestion, and of the exportation to the deep ocean layers.

2. MATERIALS AND METHODS

2.1 Site description and field sampling

The data set whereon this research is based was collected during the second leg of the European Polarstern Study (EPOS Leg 2) in the Scotia–Weddell Sea sector of the Southern Ocean, from November 22th 1988 to January 9th 1989. In this area located between the tip of the Antarctic Peninsula and the South Orkney Islands (Fig. 2.1), the open water of the Antarctic Circumpolar Current running in the Scotia Sea contacts the eastward flowing waters from the northern rim of the Weddell Gyre along a broad frontal zone. This boundary zone, with accompanying intense mesoscale activity, has been referred to as the Weddell–Scotia Confluence (WSC) by Gordon (1967). The hydrographical structure of the Confluence area is dominated by a sharp temperature gradient at its northern edge (the Scotia Front), extending from about 200 to 2500 meters. During late November, the Scotia Front was located between 57 30^0 and 58^0 S; one month later, it was wider and had expanded southward to 59^0 S (Cederlöf *et al.*, 1989).

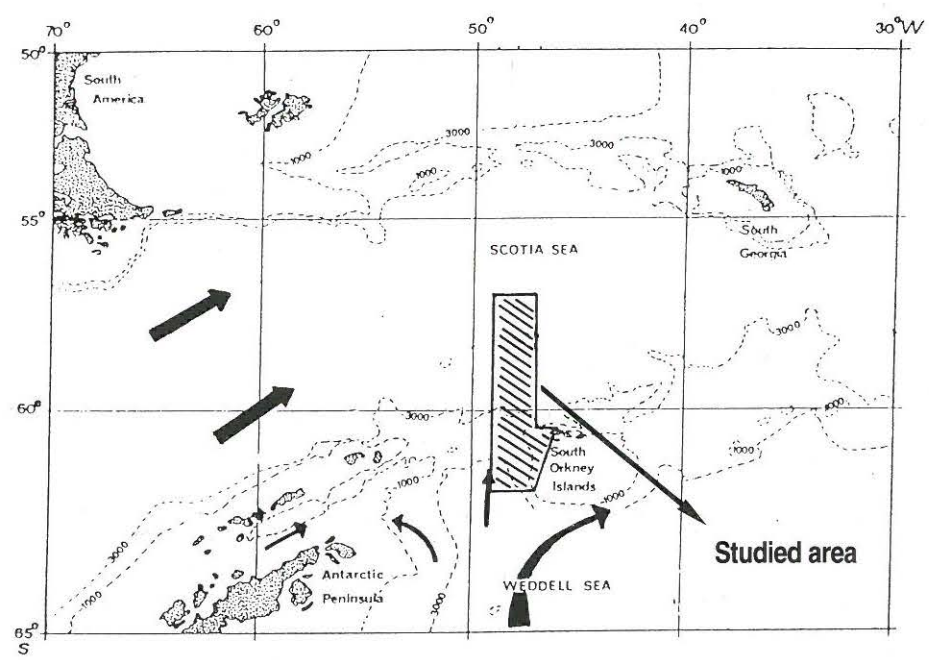

Figure 2.1 : Hydrodynamical characteristics of the studied area.

Superimposed to this frontal structure, seasonal sea ice covers this area up to latitude 58 30⁰ S at its maximal extent. At the time of the cruise beginning, the process of ice melting has already started in this area since the end of October. Data collected in that part of the Weddell Sea during EPOS Leg 1 are therefore included in the present study. The whole data set thus refers to four North–South transects carried out along 49⁰ W (stations 100–113, 26–30 October; stations 143–153, 26–30 November; stations 172–179, 20–24 December; stations 182–194, 27–31 December) and two along 47⁰ W (stations 130–139, 11–13 November; stations 160–169, 13–17 December), between latitude 57⁰ S and 62⁰ S (Fig. 2.2). Precise coordinates and sampling conditions are described in details in Larsson (1990, EPOS Leg 1) and Veth *et al.* (1991, EPOS Leg 2).

Water column sampling : Sampling for physical, inorganic nutrients and chlorophyll *a* measurements was conducted at each half degree of latitude using a standard CTD rosette sampler equipped with 12 L Niskin bottles. Samples for biological activity measurements were collected within the upper mixed layer of annotated stations (see Fig. 2.2). Sampling for planktonic communities analysis (Chapter 4) was concentrated on two transects performed along the meridian 49⁰W and 47⁰W between 59⁰S and 62⁰S as well as two stations located at 59⁰S (station 147) and 61⁰S (station 151) which were visited several times during the cruise (see Fig. 2.2).

Ice sampling : Ice sampling was carried out randomly at three particular sites of the marginal ice zone of the northwestern Weddell Sea, namely stations 169, 178 and 194. According to the terminology proposed by Horner *et al.* (1988), three broad categories of microbial assemblage can be distinguished in the ice (Fig. 2.3) : surface assemblages which include infiltration assemblages at the snow–ice interface of floes as well as meltpool and tide crack microorganisms; interior assemblages (including brine channel and band assemblages) at depth within the ice; and bottom assemblages that develop in different types of ice near the ice–seawater interface. Whilst the two first groups of ice assemblages are frequently encountered in the pack ice of the northern Weddell Sea, the latter one is inconspicuous, being more typical of the land fast ice common in the Ross Sea (Horner, 1985). Thus samples from stations 169 and 194 are typical infiltration assemblages, whereas the brown coloured band sampled in the middle (60 to 80 cm from top of ice floe) of cores taken at station 178 presented the characteristics of a band assemblage.

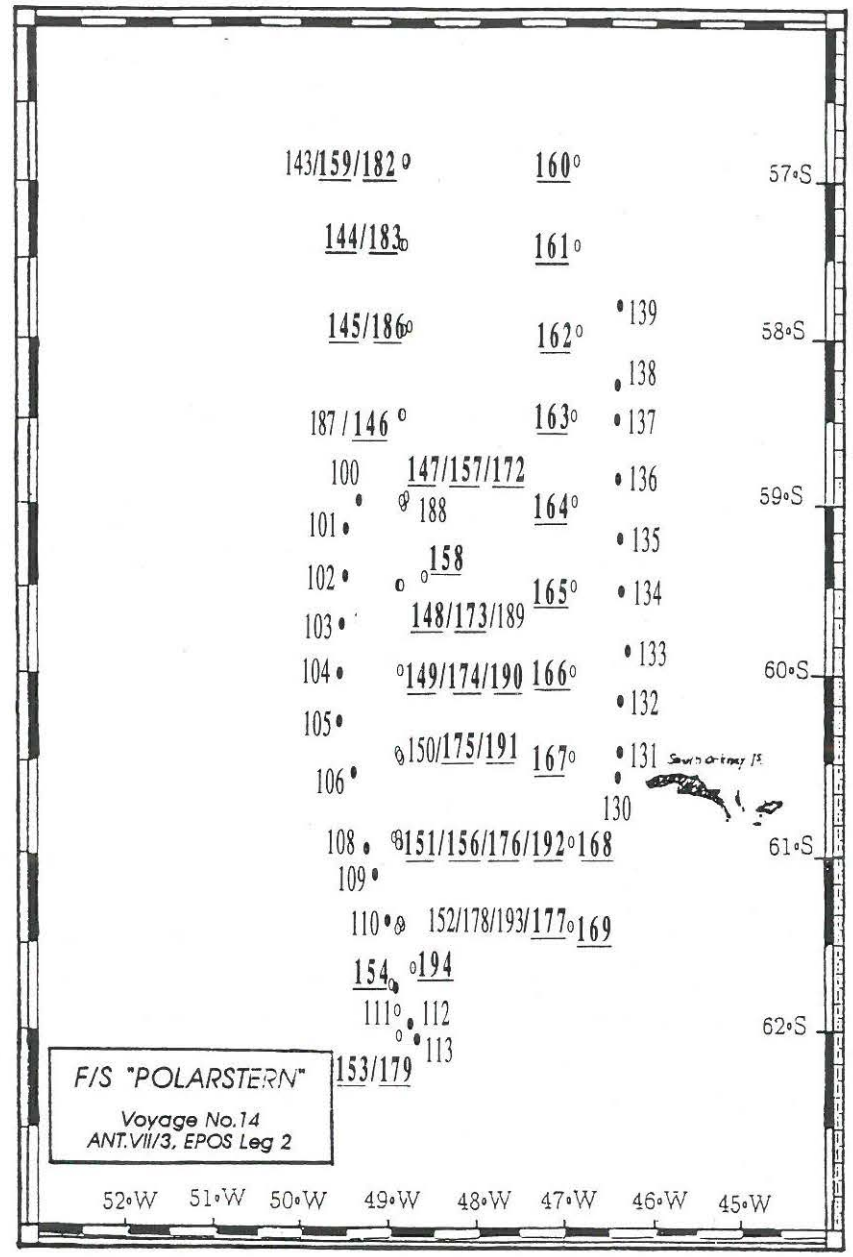

Figure 2.2 : Studied area and sampled stations (EPOS legs 1 and 2). Biological activity measurements at the annotated stations (for example 157).

To reduce osmotic shock (Garrison & Buck, 1986), ice samples were melted in GF/F, filtered sea water (1:20, v:v) in the dark prior to fixative addition or experimental study. For comparison between ice and water environments, samples of seawater were also collected directly under the ice floes.

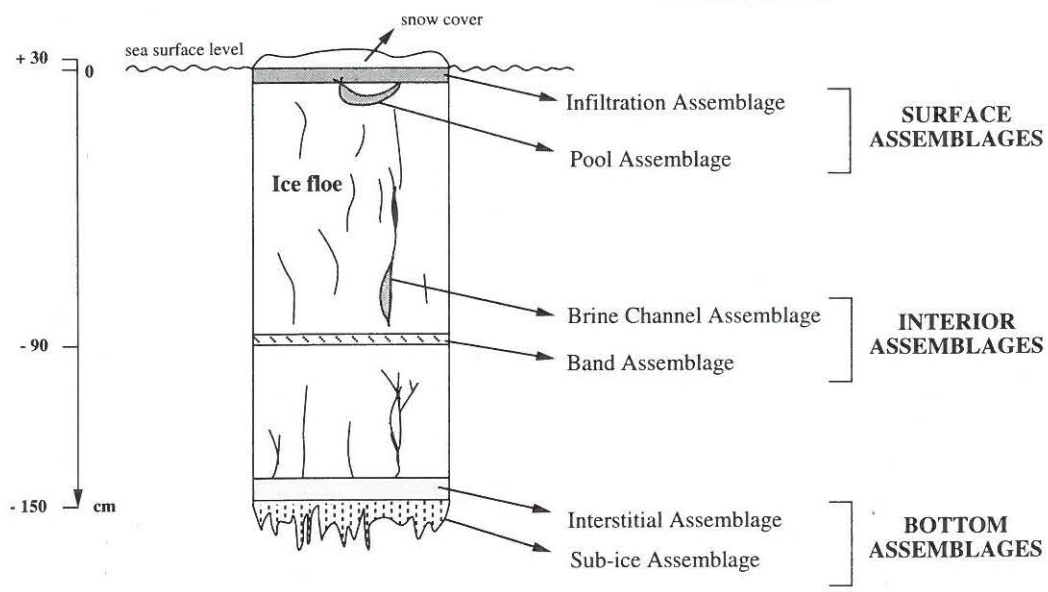

Figure 2.3 : Schematic representation of the kinds of algal assemblages found in sea ice (from Horner *et al.*, 1988).

2.2. Physical and optical measurements

Vertical profiles of salinity and temperature (EPOS–Leg 2 data report, 1989) were determined by use of a Neil Brown Mark IIIb CTD–profiler (EG & G Ocean Products). *In situ* temperature and salinity calibrations were conducted regularly during the cruise. Hydrographical data can be found in Larsson (1990, EPOS Leg 1) and Veth *et al.* (1991, EPOS Leg 2).

Incident Photosynthetically Available Radiation (PAR) was continuously measured by means of a cosine Li–Cor sensor set up on the upper deck of the ship. Subsurface light was calculated from the knowledge of ice coverage estimates (Lange & Eicken, 1989; van Franeker, 1989), using a mean of 0.15 and 0.95 for sea and snow–ice albedo respectively. Available light in the water column was calculated from the vertical light attenuation coefficient determined from light profiles measured by use of an underwater quantameter (Magas & Svansson, 1989). The depth of the euphotic zone was determined at the 0.1 % level of incident surface light.

2.3. Chemical measurements

Nitrate + nitrite was determined with a Technicon Autoanalyzer II according to the method of Tréguer & Le Corre (1975). Calibration was carried out in the range of 20 to 40 µmol.N l^{-1}. Nitrate depletions were calculated from vertical distribution of nitrate concentration, and integrated down to the depth where nitrate reaches the winter value of 31.5 µmol.N l^{-1} (see Goeyens *et al.*, 1991a for details). Ammonium concentrations were determined manually as described by Koroleff (1969 and 1976). Standardization was carried out between 0 and 3 µmol.N l^{-1} (see Goeyens *et al.*, 1991b for details).

Chlorophyll *a* was determined by both spectrofluorometry (Neveux & Panouse, 1987) and spectrophotometry (Lorenzen, 1967).

2.4. Biomasses

Microbial biomasses were determined from the qualitative and quantitative analysis of auto– and heterotrophic microorganisms carried out with different microscopic techniques. Preservation solution, staining dye when required, and microscopy method specific to each taxonomic group (Taxon) considered are gathered in Table 2.I. Carbon biomass of each selected trophic group was calculated from biovolume measurement using the conversion factors listed in Table 2.II.

Table 2.I : Taxons, sampling treatment and microscopy analysis.

Taxon	Sampling volume, ml	Preservation solution	Microscopic analysis
Diatoms > 20µm Diatoms < 20µm	50 – 100 10 – 20	Glutardialdehyde-lugol ($35^{o}/_{oo}$, v/v), (1% final conc.)	Inverted light microscopy (Utermöhl, 1958)
Flagellates	10 – 20	Glutardialdehyde (0.5% final conc.)	Epifluorescence microscopy after DAPI staining (Porter & Feig, 1980)
Ciliates	50 – 100	Glutardialdehyde-lugol ($35^{o}/_{oo}$, v/v), (1% final conc.)	Inverted light microscopy (Utermöhl, 1958)
Bacteria	2 – 5	Formalin (2% final conc.)	Epifluorescence microscopy after DAPI staining (Porter & Feig, 1980)

Table 2.II : Conversion factors for biomass estimate from biovolume measurement.

Taxon	Carbon/Biovolume, $pgC\ \mu m^{-3}$	Reference
Diatoms	0.11	Edler, 1979
Flagellates	0.11	Edler, 1979
Ciliates	0.08	Beers & Stewart, 1970
Bacteria	Biovolume dependent ratio*	Simon & Azam, 1989

*: $\frac{\text{Carbon}}{\text{biovolume}} = \left[130 + 350 * e^{-\text{biovolume}/0.095}\right] * 10^{-3}$

2.5. Biological activities

Phytoplankton: Daily integrated gross and net primary production and phytoplankton respiration were calculated, using the AQUAPHY set of equations (Lancelot *et al.*, 1989; Lancelot *et al.*, 1991), from data on phytoplankton ^{14}C assimilation rates in combination with the knowledge of daily light variations with depth.

ANTAR II/05

Basically, the AQUAPHY model is based on the concept of reserve material storage by phytoplankton cells, according to the future requirements of their growth. The model considers thus phytoplankton cells as composed of monomeric precursors for macromolecule synthesis, of reserve products (lipids and polysaccharides), and of functional products (composed at 85% of proteins; Dorsey *et al.*, 1978), and assimilates protein synthesis to the measurement of *net* primary production, owing to the functional and structural nature of this cellular constituent. Photosynthesis directly, and storage products catabolism indirectly provide required energy and reductors for the biosynthesis of new cellular material as well as for the basal metabolic maintenance of the cell. So, the model explicitely calculates the **photosynthetic process (*gross* primary production)** – occurring only during the light period of a circadian day, and fueling the different pools of cellular metabolites – and the **phytoplankton growth process (*net* primary production)** reflected by the protein synthesis – continuing along the whole day, at the expense of reserve products accumulated by the phytoplankton cell during the light period. This model was chosen because it takes explicitly into account the interaction between phytoplankton physiology and the turbulent structure of its habitat, by describing the light history of the cells as reflected by the pool size of the storage products.

Experimental determination of the AQUAPHY parameters involved two kinds of tracer experiments conducted in parallel under simulated *in situ* conditions. For all these incubations, 250 to 700 ml seawater sample – which amount was chosen according to phytoplankton biomass – were incubated in transparent culture flasks with $NaH^{14}CO_3$ at a rate of 10 µCi/100 ml sample (Amersham, specific activity = 56 mCi $mmol^{-1}$). Photosynthetic parameters were calculated, using the Platt *et al.* (1985) equations, from short–term (4 hours) ^{14}C incubations performed at various light intensities at *in situ* temperature. Phytoplankton growth and respiration parameters were calculated, using the AQUAPHY equations through an isotopic model (Lancelot *et al.*, 1989), from data on long–term (24 hours) light–dark kinetics of ^{14}C assimilation into four pools of cellular constituents (lipids, small metabolites, polysaccharides and proteins).

Details on experimental procedure, biochemical fractionation and calculations are described in Lancelot & Mathot (1985), Lancelot *et al.* (1991a) and Mathot *et al.*(1992).

Microheterophs: Protozoan (mostly heterotrophic dinoflagellates and ciliates) grazing on algal cells was calculated from cell counts followed by carbon biomass calculation as described above, using the maximal hourly clearance rate of 10^5 body volume per protozoa determined by Björnsen & Kuparinen (1991). In this calculation, only protozoa greater than 7 µm were considered as effective phytoplankton grazers; smaller heterotrophs were assumed to feed on bacteria.

Bacterial production rates were measured according to the ^{3}H–thymidine incorporation method of Fuhrman & Azam (1982). ^{3}H–thymidine was added at a final concentration of 10 nmol l^{-1}, a concentration shown saturating for the process of incorporation. The uptake of radioactivity in the cold TCA fraction was determined after 3–4 hours incubation. Empirical calibration with cell number increase in 0.2 µm filtered seawater reinoculated with 2 µm filtered seawater (the procedure of Riemann *et al.*, 1987) was carried out several times. The conversion factor found was 1.25 10^9 cells/nmol thymidine incorporated. Bacterial mortality was measured according to the method developed by Servais *et al.* (1985, 1989). Within this overall mortality rate, the part being attributed to grazing by nanoprotozoa was estimated by comparing the mortality rate of an unscreened sample to that of a 0.2 µm filtered sample membrane and poisoned with a colchicine– cycloheximide mixture.

Total ammonium remineralization by heterotrophic microorganisms was determined by isotope (^{15}N) dilution experiments. A detailed description of the methodology is given in Goeyens *et al.* (1991b). Ammonium regeneration by bacteria was calculated from bacterial growth rates using a carbon:nitrogen (w:w) ratio of 4 for the bacterial biomass as well as for its direct substrates. Ammonium regeneration by protozoa was calculated from grazing rates using a growth yield of 0.38 and carbon:nitrogen ratios of 4.5 and 5.6 for phytoplankton and protozoa respectively.

3. SEA ICE RETREAT AND PHYTOPLANKTON ICE–EDGE BLOOM DEVELOPMENT

Many evidences (Smith & Nelson, 1986; Sullivan *et al.*, 1988; Comiso *et al.*, 1990) indicate that the circumpolar marginal ice zone is a region of enhanced primary production owing to the formation, at the time of ice melting, of a shallow vertically stable upper layer as a result of the production of meltwater and the subsequent seeding by actively growing sea ice microbes (Garrison *et al.*, 1987). Their relative contribution in initiating phytoplankton ice–edge development in the marginal ice zone of the northwestern Weddell Sea is considered here below.

3.1. Sea ice microbial communities and their impact on the water column at the time of ice melting

Sea ice offers a set of physico–chemical conditions for microorganisms living in close association with it, either attached to ice crystal or suspended in the interstitial water between ice crystal (Horner, 1985). These microorganims, originally planktonic or benthic, were incorporated within the ice during fall, at the time of frazil ice formation (Garrison *et al.*, 1983). Sea ice microalgae grow in early spring when incident light reachs sufficient levels, and are accompanied by the development of a microbial network composed of bacteria and various protozoa (Whitaker, 1977; Ackley *et al.*, 1979; Palmisano & Sullivan, 1983; Horner, 1985; Garrison & Buck, 1989; Garrison & Gowing, 1992; Sulllivan, 1985; Kottmeier & Sullivan, 1987). When released from the ice upon melting, fate of these sea ice–associated microorganisms is variable : part is grazed by pelagic herbivores like krill (Marschall, 1988) and copepods (Fransz, 1988); part aggregates and settles down (Schnack *et al.*, 1985; von Bodungen *et al.*, 1986; Riebesell *et al.*, 1991) and part survives in the water column (Garrison & Buck, 1985). This latter part has been suggested to constitute an inoculum for phytoplankton ice–edge bloom development and associated secondary producers. The genesis of a phytoplankton ice–edge bloom through the release of living cells seeded into the water column depends however on the dilution factor related to the physical properties of the water column but also on the viability of the released microorganims. Two approaches were developed to study the seeding capability of microalgae released in the northwestern Weddell Sea at the time of ice melting. One is based on the measurement of potential metabolic activities of released sea ice microalgae. The second approach, based on the direct comparison of microbial inhabitants of sea ice assemblages originating from various sea ice habitats and of adjacent surface waters,

will give an indirect estimate of the importance of sea ice microbial communities as inoculum for the ice–edge bloom development in this part of the circumpolar marginal ice zone of the Southern Ocean.

3.1.1. Potential photosynthetic activity of released sea–ice microalgae

The potential photosynthetic activity of sea ice microalgae released in the water column upon melting was measured through shipboard simulating seeding experiments under controlled conditions (Mathot *et al.*, 1991).

Comparison between photosynthetic parameters characteristic of sea ice communities collected at the snow ice interface (***infiltration assemblages***) and deeper within the ice (***band assemblages***) with those of phytoplankton communities sampled in the corresponding adjacent waters (Fig. 3.1, Table 3.I) indicates that infiltration layer microalgae are as efficient photosynthetizers as surface planktonic cells. These assemblages could then act as efficient inoculum when released in the water column. Microalgae released from band assemblages appear however less efficient, their photosynthetic capacity being lower by a 3.5 factor than that of local phytoplankton (Table 3.I). The relative importance of infiltration layer and band assemblages is however difficult to assess owing to the high spatial variability of the sea ice habitat (Eicken *et al.*, 1991). Accordingly, visual observation of the ice field of the northwestern Weddell Sea in 1988 evidenced high patchiness in the spatial distribution of algal–rich ice floes of strong brown or yellow coloration (the ***brown ice***), these latter contrasting severly with the white algal–poor ice floes (Fig. 3.2). Following Horner (1985) however, ice assemblages encountered in the pack–ice of the northwesten Weddell Sea are mainly infiltration assemblages and to a lesser extent interior assemblages.

Table 3.I : Photosynthetic characteristics of the infiltration assemblage and the band assemblage (= vegetative cells only, with exclusion of the resting spores) from ice communities and of phytoplankton from the water column.

	n	α	K_m	I_k
Infiltr. Ass.	2	0.00066 $\pm$0.00007	0.049 $\pm$0.003	75 $\pm$12.8
Band Ass.	2	0.00018 $\pm$0.00007	0.012 $\pm$0.007	62 $\pm$15.7
Phytoplankton	6	0.00042 $\pm$0.00016	0.041 $\pm$0.014	92 $\pm$19

n = number of samples
α = photosynthetic efficiency $[h^{-1} (\mu E\ m^{-2}\ s^{-1})^{-1}]$
K_m = maximal specific rate of photosynthesis (h^{-1})
I_k = light adaptation parameter $(K_m/a : \mu E\ m^{-2}\ s^{-1})$

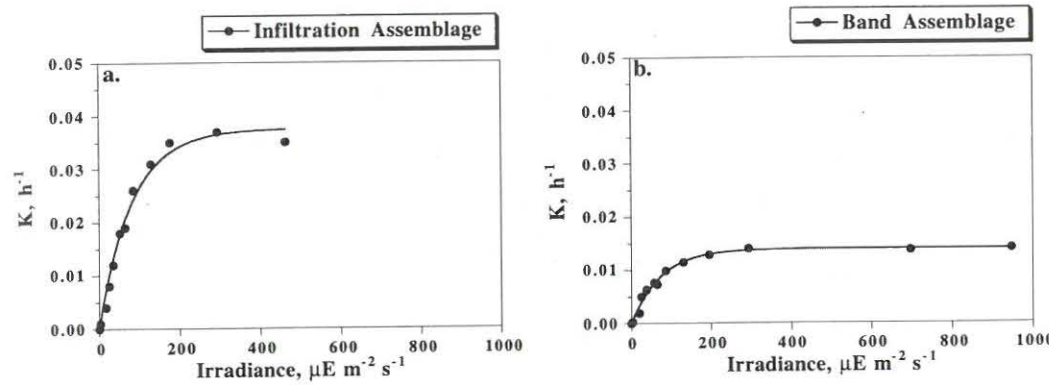

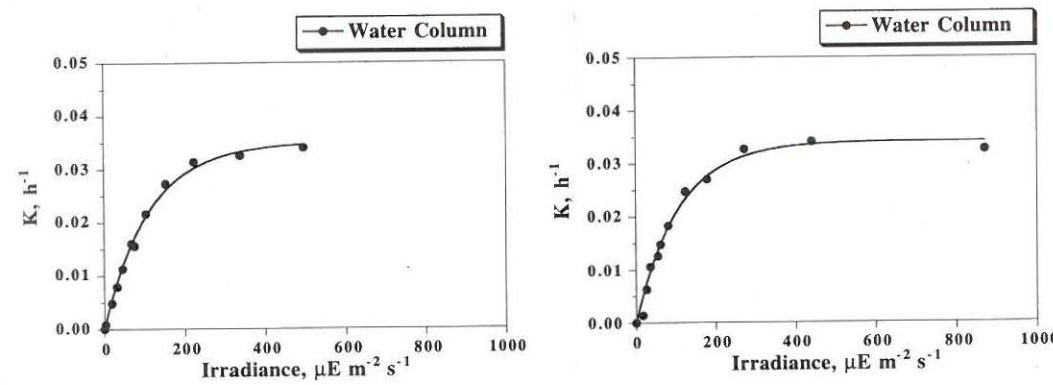

Figure 3.1 : Photosynthesis–irradiance relationship of surface layer phytoplankton and sea ice microalgae from the infiltration layer (a) and the interior layer (b).

Figure 3.2 : Algal–rich ice floes of brown coloration (a), and white algal–poor ice floes (b) in the northwestern Weddell Sea (photographs by S. Mathot).

3.1.2. Sea ice microbial assemblages : complexity and patchiness

Microscopical analysis of sea ice infiltration layer and band assemblages randomly collected in the northwestern Weddell Sea revealed the existence of a complex microbial network composed of diatoms, autotrophic flagellates, bactivorous and herbivorous protozoa and bacteria (Table 3.II). As a general trend, autotrophs contributed to a mean of 90 % (range : 76–96 %) of total microbial carbon, with little difference between assemblages from different sea ice habitats (Table 3.II). Bacterial biomass was relatively abundant contributing to 41 and 62 % of the total heterotrophic biomass in infiltration and band assemblages respectively. However, the taxonomic composition of both microalgae and protozoa varied greatly, according to the physical characteristics of the sea ice habitat. Whilst diatoms dominated dramatically the algal composition of all investigated ice areas (Table 3.II), the bulk of their biomass considerably differed from one sea ice habitat to another, with nano–sized *Nitzschia* sp. and micro–sized *Tropidoneis* sp. prevailing in infiltration assemblages, and micro–sized

Table 3.II : Composition of microorganisms in the sea ice & adjacent water column samples. Results expressed in % of total carbon biomass (autotrophs + heterotrophs). Diatoms R.S. = Resting Spores; Diatoms V.C. = Vegetative Cells; (–) = negligible.

Taxon	Infilt. Assembl. n = 4		Band Assemblage n = 2		Water Column n = 3	
	Range,	$\bar{x}$	Range,	$\bar{x}$	Range,	$\bar{x}$
Autotrophs						
Diatoms R.S.	(–)		12–45	29±16.2	(–)	
Diatoms V.C.	65–93	77 ±8.7	50–63	56.5±6	11–15	13.4±1.6
Phaeocystis col.	0–3.3	1.2±1.2	(–)		(–)	
Dinoflagellates	1–11	5.6±3.2	0–0.3	0.2±0.2	2–10	6.7±3.2
Nanoflagellates	3–13	6.9±4.3	0.2–1	0.6±0.4	38–50	43.6±4
Aut.procaryotes (= cyanobact.?)	0.1–1.8	0.9±0.6	(–)		(–)	
Total	82–97	92±4.8	76–96	86±10	60–71	64±14.7
Heterotrophs						
Protozoa						
. Ciliates	0.1–2.4	0.9±0.7	1.4–2.9	2.2±0.8	1.9–3	2.5±0.4
. Dinoflag.	0.4–4.5	2.1±1.2	0–0.1	0.05±0.05	3.8–9	6.5±1.8
. Nanoflag.	0.2–3	1.6±0.7	0–0.6	0.3±0.3	7 –12	9 ±2.1
Bacteria	1.3–11	3.8±3.5	1.3–22	12 ± 10.4	9 –27	18.2±5.9
Total	3–18	8.3±4.9	4–24	14+10	29 –40	36.3±4.9

Thalassiosira sp. and *Amphiprora* sp. in interior layers. Ciliates constituted the bulk of protozoa biomass of band assemblages. Within infiltration layer reversely, ciliates were scarce, whereas dinoflagellates and heterotrophic nanoflagellates contributed almost equally to protozoan biomass.

3.1.3. Fate of microbial assemblages at the time of ice melting : the role of krill

Contrasting with sea ice assemblages, microorganisms of adjacent surface waters were dominated by nano–sized microorganisms mainly autotrophic and heterotrophic flagellates, diatoms – mainly *Nitzschia* – representing a maximum of 15% of the total microbial biomass. Obviously the ice melting process in the northwestern Weddell sea gives rise to a shift from a diatom–dominated community in the ice environment to a nanoflagellate–dominated community in the water column (Fig. 3.3). This shift, in other respects not due to the inability of ice microorganisms to develop in sea water, has to be explained by an effective disappearance of ice microorganisms from the water column, either by grazing pressure or by sedimentation. The presence of numerous krill swimming around ice floes, scraping on concentrated sea ice assemblages (Cuzin–Roudy & Schnack, 1989) and the propensity of ice algae to aggregate formation followed by rapid sedimentation (Riebesell *et al.*, 1991) supports this assumption, so minimizing the contribution of ice algae to phytoplankton ice–edge development. Accordingly, a low seeding stock of 0.05 µg Chl *a* l^{-1} was calculated by Lancelot *et al.* (1991a) from the empirical relationship between chlorophyll *a* concentrations in surface waters at the early beginning of ice melting and ice cover percentage (Fig. 3.4).

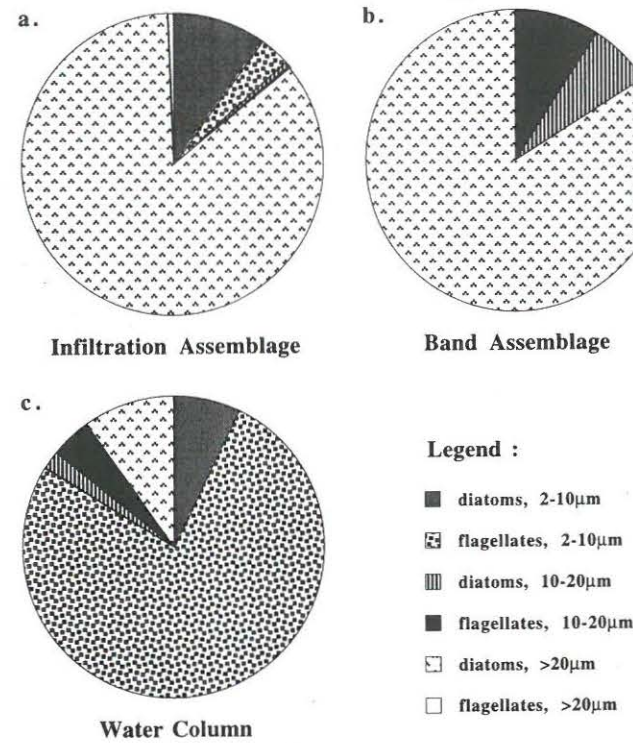

Figure 3.3 Distribution of autotrophic carbon biomass in three size classes with distinction between diatoms and flagellates typical of infiltration (a) and band (b) assemblages, and surface phytoplankton (c).

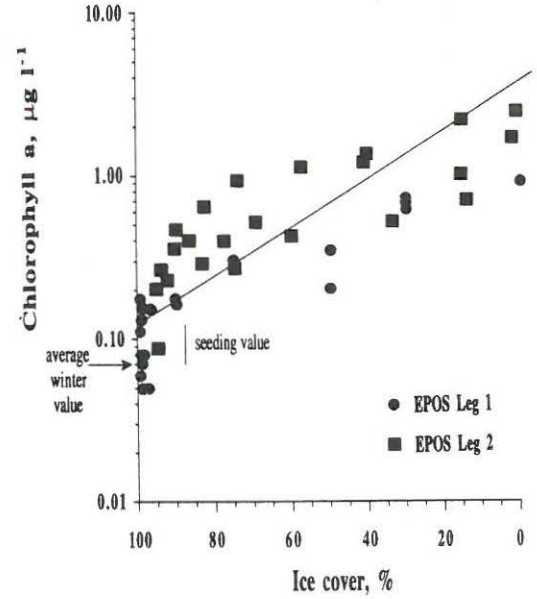

Figure 3.4 : Relationship between chlorophyll *a* concentration of surface waters and ice cover as measured in the marginal ice zone at the beginning of ice melting.

3.2. Physical processes associated to sea ice retreat and phytoplankton ice–edge bloom initiation

3.2.1. Phytoplankton bloom and the receding ice–edge

In 1988, the marginal ice zone around the 49° W meridian extended from latitude 58 30° to 61° S, covering a distance of about 300 km. This zone is a dynamic frontal system which is not a sharply delimited line between the ice and the open ocean, but rather a wide transitional zone with large spatial (especially North–South) and temporal differences in its environmental properties. Figures 3.5 and 3.6 respectively show the spatio–temporal variation of ice cover (Fig.3.5) estimated by Lancelot *et al.* (1991b) in the studied sector during spring 1988, and the shift of the ice–edge further South (Fig.3.6). As seen on these figures, the process of ice retreat initiated in end October and completed in end December, proceeding at a mean rate of 5.5 km per day. Nevertheless, the ice–edge in this sector of the Weddell Sea does not retreat further south than 61° S because of a continuous supply of sea ice from the Weddell Gyre (Ackley, 1981). In agreement with previous observations (Comiso & Zwally, 1984), ice retreat did not occur at the same rate throughout the whole period, being minimal at the beginning (end October) and at the end (end December) of the process. During the period in between, intense ice melting occurred and sea ice retreat could cover distances as great as 9 km per day.

In close relationship with sea ice retreat, maximum chlorophyll *a* concentrations of about 4 $\mu g\ l^{-1}$ were systematically recorded close to the ice–edge , at a distance of about 50 km from its northern boundary (Fig. 3.6) and coincided with nitrate concentration minima (about 20 $\mu mole\ l^{-1}$). Moreover a 100 to 150 km–width belt of relatively elevated phytoplankton biomass (higher than 2 $\mu g\ l^{-1}$) was strongly associated with the receding ice–edge, moving in parallel with this latter (Fig. 3.6). On both sides of this region of enhanced primary production, mean chlorophyll *a* concentrations were very low (0.4 μg chl $a\ l^{-1}$), reaching 1 $\mu g\ l^{-1}$ at a maximum.

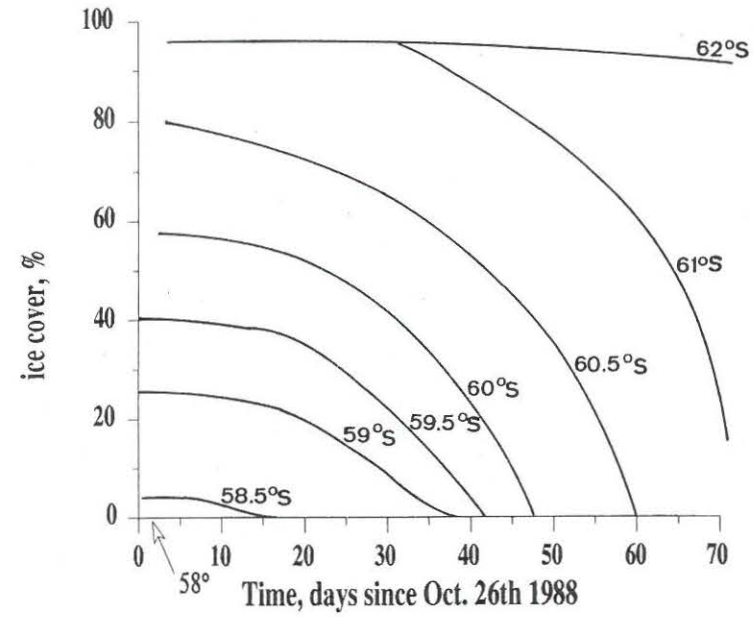

Figure 3.5 : Spatio–temporal evolution of ice cover around meridian 49° W during sea ice retreat 1988.

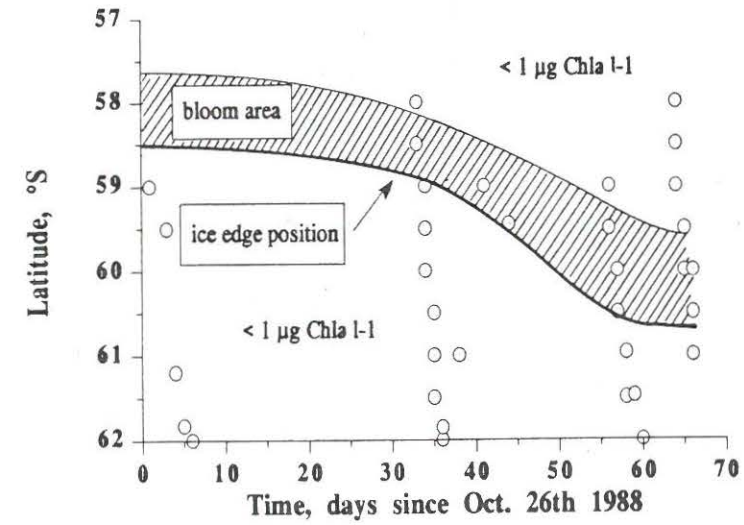

Figure 3.6 Sea ice retreat and related chlorophyll *a* spatio–temporal distribution. Sampling stations (□, EPOS Leg 1; O, EPOS Leg 2) and position of the ice–edge .

The strong relationship between the receding sea ice and phytoplankton bloom development is clearly evidenced by Fig. 3.7 that shows synoptic distribution of ice cover, averaged chlorophyll *a* concentrations over the upper wind mixed layer and nitrate depletions (the amount of nitrate removed from the water column by phytoplanktonic uptake during the ongoing growth season) observed or calculated over a one–month interval. During this period, sea ice retreated over a distance of 270 km (Fig. 3.7a). Accordingly, the peak of phytoplankton shifted from latitude 58 30^0 to 60^0 S (Fig. 3.7b), at a similar rate as the receding ice–edge (9 km day^{-1} at this period of intense ice melting). Also, nitrate depletion (Fig. 3.7c) reached a maximum of 500 mMN m^{-2} that moved southward, closely following the sea ice retreat. More noteworthy is the similar feature of both phytoplankton blooms, in magnitude as well as in extent, suggesting that their controlling mechanisms are identical. Unexpected however is the moderate magnitude of spring bloom regarding the high ambient nutrient concentrations. The latter remained indeed well above depletion throughout the spring season (Goeyens *et al.*, 1991a; van Bennekom *et al.*, 1989). Such a low biological performance cannot be ascribed to low temperature stress on phytoplankton physiology, as photosynthetic and growth capacity at temperatures ranging from –1.8 to +2^0 C were of the same order of magnitude as those of temperate phytoplankton (Lancelot *et al.*, 1991a). Other factors likely prevent massive biomass development in this part of the circumpolar marginal ice zone. They are discussed in details in the following sections.

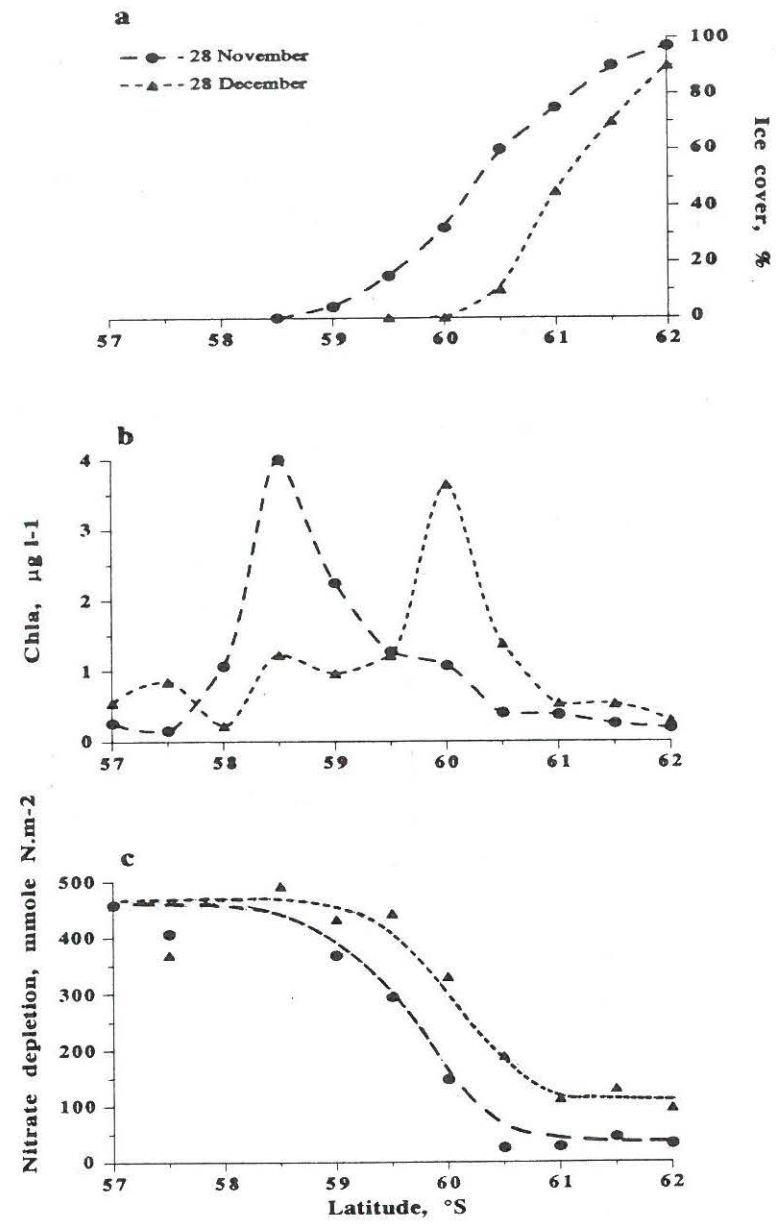

Figure 3.7 : Ice cover percentage (a), averaged chlorophyll *a* concentration over the upper mixed layer (b) and nitrate depletion (c) measured at one–month interval along the 49^0 W meridian.

3.2.2 The dual role of ice melting in phytoplankton initiation

Vertical stability caused by ice melting has been shown to be the necessary condition for phytoplankton ice–edge bloom initiation (Smith & Nelson, 1985; Sullivan *et al.*, 1988). The relationship between phytoplankton bloom development in the upper mixed layer and the density field of surface waters, as observed during the cross section in the marginal ice zone of early summer (Fig. 3.8), strongly suggest that vertical stability is a necessary but not sufficient condition to allow high biomass development. Indeed, the strong vertical stability of surface waters, created at about 20 % ice cover (Fig. 3.8), maintained itself in the recently ice–free area over a distance of about 250 km (close to the maximum winter sea ice extent around this meridian). On the contrary, corresponding chlorophyll *a* concentrations exhibited one order of magnitude variations around a sharp phytoplankton peak of 4 µg l^{-1} occurring at latitude 60° S (Fig. 3.8). Comparing this with average light in the upper mixed layer (this latter being calculated by taking into account the subsurface irradiance corrected for ice cover, the vertical light extinction coefficient and the depth of the wind mixed layer, see Fig. 3.8a) highlights the dual role of ice–melting in initiating phytoplankton bloom by providing optimal light conditions to phytoplankton cells owing to both the installation of a shallow vertically stable environment as well as the progressive removal of sea ice (Fig. 3.8). At ice coverage higher than 20 % however, phytoplankton development is prevented due to light limitation, despite relatively shallow upper mixed layers (Fig. 3.8a & b). In this ice covered area, environmental light is highly reduced by sea ice albedo to values well below than the light saturation level (Ik) of 100 µE m^{-2} s^{-1} typical of phytoplankton cells growing in this sector of the Southern Ocean (Lancelot *et al.*, 1991a). Consequently, very low chlorophyll *a* concentrations (less than 0.5 µg l^{-1}) are characteristic of these ice covered areas, apparently regardless the vertical stability (Fig. 3.8c).

In most marginal ice areas, the geographical extent of the bloom has been related to that of vertical stability, i.e. the persistence of optimal light conditions, whilst its decline has been attributed to dilution due to the northward degradation of the shallow upper mixed layer by either vertical or lateral processes (Smith & Nelson, 1985; Sullivan *et al.*, 1988; Mitchell & Holm–Hansen, 1991). Deepening of the upper mixed layer by decreasing average water column light to values lower than the phytoplankton light saturation level (Fig. 3.8) might well explain the low chlorophyll concentrations typical of the permanently ice–free area measured North of latitude 58° S. In the recently free of ice zone (between 58° and 60 30° S), on the contrary, vertical stability persisted seawards from the ice–edge, providing optimal light conditions to

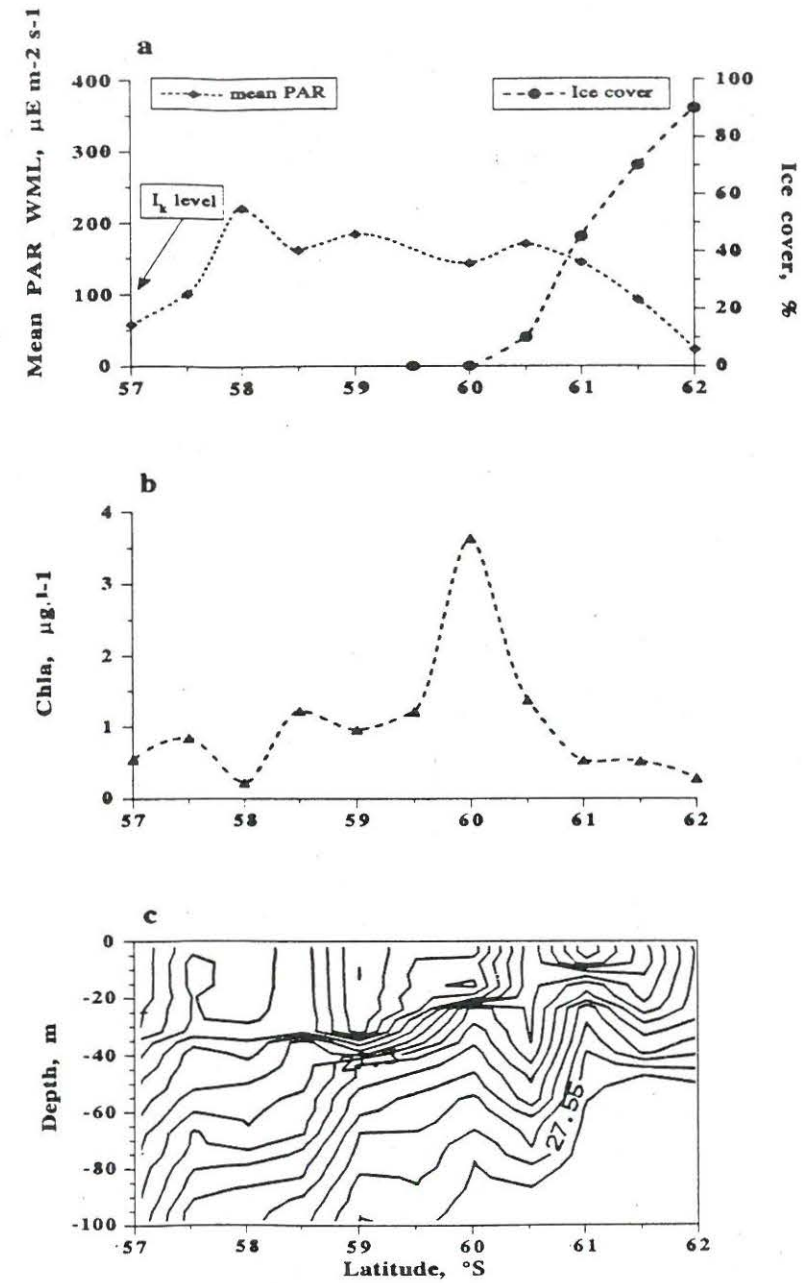

Figure 3.8 : Average light in the upper mixed layer (a), averaged chlorophyll *a* Concentration over the upper mixed layer (b) and density field (c) measured in end–December along the 49° W meridian.

phytoplankton cells (Fig.3.8). Northwards maintenance of vertical stability created in the marginal ice zone by sea ice melting is however a common phenomenon due to heating input (Veth *et al.*, 1992). In their comprehensive analysis of the physical processes contributing to the buoyancy flux in the marginal ice zone of the northwestern Weddell Sea during sea ice retreat 1988, these authors demonstrate that the total buoyancy flux is rather constant with the distance to the ice–edge, being mostly due to ice melting in the marginal ice zone and solar heating in the recently free of ice area. Consequently, similar wind mixed layers are expected in marginal ice zone and adjacent open areas under similar weather conditions. This means that the suboptimal performance of phytopankton in the open ocean adjacent to the marginal ice zone, after an initial peak following the receding ice–edge, is not caused by turbulent mixing as is often assumed.

3.3. The role of trace metals

The hypothesis that Southern Ocean phytoplankton bloom is limited by deficiency of a trace metal, notably iron (Fe), was recently suggested by Martin & Fitzwater (1988) who extrapolated from bioassays conducted in a similar high nutrient region – the subarctic North Pacific Ocean (Martin & Fitzwater, 1988; Coale *et al.*, 1991). This iron limitation hypothesis for the Southern Ocean was tested in a suite of five experimental runs in different sub–areas of the studied sector of the marginal ice zone (de Baar *et al.*, 1990; Buma *et al.*, 1991). Despite a clear stimulation of growth in every single experiment due to Fe addition, the control bottles (no addition) also rapidly outgrew the levels of chlorophyll *a* in the field (Fig. 3.9). Firstly, this indicated the presence of enough dissolved Fe levels to sustain some growth, as later confirmed by seawater Fe concentrations exceeding 1 nM in the Weddell/Scotia Sea region and upstream Peninsula waters (Nolting *et al.*, 1991; Westerlund & Öhman, 1991; Martin *et al.*, 1990b). Secondly, the bottle effect of controls outgrowing the field was suggested to result from the exclusion of larger grazers (mesozooplankton, e.g. copepods, *Euphausia superba*, salps), allowing the accumulation of both phytoplankton (notably diatoms) and microzooplankton (Buma *et al.*, 1991). Experiments conducted one year later in the Ross Sea showed very similar trends in three out of four experiments, the fourth at the most offshore station more likely suggesting the sought after true Fe limitation (Martin *et al.*, 1990a). These results were interpreted to suggest that, despite observed Fe stimulation, the low phytoplankton stock in the Ross Sea is mostly controlled by loss terms (Dugdale & Wilkerson, 1990). However, in more offshore Antarctic waters, severe Fe limitation is still a valid hypothesis for testing, as

indicated by the results of the one offshore Ross Sea bottle experiment (Martin *et al.*, 1990b). Otherwise, assessments other than bottle enclosures are needed to provide unequivocal evidence for Fe limitation.

Summarizing it may safely be concluded that the Weddell–Scotia region of the EPOS study (as well as at least part of the Ross Sea) is not Fe limited *per se*. Other factors are likely responsible for the moderate ice–edge blooms here observed. Top down grazing control appears one of the more viable proposition, as low sedimentation rates of 0.005 – 0.03 d^{-1} were actually calculated from sediment trap data (G. Cadée, pers. com., 1991). This hypothesis is examined in the following section.

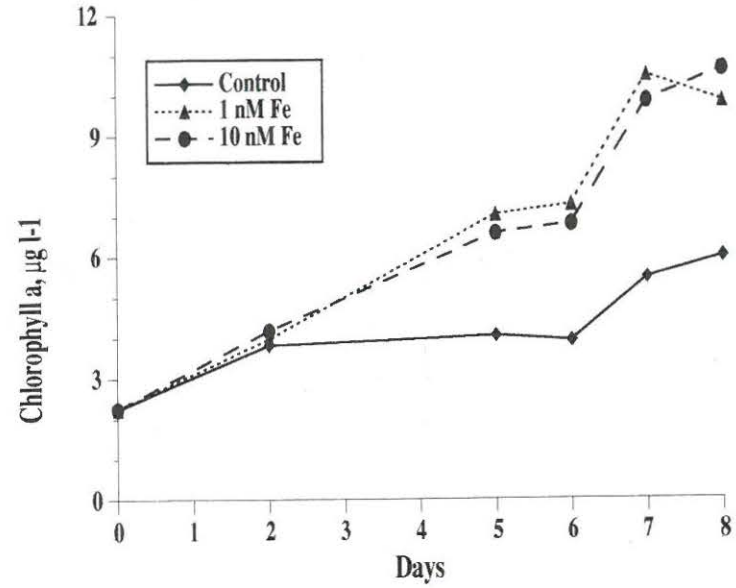

Figure 3.9 : Iron enrichment experiment carried out at latitude 59° S (after de Baar *et al.*, 1990).

4. STRUCTURE AND FUNCTIONING OF THE PLANKTONIC FOOD WEB AT THE RECEDING ICE–EDGE

4.1. The complex structure of the planktonic food–web

The development of phytoplankton blooms at the receding ice–edge is accompanied by the development of various heterotrophic organisms. The complex structure of the planktonic food web characteristic of the marginal ice zone (Fig. 4.1.) has been established on the basis of the identification of key planktonic organisms together with the analysis of their spatio–temporal variations as well as their mutual interactions.

4.1.1. Identification of key planktonic organisms

Auto– and heterotrophic microorganisms

Average carbon biomass distribution among the main taxonomic groups characterizing microbial communities of the marginal ice zone of the northwestern Weddell Sea is shown on Table 4.I. These taxons were chosen according to the size (nano–, micro–) and the trophic mode (phyto–, protozoo–, bacterioplankton). Within each trophic mode, additional taxons were considered on the basis of their relative abundance. This analysis revealed the dominance of nano–sized–microorganisms, both autotrophs and heterotrophs.

Phytoplankton biomass, ranging between 7.7 and 79.8 $\mu gC\ l^{-1}$ with a mean value of 25.7 $\mu gC\ l^{-1}$, constituted by far the bulk of the microbial biomass, contributing on an average to 65 % of the total microbial carbon (Table 4.I). Among autotrophs (mean carbon biomass = 25.7 $\mu gC\ l^{-1}$), the nanophytoplankton forms were the most important, representing 74 % of the total phytoplankton biomass with an average of 18.9 $\mu gC\ l^{-1}$. As a general trend, flagellates were shown to dominate the nanoplanktonic autotrophic community (87 %), whilst diatoms constituted the bulk of microphytoplankton (99 %). In one case however (station 147), when small *Chaetoceros* sp. were abundant, diatoms could significantly contribute to nanophytoplankton. Naked flagellates identified as *Prasinophyceae*, *Cryptophyceae* and *Prymnesiophyceae* were the dominant nanophytoplankters. Among these, *Cryptomonas* spp. (Fig. 4.2a) was by far the most important genus. Centric diatoms constituted the bulk of microphytoplankton, with *Corethron* sp., *Thalassiosira* sp. and *Rhizosolenia* sp. being the principal genus (Fig. 4.2b).

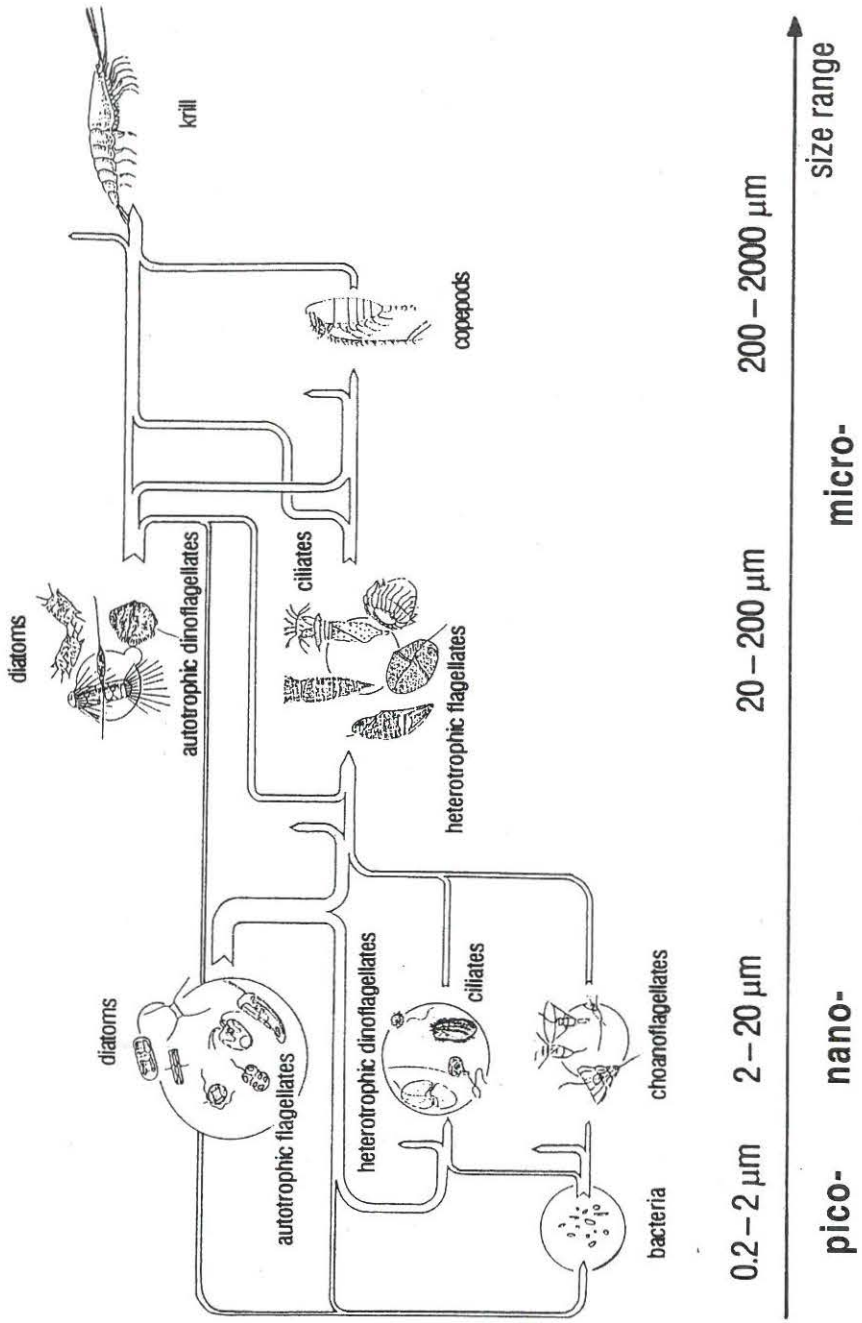

Figure 4.1 : Structure of the planktonic food web at the receding ice-edge of the northern Weddell Sea.

Table 4.I : Mean and extreme values of biomass for main microbial groups. Number of observations = 16. Units are µgC l^{-1}.
Abbreviation : n.s. = not significative.

Taxon	Nano-size, (<20µm) Mean (min. – max.)	Micro-size, (>20µm) Mean (min. – max.)	Total Mean (min. – max.)
Phytoplankton			
Diatoms	**2.0** (0.1 – 18.6)	**6.7** (n.s. – 50.3)	**8.7** (0.1 – 68.9)
Dinoflagellates	**0.5** (0 – 2.1)	**n.s.** (0 – 0.5)	**0.5** (0 – 2.1)
Other flagellates	**16.4** (4.4 – 79.1)	**0.1** (0 – 2.0)	**16.5** (0.2 – 79.1)
Total	**18.9** (3.4 – 79.3)	**6.8** (n.s. – 52.8)	**25.7** (7.7 – 79.8)
Protozooplankton			
Choanoflagellates	**0.1** (n.s. – 0.4)	–	**0.1** (0 – 0.7)
Dinoflagellates	**1.3** (0.3 – 3.4)	**1.3** (0 – 7.4)	**2.6** (0.7 – 7.7)
Other flagellates	**3.4** (0.3 – 20.3)	–	**3.4** (0.3 – 20.3)
Ciliates	**0.2** (0 – 1.0)	**1.6** (0.5 – 6.5)	**1.8** (0.5 – 6.7)
Amoeba	**1.2** (0 – 5.6)	–	**1.2** (0 – 5.6)
Total	**6.2** (0.7 – 27.6)	**2.9** (0.5 – 11.2)	**9.1** (1.8 – 29.2)
Bacterioplankton			**4.2** (1.4 – 10.0)

Among heterotrophs, protozooplankton was the most important in terms of biomass. Its mean biomass amounted to 9.1 µgC l^{-1}, contributing to 23 % of the total microbial biomass. On an average, it represents 35 % of the phytoplankton biomass. Like phytoplankton, protozooplankton was dominated by nano–sized taxons, in which heterotrophic dinoflagellates and other heterotrophic flagellates contribute respectively to 29 and 37 % of the total nanoprotozooplankton biomass. The microzooplankton was composed of dinoflagellates and ciliates, these latter dominating at 55 % in biomass.

Bacterioplankton biomass varied around 4.6 µgC l^{-1}, averaging 16 % of phytoplankton biomass. At one occasion, however, (station 147), a particularly high bacterial biomass of 10 µgC l^{-1} and 1.3 times greater than the phytoplanktonic standing stock was observed. This elevated bacterial biomass follows the passage of a krill swarm literally cleaning the water from its phytoplankton standing stock (Jacques & Panouse, 1991). Organic matter released through krill feeding activity might have thus stimulated bacterial growth.

a.

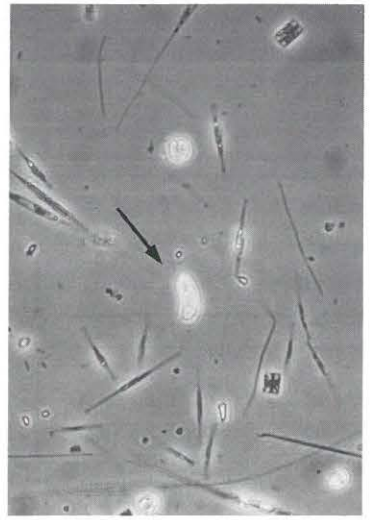

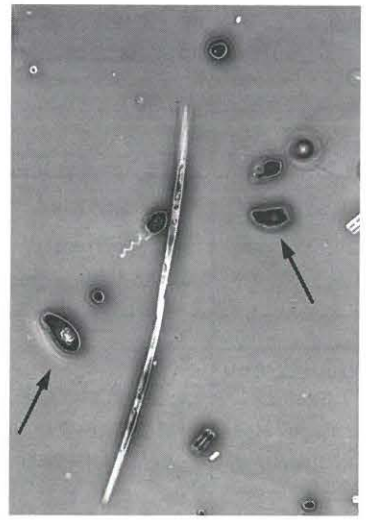

b.

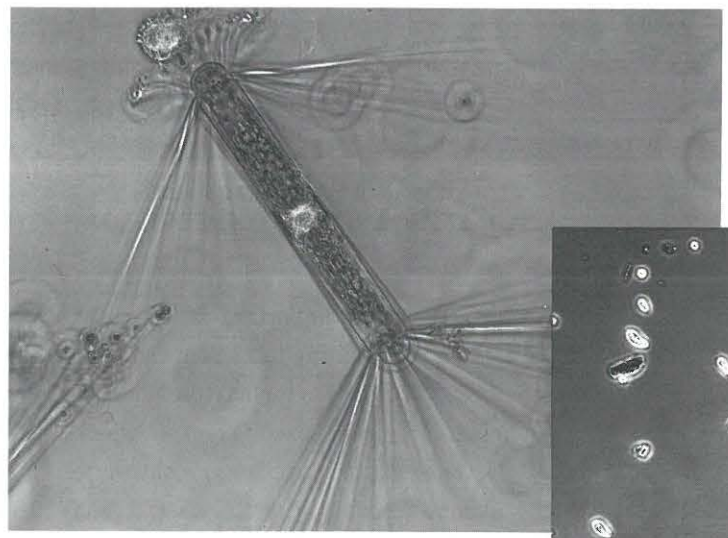

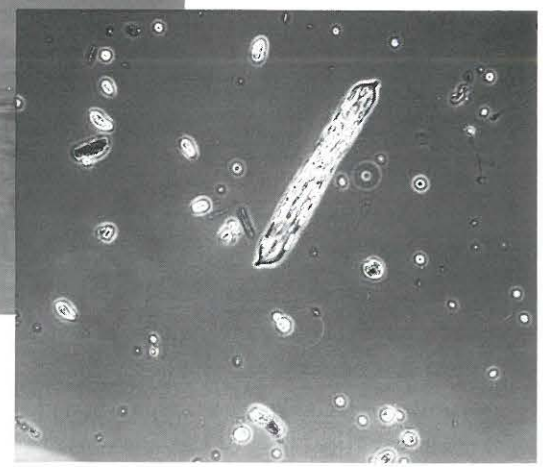

Figure 4.2 : Dominant phytoplankton species : (a) *Cryptomonas* spp.; (b) *Corethron* sp. and *Rhizosolenia* sp. (photographs by S. Mathot).

Mesozooplankton and krill

Oithona similis was the most abundant herbivorous copepod in the marginal ice zone of the northwestern Weddell Sea, the total biomass of which was however low in comparison with protozooplankton, varying between 0.5 and 13 µgC l^{-1} (Fransz & Gonzalez, 1992). Higher copepod biomass reaching 50 µgC l^{-1} was however recorded in the permanently open sea, North of the marginal ice zone.

The Antarctic krill *Euphausia superba*, one of the major components of mesozooplankton in the sea ice–associated area of the Southern Ocean (Hempel, 1985), leads a double life behavior : under–ice during winter, shifting to pelagic in summer (Smetacek *et al.*, 1990; Siegel *et al.*, 1990). By exploiting alternatively the sea ice algae and phytoplanktonic ressources, krill might control the phytoplankton ice–edge bloom at different stages during the course of its development. Overwintering krill in the pack ice zone likely has a predominant role on phytoplankton ice–edge bloom initiation and magnitude, as it reduces the water column seeding by scraping the ice, especially when sea ice algae are released in the water column at the time of ice melting (Marschall, 1988; Stretch *et al.*, 1988; Smetacek *et al.*, 1990). High krill biomass (1–27 g m^{-2}) was recorded in the closed pack ice zone of the northwestern Weddell Sea in the early beginning of the ice melting process (Siegel *et al.*, 1990). These numbers underestimate however the existing krill standing stock, representing only organisms that could be sampled by trawls (Siegel *et al.*, 1990). Indeed, dense krill populations were effectively observed in the marginal ice zone, either evolving in the ridges resulting from piling ice floes (Bergström *et al.*, 1989, 1990) or washed onto the ice in the ship's wake (Cuzin–Roudy & Schalk, 1989).
High patchiness characterizes the distribution of krill swarms in their pelagic life, owing to their great mobility. During the 70 day–EPOS expedition, one single krill swarm was sampled, which biomass amounted 119 g m^{-2} (Schalk, 1990).

4.1.2. Trophic interactions at the receding ice–edge

The trophic interactions between the planktonic organisms of the marginal ice zone of the northern Weddell sea were determined indirectly from the analysis of the sequence of events occurring during the process of sea ice retreat, as deduced from the analysis of spatio–temporal variation of organisms biomass with regards to ice cover, and of the mutual interactions between auto– and heterotrophs established by correlation analysis between specific taxonomic groups.

The spatio–temporal variations of microorganisms (phytoplankton, bacteria and protozoa) and herbivorous copepods biomass averaged over the depth of the upper homogeneous surface layer (Fig 4.3, 4.4) clearly indicates that protozoa are the first heterotrophs to respond to phytoplankton ice–edge bloom. As shown on Fig.4.3, protozoan biomass closely follows phytoplankton biomass by increasing at the time of phytoplankton bloom. However, the high protozoan biomass reached at phytoplankton maximum maintains itself during the decline of the autotrophs, suggesting that these micrograzers do actively control phytoplankton development in this area of the Weddell Sea. Accordingly, a highly significant positive correlation ($r = 0.6$, $P < 0.005$; Table 4.II) relates the variations of phyto– and protozooplankton biomass.

Further investigation on trophic relationships between phytoplankton and protozoa was carried out through multiregression analysis of each dominant taxonomic group of either nano– or micro–sized protozooplankton on each different potential food resource (bacterioplankton, nano– or micro–sized phytoplankton, see Table 4.II). This statistical analysis indicated strong trophic interactions between food and consumers within the same size range, especially between heterotrophic nanoflagellates and nanophytoplankton and between heterotrophic dinoflagellates and microphytoplankton. This size overlapping of autotrophic food and herbivorous consumers is more evidenced by Fig. 4.5 that shows the size distributions of microbial (phytoplankton and protozoa) carbon biomass on a logarithmic scale of microorganism diameter for two typical patterns (Fig. 4.5a & 4.5b) of phytoplankton size distribution. Thus, the highly significant correlations existing between distinct taxonomic groups (Table 4.II) together with the overlapping of the peaks of both protozoan biomass and phytoplankton biomass (Fig. 4.5) show that the trophic organisation of the microbial community can be as complex as that presented on Fig.4.1. In this case indeed, the size ratio of about 1:10 between prey and predator suggested by Azam *et al.* (1983) does not hold, and the energy flux is thus not always oriented towards an increasing particle size as generally admitted.

Protozoa together with phytoplankton are in turn susceptible to be ingested by herbivorous copepods whose biomass, whilst maintained at low level in the area concerned by ice retreat, slightly increased in the recently free of ice area at the time of phytoplankton and protozoa biomass decline (Fig.4.3).

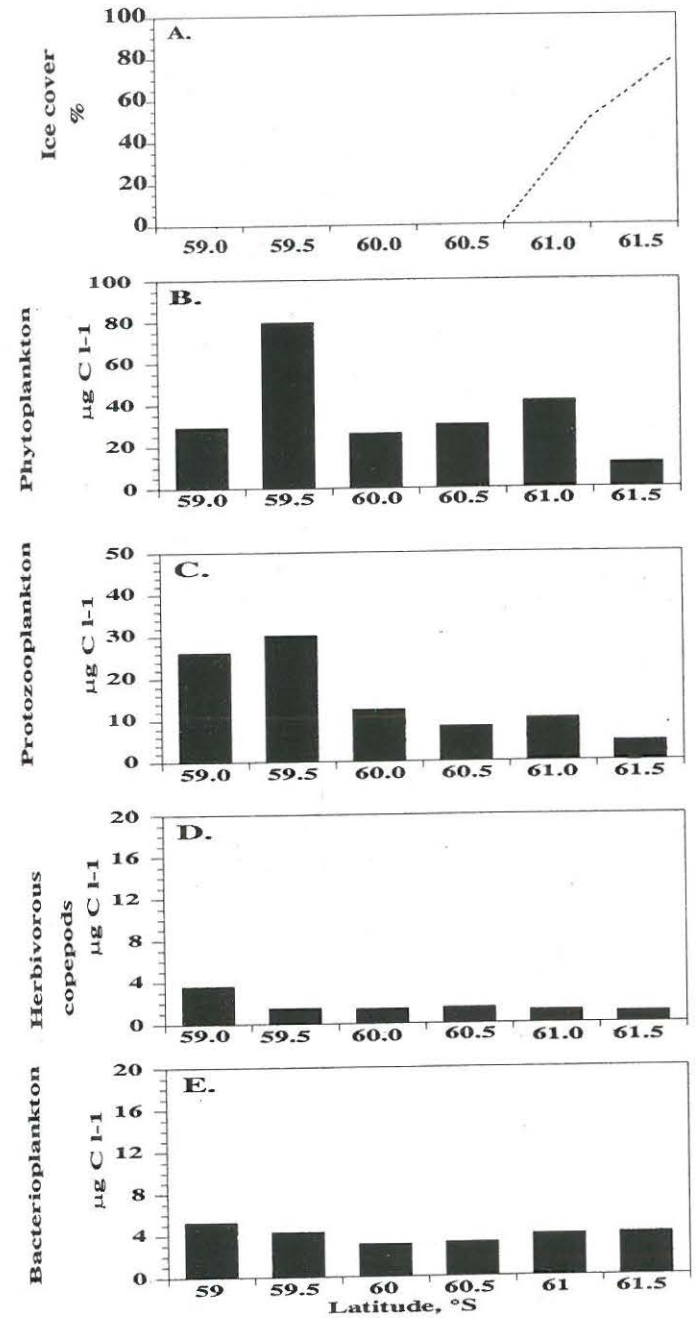

Figure 4.3 : Spatial variations of ice cover (a), phytoplankton (b), protozoa (c), herbivorous copepods (d) and bacterioplankton (e) carbon biomass along the meridian 49° W in end December 1988 (Transect 172–179, 20–24 Dec.).

meridian 49°W

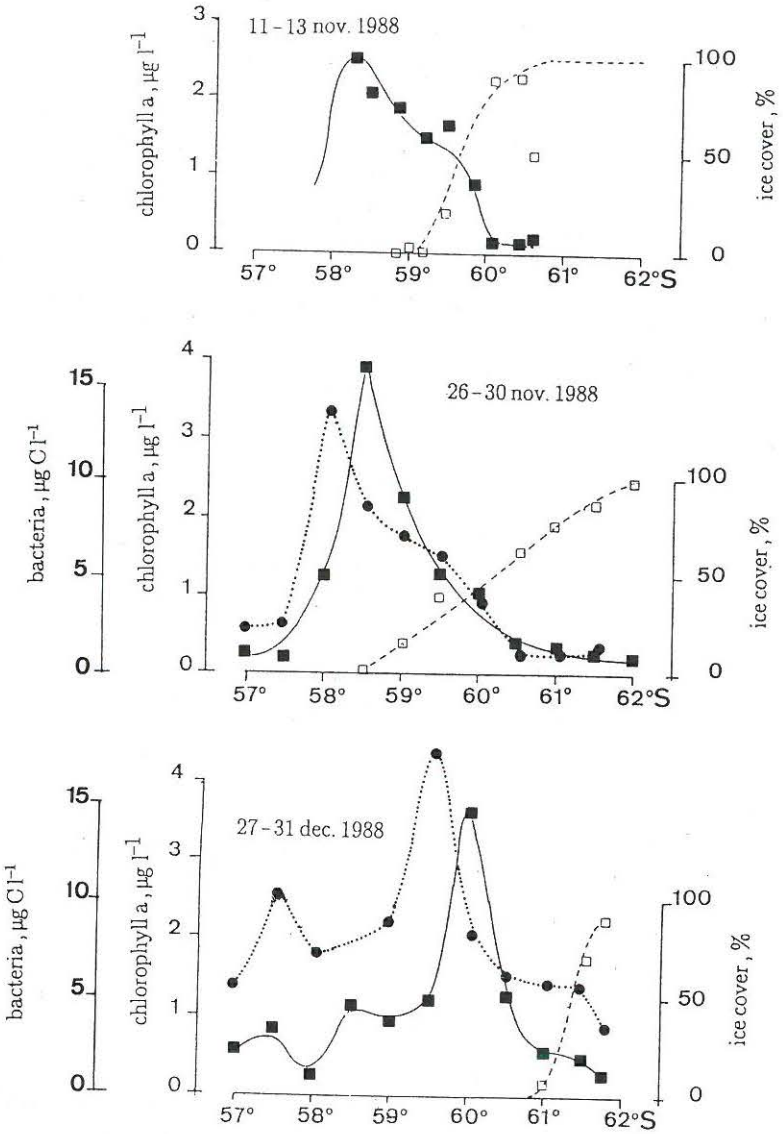

Figure 4.4 : Spatio–temporal variation of phyto– (▬) and bacterioplankton (●), and ice cover (□) along the meridian 49° W during spring 1988. Bacteria were not measured in early November.

Table 4.II : Correlation analysis between biomasses of selected taxonomic groups of microorganisms. Pearson's method followed by the Student test. Coefficients r and (P) are reported for the significant correlations (n.s. = not significant, i.e. P > 0.05).

ANTAR II/05

Consumer \ Food resource	Bacterio-plankton	Nanophyto-plankton	Microphyto-plankton	Total phyto-plankton
Bacterioplankton	–	–	–	n.s.
Nanoprotozooplankton				
Choanoflagellates	0.86 ***	n.s.	n.s.	n.s.
Other flagellates	n.s.	0.85 ***	n.s.	n.s.
Ciliates	0.44 *	n.s.	n.s.	n.s.
Total	n.s.	0.80 ***	n.s.	n.s.
Microprotozooplankton				
Dinoflagellates	n.s.	n.s.	0.84 ***	n.s.
Ciliates	n.s.	n.s.	0.67 **	n.s.
Total	n.s.	n.s.	0.95 ***	0.63 **
Total protozooplankton	n.s.	0.83 **	n.s.	0.68 **

* : P < 0.05

** : P < 0.005

*** : P < 0.0005

On the other hand, no significant correlation was found between bacterial and phytoplanktonic biomasses (Table 4.II). Accordingly, the spatio–temporal evolution of chlorophyll *a* concentration and bacterial biomass (Fig. 4.4) clearly indicates a delay in the response of bacteria to phytoplankton development which follows the southward retreat of the ice–edge. Taking into account the rate of ice retreat, this delay can be estimated to about 10 days. This lag in the response of bacteria to phytoplankton development has been attributed to the macromolecular nature of the dissolved organic matter released from phytoplankton either by autolysis or sloopy feeding, which requires extracellular hydrolysis before being taken up (Billen & Becquevort, 1991). Among protozoa, only the filter–feeding ones, mainly the choanoflagellates and to a lesser extent nano–sized ciliates, should be active bacteria consumers according to the significant correlation relating these taxonomic groups to bacteria (Table 4.II).

a.

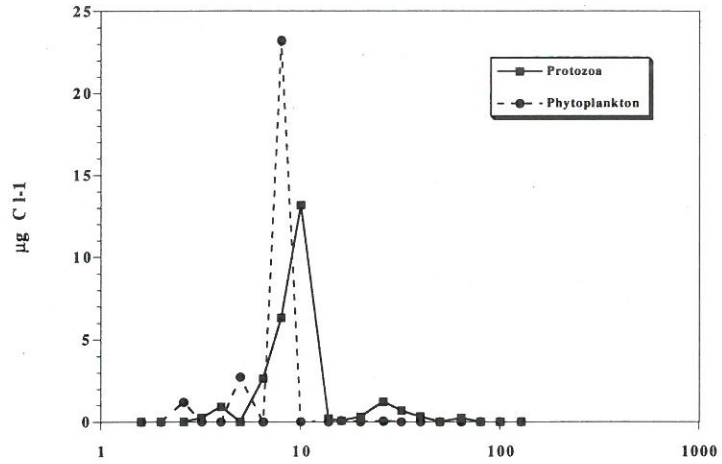

b.

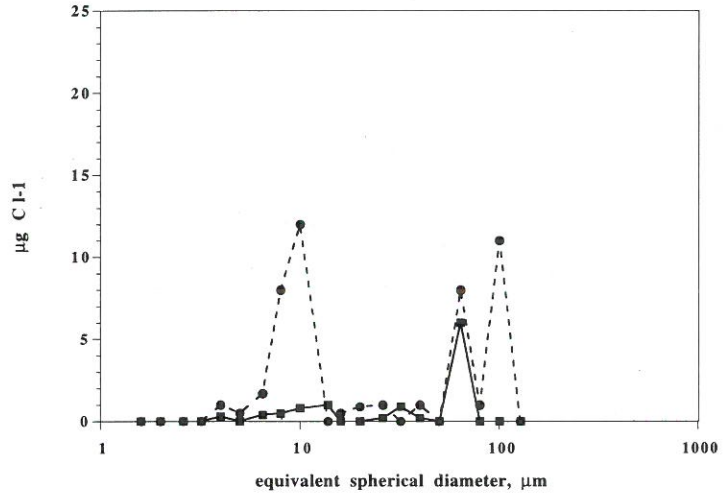

Figure 4.5 : Typical pattern of size distribution of phytoplankton and protozoo–plankton biomass.

4.2. The relative role of micro– and mesograzers in controlling phytoplankton activity in the northwestern Weddell Sea

4.2.1. The sustained grazing pressure exerted by protozoa and copepods and its implication for new to regenerated production ratio.

The relative role of herbivorous protozoa and copepods in controlling phytoplankton ice–edge bloom development was assessed by comparing calculated potential ingestion rates by these two grazers with daily integrated net primary production (Fig.4.6). This comparison strongly suggests that at least protozoa do actively control phytoplankton development at the receding ice–edge. Accordingly, potential ingestions higher than net primary production were occasionally calculated in the recently free–of–ice area. The role played by copepods on the other hand appears neglectable. Its food requirements should primarily be met by protozoa production in the recently free of ice area (Fig.4.6).

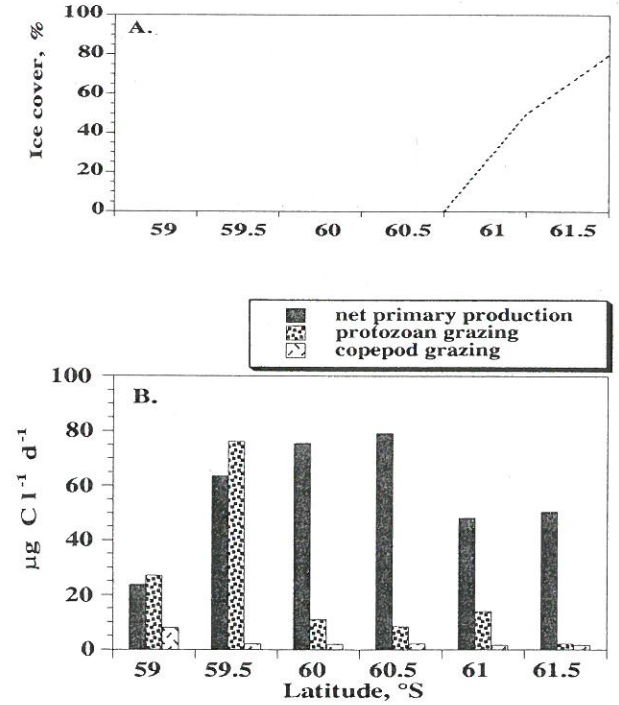

Figure 4.6 : Spatial variations of ice cover (a) and daily net primary production, protozoa and copepod grazing (b) along the meridian 49^0 W in end December 1988.

As a consequence of the high protozoa activity in the area concerned by ice retreat, ammonium concentration dramatically increases with the distance to the ice–edge (Fig.4.7). The balance of inorganic nitrogen forms available to phytoplankton is therefore modified in favor of ammonium, inducing a shift from a phytoplankton community preferably utilizing nitrate as nitrogen source to a predominance of ammonium–based primary producers. This is clearly evidenced by the sharp decrease of measured f_{NO_3} (the ratio between nitrate utlization and total nitrogen uptake by phytoplankton) with the distance to the ice–edge (Fig.4.7).

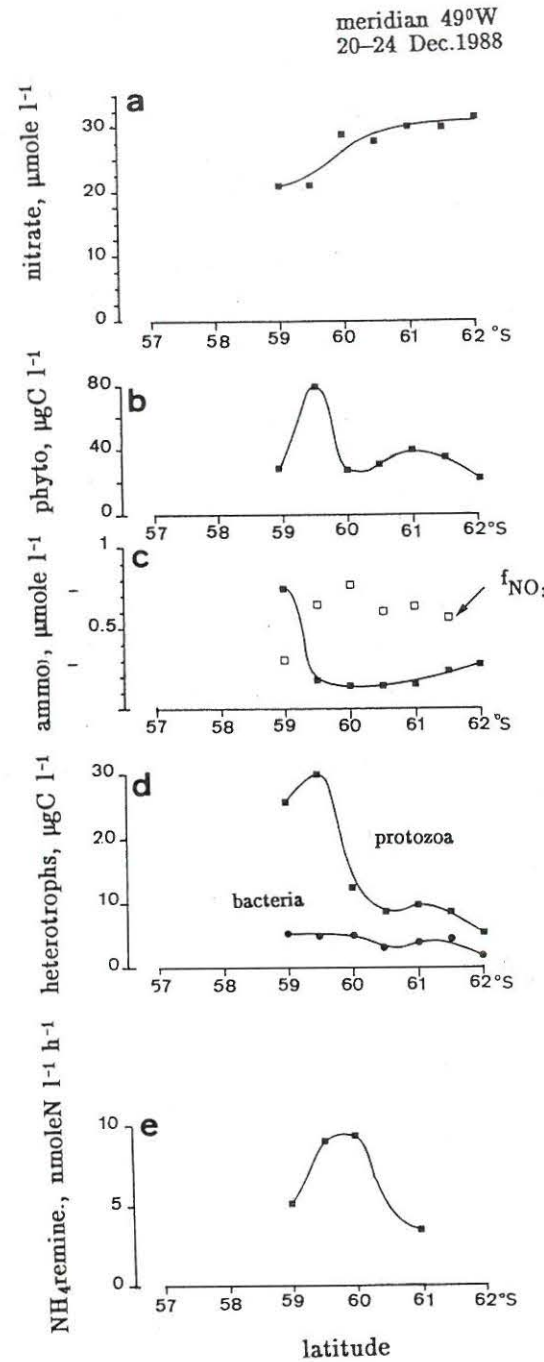

Figure 4.7 : Spatial variations of nitrate (a) and ammonium (c) concentration, of autotrophic (b) and heterotrophic (d) biomass, and of remineralization rate (e) along the meridian 49° W in end December 1988. Average values over the depth of the upper homogeneous layer.

4.2.2. The episodic role of krill

In the previous section, overwintering krill has been suggested to play a significant role in phytoplankton bloom initiation by grazing on sea–ice algae when released in the water column. In its pelagic life, krill, which is an excellent swimmer covering large distances, clears water column by grazing on meso– and microorganisms and controls the overall structure of the planktonic food–web. Such a krill passage was observed in the marginal ice zone of the northwestern Weddell sea during spring 1988. Its impact on the structure and functioning of the microbial network was drammatic. Phytoplankton and protozooplankton biomass was reduced to unsignificant value. Chlorophyll *a* concentrations in particular (Fig. 4.8) were reduced from 2.5 to 0.3 $\mu g\ l^{-1}$ within less than 10 hours and the phytoplankton species composition shifted from a diatom– to a nanoflagellate–dominated community (Jacques & Panouse, 1991). Bacterial activity, on the other hand, was significantly enhanced due the increase of dissolved organic matter released by krill feeding activity.

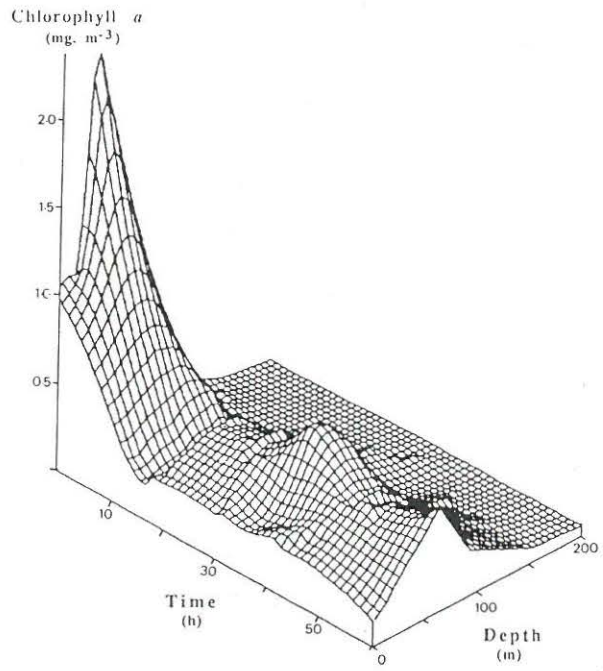

Figure 4.8 : Three–dimensional evolution of a diatom bloom at station 157 in the Weddell Sea (5th December 1988). The diatom bloom vanished in less than 10 h, probably grazed down by a krill swarm, and the phytoplankton community toppled towards a flagellate–dominated system (from Jacques & Panouse, 1991).

4.3. Food–web structure and krill distribution in the circumpolar marginal ice zone of the Southern Ocean : some scenarios

The comprehensive analysis of the structure and functioning of the food web at the receding ice–edge of the northwestern Weddell Sea outlines the key role played by krill in determining the local structure of the microbial network either as overwintering organism, by selectively eliminating micro–sized ice microorganisms released in the water column upon melting, and/or as mobile swarms in the free of ice areas by grazing on microorganisms and mesoplankton. Depending on the presence of active overwintering krill underneath the ice, the following microbial food web (Fig.4.9) are expected to prevail in the part of the Southern Ocean concerned by sea ice retreat :

In the absence of overwintering krill, sea ice diatoms and to a lesser extent *Phaeocystis* – the dominant composant of sea ice biota (Horner, 1985; Mathot *et al.*, 1991) – seed surface waters at the time of ice melting. Fabulous ice–edge blooms dominated by large diatoms or *Phaeocystis* are therefore expected (Fig. 4.10a). Such blooms have been observed in the marginal ice zone of the Ross Sea, an area where krill density is more scarce (Marr, 1962), compared to the Weddell Sea.

In the presence of overwintering krill scraping on sea ice assemblages, sea ice diatom seeding is considerably reduced and ice–edge blooms are dominated by nanophytoplankton. At the same time, an efficient microbial network (Fig.4.10b) develops due to the concomitant development of protozoa probably originated from the sea ice biota (Garrison *et al.*, 1987; Mathot *et al.*, 1991). Resulting ice–edge blooms are relatively moderate.

Ice–free planktonic communities are regulated by episodic passage of krill swarms able to follow blooms spatially, thus grazing heavily on large diatoms, nanophytoplankton, protozoa and copepods (Fig.4.9). Resulting biomasses are very low, excepted bacteria (Fig.4.10b).

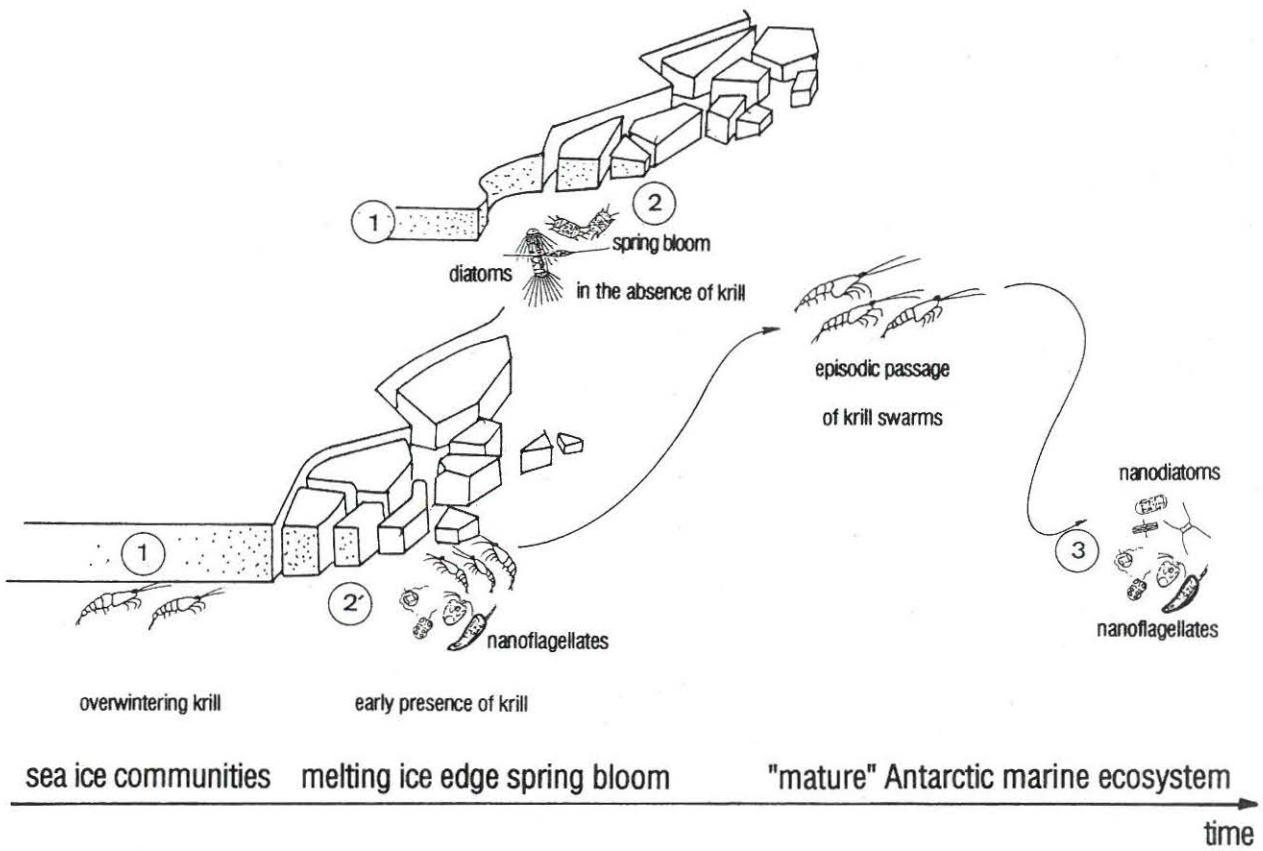

Figure 4.9 : Scenario relating spring and summer phytoplankton and the hypothetical annual cycle of krill suggested by Smetacek *et al.* (1990).

a.

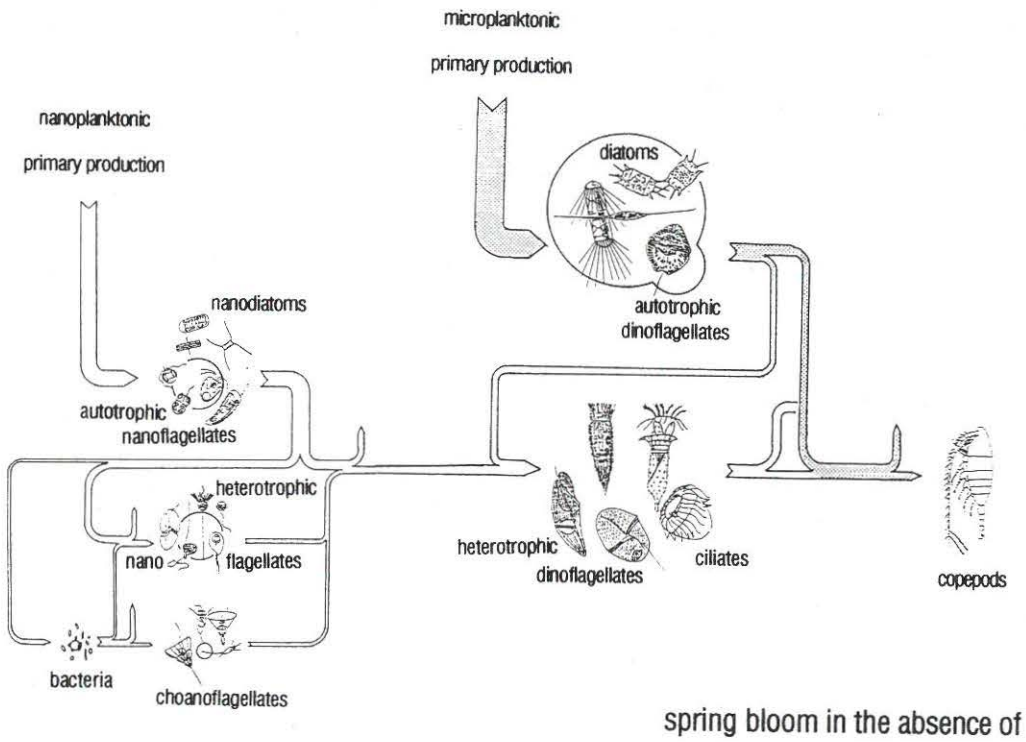

b.

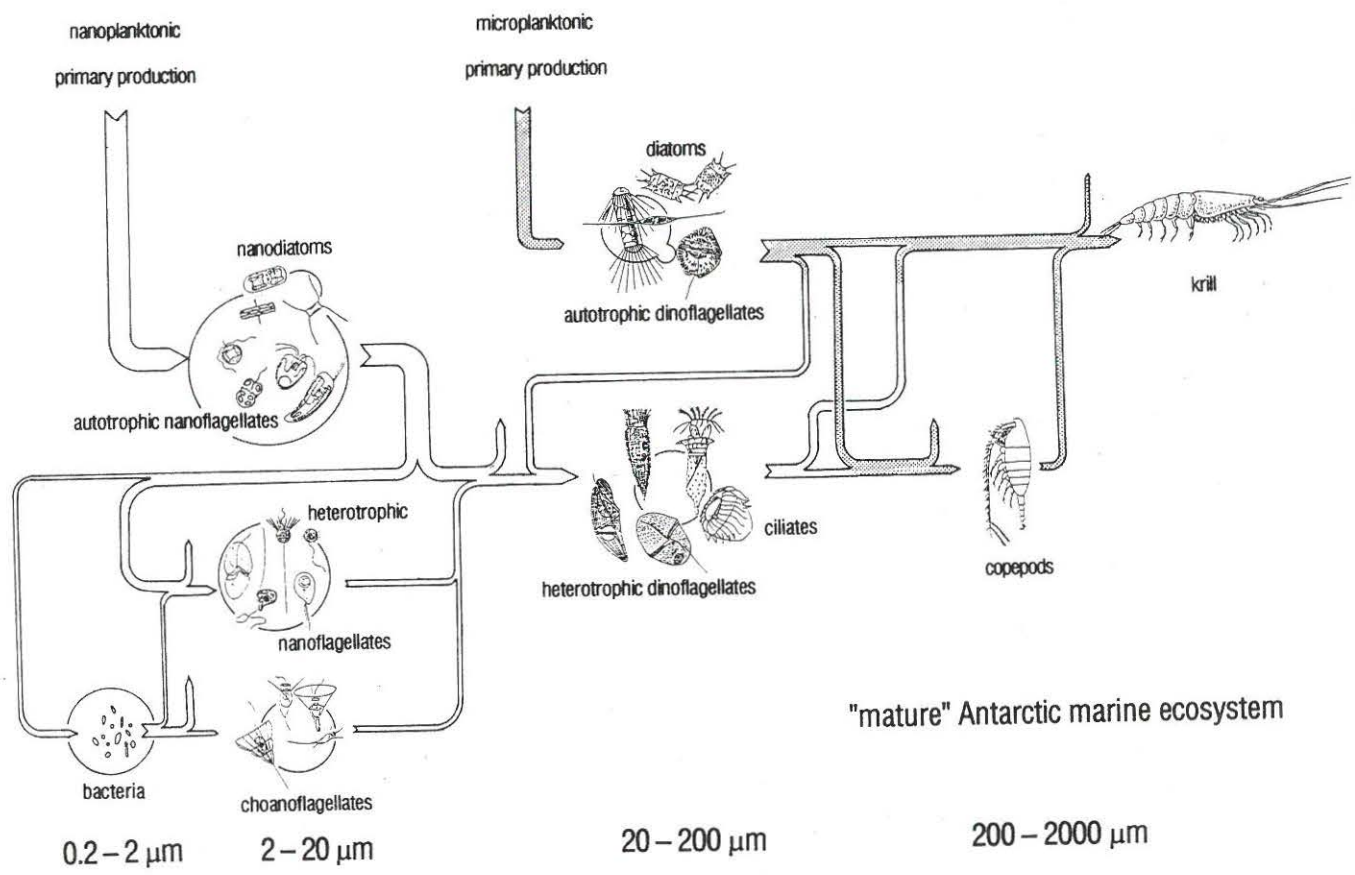

Figure 4.10 : Proposed structure of the Antarctic planktonic food web in the absence (a) and presence (b) of overwintering krill.

5. THE ECOLOGICAL MODEL : DESCRIPTION, FORMULATION AND PARAMETRIZATION

5.1. General structure of the ecological model

The general structure of the ecological model (Figure 5.1) has been established from the above analysis of the physical, chemical and biological events occurring in the marginal ice zone of the northwestern Weddell Sea at the time of ice melting. It is a two–layer 1D model composed of a well–mixed upper layer and a stratified deeper layer restricted to the euphotic depth (about 70 m in this area). No net horizontal advection is considered. This ecological model consists in a 1D hydrodynamical model calculating the thickness of the upper mixed layer from meteorological and ice cover observations coupled with a biological model composed of two submodules describing phytoplankton and microbial loop dynamics respectively. The model of phytoplankton growth calculates algal development using the output of the hydrodynamical model along with measured surface light as forcing variable, protozoan grazing as biological control and seeding as initial conditions. The model of microbial loop dynamics calculates bacterioplankton development using predicted temperature and dissolved organic matter calculated from predicted phytoplankton exudation and autolysis as forcing variables and grazing by small heteronanoflagellates as direct biological control. Both nitrate and ammonium are assimilated by phytoplankton whilst ammonium is occasionally taken up by bacteria according to the chemical composition of their substrates. Ammonium is regenerated through bacteria and bactivorous and herbivorous protozoan activity. Losses by sedimentation calculated from sediment trap data (Cadée, pers. com.) are neglected due to their generally low value (0.005 to 0.03 d^{-1}) compared to grazing (0.01 – 0.3 d^{-1}). Also trace elements, being not considered as limiting factor of phytoplankton development in this part of the circumpolar marginal ice zone (de Baar *et al.*, 1990; Buma *et al.*, 1991), are ignored by the model.

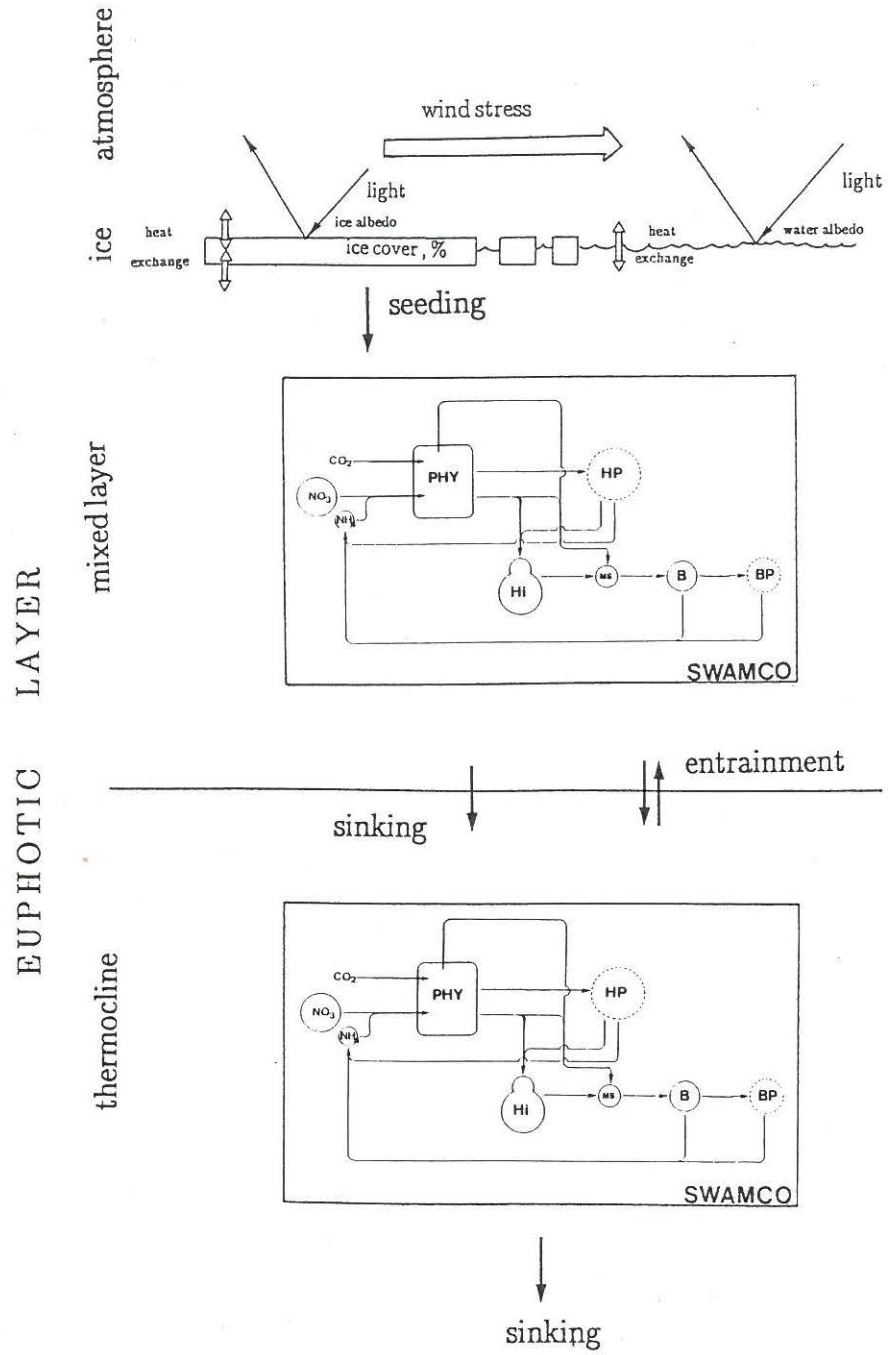

Figure 5.1 : Diagrammatic representation of the coupled hydrodynamical–biological model.

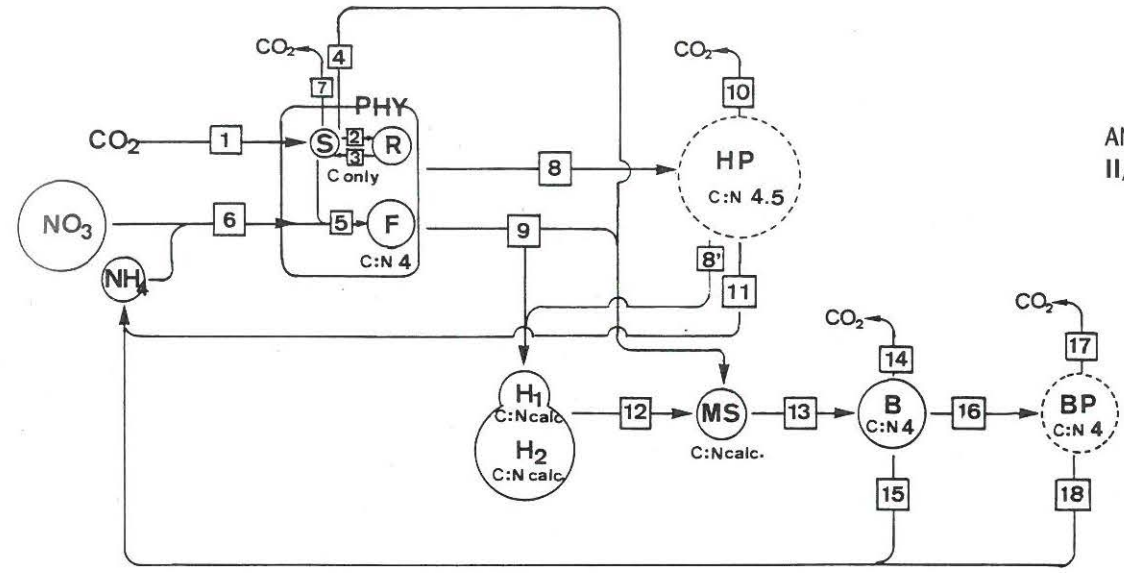

Figure 5.2 : Structure of the biological model SWAMCO. PHY = phytoplankton; HP = herbivorous protozoa; BP = bactivorous protozoa.

State variables :

NO_3	Nitrate ($\mu gN\ l^{-1}$)
NH_4	Ammonium ($\mu gN\ l^{-1}$)
F	Functional cellular constituants of phytoplankton ($\mu gC\ l^{-1}$); invariant nitrogen:carbon (w:w) ratio $NC_F = 0.28$
R	Cellular reserves of phytoplankton ($\mu gC\ l^{-1}$)
S	Small metabolites pool of phytoplankton ($\mu gC\ l^{-1}$)
MS	Dissolved organic matter of low molecular weight ($\mu gC\ l^{-1}$); variable nitrogen : carbon ratio
H_1	Dissolved organic matter of high molecular weight with high biodegradability affinity ($\mu gC\ l^{-1}$); variable nitrogen : carbon ratio
H_2	Dissolved organic matter of high molecular weight with low biodegradability affinity ($\mu gC\ l^{-1}$); variable nitrogen : carbon ration
B	Bacteria ($\mu gC\ l^{-1}$) invariant nitrogen : carbon (w:w) ratio $NC_B = 0.25$

Processes :

1	Phytopl. photosynthesis	10	Herbivorous protozoa (HP) respiration
2	Phytopl. reserve synthesis	11	Ammonium regeneration by HP
3	Phytopl.reserve catabolism	12	Exoenzymatic hydrolysis of H_1, H_2
4	Phytoplankton exudation	13	Uptake of monomeric substrates by bacteria
5	Phytoplankton growth	14	Bacteria respiration
6	Inorganic nitrogen uptake	15	Ammonium regeneration by bacteria
7	Phytoplankton respiration	16	Bactivorous protozoa (BP) grazing
8	Herbivorous protozoa (HP) grazing		
8'	Sloppy feeding	17	Bactivorous protozoa (BP) respiration
9	Phytoplankton autolysis	18	Ammonium regeneration by BP

The chemical and biological state variables of the model and the associated biological processes are described on Fig. 5.2. The differential equations describing changes in the main state variables of the model as the result of biological activity are gathered in table 5.1.

Table 5.I : Differential equations of the biological model (without considering its coupling with the physical model).

Phytoplankton :

$\frac{dF}{dt}$ = synthesis – grazing – autolysis

$\frac{dR}{dt}$ = synthesis – catabolism – grazing – autolysis

$\frac{dS}{dt}$ = synthesis – R&F synthesis + R catabolism – exudation – respiration – grazing – autolysis.

Microbial loop :

$\frac{dH_{1,2}}{dt}$ = R&F autolysis – $H_{1,2}$ exoenzymatic hydrolysis

$\frac{dMS}{dt}$ = $H_{1,2}$ exoenzymatic hydrolysis – bacteria uptake + phytoplankton exudation + sloppy feeding

$\frac{dB}{dt}$ = growth – mortality

Inorganic nitrogen loop :

$\frac{dNO_3}{dt}$ = – phytoplankton uptake

$\frac{dNH_4}{dt}$ = – phytoplankton uptake – bacteria uptake + bacteria regeneration + herbivorous protozoa regeneration + bactivorous protozoa regeneration

5.2. The physical model

The model consists of a 1D turbulent hydrodynamical model that calculates the thickness of the wind mixed layer from the balance between the kinetic turbulent energy induced by the wind and the buoyancy input by surface heating and ice melting from the top and entrainment of heavy water from below. This model is an adaptation to polar waters of the 1D mixed–layer model developed by Denman (1973) for the open area and extended by van Aken (1984) with terms describing salt fluxes. The principal attributes and the mathematical formulation have been described in details in Veth (1991).

5.3. The phytoplankton model

Concept: The model of phytoplankton development (AQUAPHY model) considers one single phytoplankton taxonomic group characterized by three state variables : the functional and structural cellular componants **F**, the internal reserves **R** and the monomers **S**. This model, based on the concept of energy storage theory developed by Cohen & Parnas (1976), was established in order to take into account the interaction between phytoplankton physiology and the turbulent structure of its habitat. It differs from most primary production models in that it explicitly distinguishes the photosynthetic process (*gross primary production*) – directly dependent on irradiance – from the process of phytoplankton growth (*net primary production*) – dependent on both ambient nutrient and energy availability related to the intracellular pool of storage products **R**. Cellular autolysis and protozoa grazing are the two phytoplankton mortality processes considered by the submodel.

Mathematical formulation : The following equations (see Fig. 5.2 and table 5.2 for symbols and units) are used for describing phytoplankton development :

$$\frac{dF}{dt} = sF - lF - gF \quad (1)$$

$$\frac{dS}{dt} = p - sR + cR - sF - e - r - lS - gS \quad (2)$$

$$\frac{dR}{dt} = sR - cR - lR - gR \quad (3)$$

In these equations :

. The rate of phytoplankton growth **sF** is assumed to depend – when non limited by inorganic nutrients – on the internal pool of monomeric carbon precursors **S** following a Michaelis–Menten kinetics characterized by the constants μF_{max} and Ks :

$$sF = \mu F_{max} \frac{S}{S + Ks} F \qquad (4)$$

. The photosynthetic process **p** depends on irradiance **I** following a relationship described by Platt *et al.* (1980); it is characterized by three parameters normalized to biomass, the maximal photosynthetic capacity k_{max}, the photosynthetic efficiency α and a description of the photoinhibition β :

$$p = k_{max} [1 - \exp(-\alpha I / k_{max})] \exp(-\beta I / k_{max}) F \qquad (5)$$

. The synthesis of storage products **sR** is governed by the size of **S** following a Michaelis–Menten kinetic characterized by the constants ϱmax and Ks :

$$sR = \varrho_{max} \frac{S'}{Ks + S'} F \qquad (6)$$

where $S' = \frac{S}{F} - Qs$

Qs being the monomers cellular quotat.

. The catabolism **cR** of storage products **R** is postulated to obey a first order kinetic characterized by the constant k_R :

$$cR = k_R R \qquad (7)$$

. The metabolic costs, in terms of a demand for ATP and reductors, are primarily met by cellular respiration **r**. This process is expressed by the sum of three terms, associated with maintenance processes, synthesis of new cellular material and motility respectively (Shuter, 1979) :

$$r = k_{1F} F + \xi \, sF + k_{2F} F \qquad (8)$$

where k_{1F} and k_{2F} are first order constant and ξ a dimensionless constant assumed to vary according to the inorganic nitrogen source.

. The exudation process **e** , the rate of cell autolysis **l** and the phytoplankton mortality by herbivorous protozoan grazing **g** are described by first order kinetics :

$$e = \varepsilon S \qquad (9)$$

$$lR = k_L R;\ lS = k_L S;\ lF = k_L F \qquad (10)$$

$$gR = k_G R;\ gS = k_G S;\ gF = k_G F \qquad (11)$$

in which ε, k_L and k_G are first order constants.

Parameters : The physiological parameters of phytoplankton photosynthesis and growth have been determined by mathematical fitting of the experimental data relative to the photosynthesis versus light curve and light–dark kinetics measurement using the above equations. One example is given by Fig. 5.3.

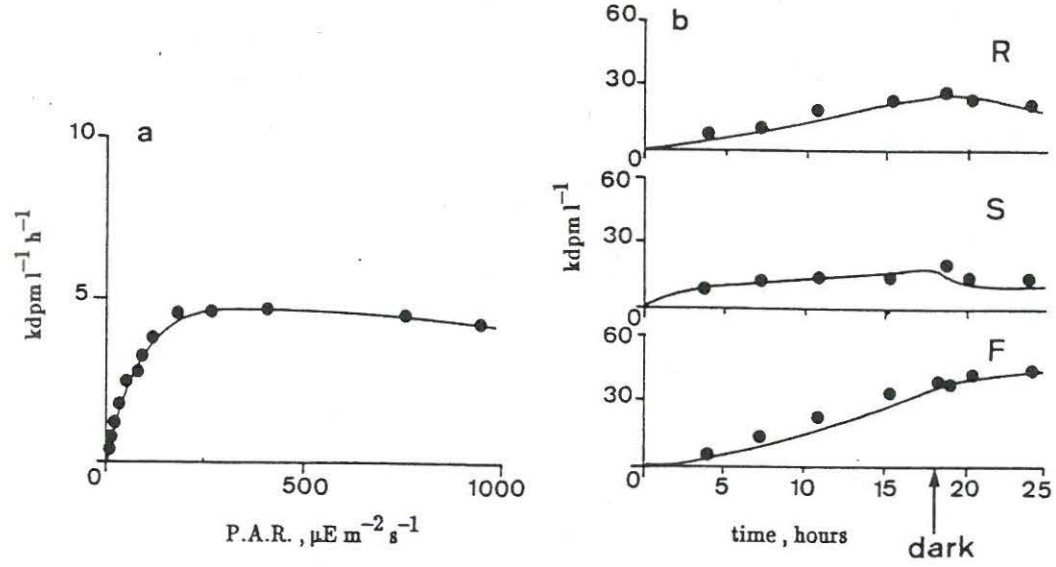

Figure 5.3 : Typical photosynthesis–light (a) and light–dark kinetics of ^{14}C assimilation into cellular constituants (b) of ice–edge phytoplankton communities of the northern Weddell Sea. Station 169, 61 30°S – 47°W.

Values were normalized to functional biomass considering a carbon/chlorophyll *a* ratio of 25 as characteristic of the *in situ* phytoplankton communities. Maximal photosynthetic capacity k_{max} (Fig. 5.5a), maximum specific growth rate μF_{max} (Fig. 5.5b) and the light adaptation parameter I_K (Fig. 5.4), derived from Platt *et al*'s equation vary within the range of those reported for antarctic phytoplankton (Tilzer *et al.*, 1986; Tilzer & Dubinsky, 1987). Our data combined with those similarly measured in the Prydz Bay area (Lancelot *et al.*, 1989) indicate however that the physiological parameters vary independently of temperature and available light (Fig. 5.4 and 5.5), suggesting that the dominant phytoplankton communities which succeed each other are the best adapted at each time to the environmental conditions. This long–term adaptation must be distinguished from the short–term dependence of photosynthetic activity on light and temperature described by Tilzer & Dubinsky (1987) which concerns only one single population at a given time. On basis of this, constant average values of physiological parameters (Table 5.2), characteristic of phytoplankton cells growing in the marginal ice zone of the Weddell Sea during spring 1988 have been chosen.

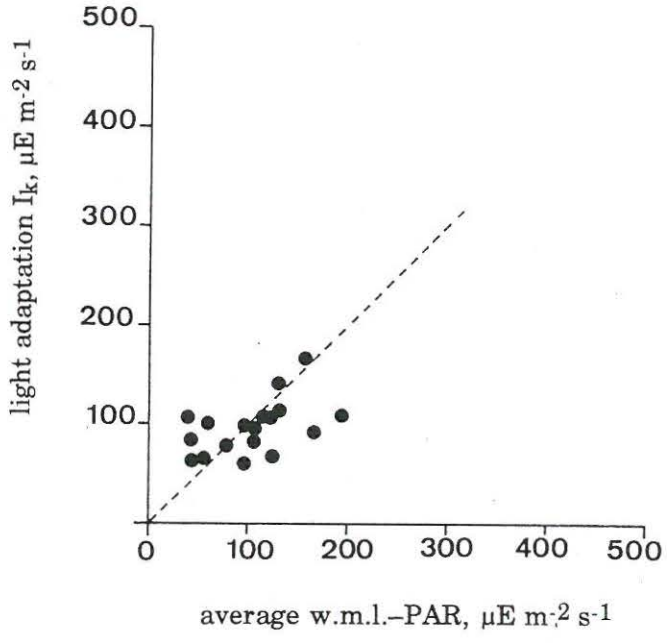

Figure 5.4 : Relationship between phytoplankton light adaptation I_K and average PAR in the upper mixed layer (dashed line shows 1/1 relationship).

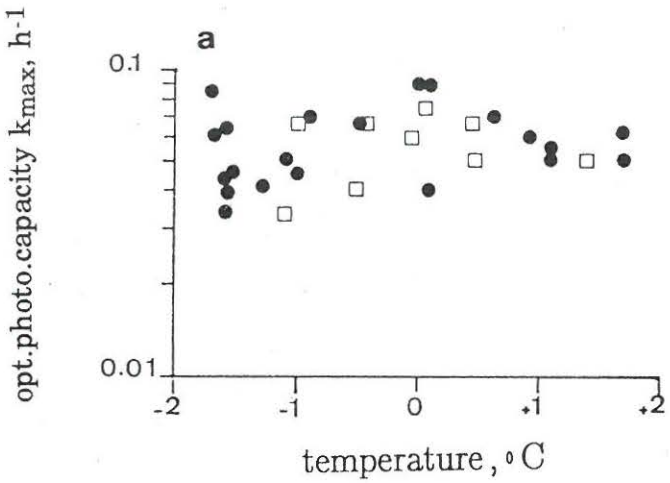

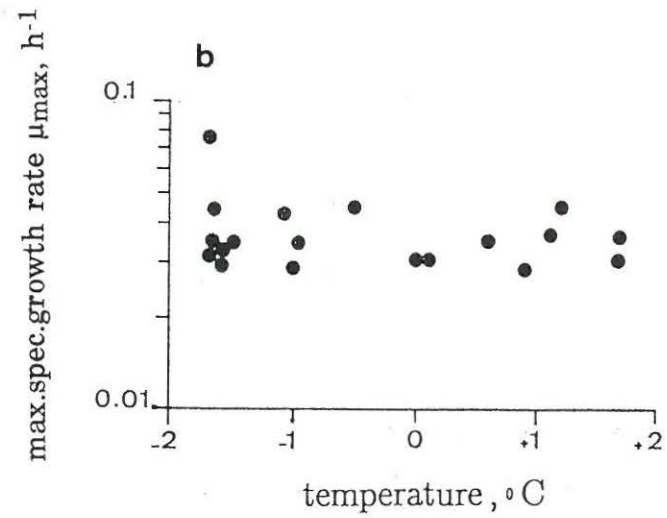

Figure 5.5 : Relationship between maximal photosynthetic capacity k_{max} (a) and maximum specific growth rate μF_{max} (b) and ambient temperature. (●): EPOS data; (□): Prydz Bay data (Lancelot *et al.*, 1989).

Phytoplankton cellular autolysis was assumed to be constant and proceeds at a rate of 0.002 h^{-1} according to Billen & Becquevort (1991). Herbivorous protozoan grazing has been considered as temperature dependent : the empirical linear regression relating specific grazing by herbivorous protozoa, as calculated from cell counts, to ambient temperature T is illustrated by Fig. 5.6. Its mathematical expression is the following :

$$k_G = 0.004\ T + 0.0075$$

For positive temperature however a constant rate of 0.01 h^{-1} was assumed.

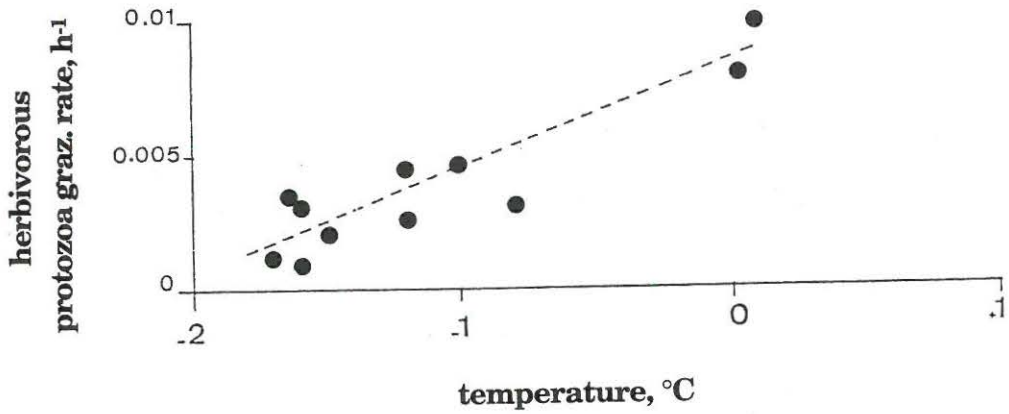

Figure 5.6 : Relationship between specific grazing rate of herbivorous protozoa on phytoplankton k_G and ambient temperature.

5.4. The microbial loop model

Concept : The model of microbial loop dynamics (HSB model, Billen & Servais, 1989) considers one single bacterioplankton group **B** (including both free–living and attached bacteria on particles and aggregates) and 3 pools of dissolved organic substrates (monomers **MS**, rapidly biodegradable polymers $\mathbf{H_1}$ and slowly biodegradable polymers $\mathbf{H_2}$) for bacterioplankton development. Basically, bacterial growth is directly dependent on the concentration of monomeric substrates whilst most of the dissolved organic matter is in the form of macromolecules requiring extracellular hydrolysis. The model thus implies that the latter process is the limiting step of the whole process of organic matter degradation and bacterial growth (for experimental evidence, see Billen, 1991). The overall process of bacterioplankton mortality results from autolysis and grazing pressure by bactivorous protozoa.

Mathematical formulation : The following set of equations (see table 5.2 for symbols and units) are used for describing microbial loop dynamics :

$$\frac{dH_1}{dt} = -eH_1 + Q\,(lR + lF + slpR + slpF) \quad (12)$$

$$\frac{dH_2}{dt} = -eH_2 + (1-Q)\,(lR + lF + slpR + slpF) \quad (13)$$

$$\frac{dMS}{dt} = eH_1 + eH_2 - uptMS + \varepsilon\, S \quad (14)$$

$$\frac{dB}{dt} = Y_B\ uptMS - mB \quad (15)$$

In these equations :

- The extracellular hydrolysis $\mathbf{eH_1}$ and $\mathbf{eH_2}$ of biopolymers H_1 and H_2 – proportional to bacterial biomass B (Fontigny *et al.*, 1987) – obeys a Michaelis–Menten kinetics (Somville & Billen, 1983; Somville, 1984) characterized by specific parameters – $e_i max$, K_{Hi} ($i = 1,2$) – owing to the different susceptibilities to extracellular hydrolysis of H_1 and H_2 :

$$eH_i = e_i max \frac{H_i}{K_{Hi} + H_i} B \quad (16)$$

  Where $i = 1, 2$.

- Q is the part allocated to H_1 of macromolecules produced by phytoplankton autolysis and by sloppy feeding of herbivorous protozoa.

. The sloppy feeding **slP** is assumed to represent a constant fraction J of herbivorous protozoa grazing.

. The uptake of direct substrates **uptSM** is assumed to obey an overall Michaelis–Menten kinetics (Parsons & Strickland, 1962; Wright & Hobbie, 1965) :

$$uptMS = b_{max} \frac{MS}{K_{MS} + MS} B \qquad (17)$$

where b_{max} and K_{MS} are the maximum rate and half–saturation constant of substrate uptake by bacteria.

. A constant fraction Y_B of the amount of substrates taken up is used for biomass production, the remaining part being respired (Servais, 1986).

. The process of bacterial mortality **mB** is represented, as a first approximation, by a first order kinetics, characterized by the constant k_{BM} :

$$mB = k_{BM} B \qquad (18)$$

Parameters : Most of the parameters involved in these equations have been determined from experiments conducted in the Weddell Sea (this study) and Prydz Bay area (Billen & Becquevort, 1991) :

. The maximum uptake rate of MS by bacteria b_{max} is calculated as $\mu B_{max}/Y_B$. The maximum specific growth rate of bacteria μB_{max} (Fig. 5.7) clearly indicates suboptimal bacterial growth at temperature characteristic of the Southern Ocean (–2 to +2°C). Interestingly, this physiological response of bacteria to cold temperature strongly contrasts with phytoplankton cells that exhibit similar maximum specific growth rate in the Southern Ocean as in lower latitudes. The temperature dependency of μB_{max} (Fig. 5.7) is described by the following sigmoid relationship :

$$\mu B_{max} = \mu' B_{max}\,(T_{opt})\ [0.1 + 0.9 \exp\,(-(\frac{T_{opt}-T}{dt})^2)\,]$$

with $\mu' B_{max}$ = μB_{max} value at optimal temperature (h^{-1}) i.e. 0.18 h^{-1}
T = ambient temperature (° C)
T_{opt} = optimal temperature (° C) i.e. 18° C
dt = sigmoid width (° C) i.e. 7° C

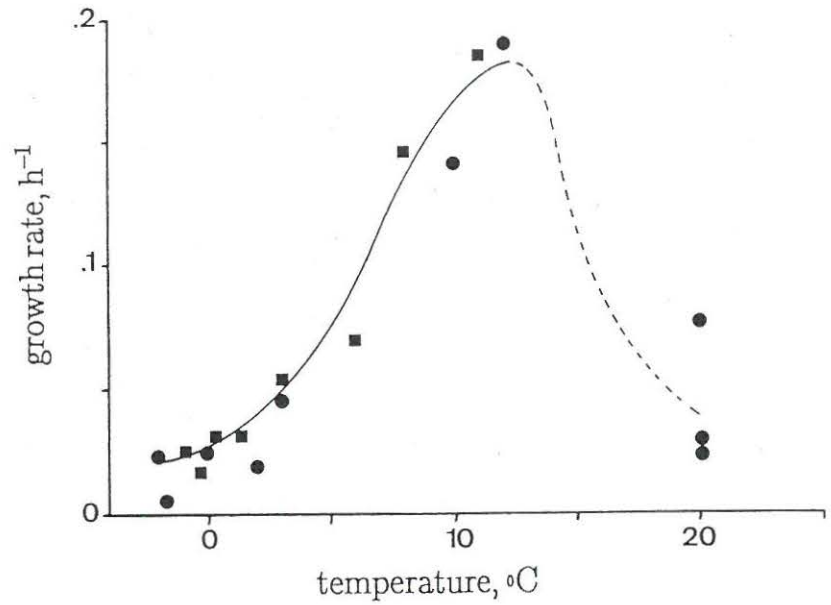

Figure 5.7 : Relationship between the maximum specific growth rate of bacteria μB_{max} and ambient temperature in the Weddell Sea (▪) and in the Prydz Bay (●).

. The value of Y_B, in the absence of nutrient limitation, is generally close to 0.3 Servais *et al.*, 1987). K_{MS} is taken arbitrarily as 0.01 mgC.l^{-1}, as this parameter does not significantly influence the results of the calculations.

. The parameters characterizing the rate of exoenzymatic hydrolysis of macro–molecules from phytoplanktonic origin have been estimated on the basis of experiments in which the kinetics of bacterial degradation of a sonicated and filtered algal culture is measured after inoculation with a natural assemblage of bacteria (Servais, 1986; Billen, 1991). The same dependence to temperature (T) as described above for μB_{max} has been considered for e_{1max} and e_{2max}.

$$e_1'_{max} = 0.75\ h^{-1}, \quad K_{H_1} = 0.1\ mgC.l^{-1}$$
$$e_2'_{max} = 0.25\ h^{-1}, \quad K_{H_2} = 2.5\ mgC.l^{-1}$$

. Measured rates of total bacterial mortality k_{BM} at *in situ* temperature vary between 0.002 and 0.005 h^{-1} (Fig. 5.8) with grazing by bactivorous protozoa (size less than 7 µm) contributing for 22 to 100 % (Becquevort *et al.*, 1992). The following empirical linear regression relating specific mortality rate of bacteria to temperature T (Fig. 5.8) has been observed :

$$k_{BM} = 0.0005\,T + 0.004$$

. The rate of H_i production through phytoplankton autolysis or protozoan sloppy feeding are the only adjustable parameters of the model. The former process was estimated to proceed at a rate of 0.002 h^{-1} whilst sloppy feeding by herbivorous protozoa was assumed to represent 10 % of the temperature–dependent grazing of herbivorous protozoa (Fig. 5.6). The model assumes in addition that the biopoly–mers of two classes of biodegradability (H_1, H_2) are produced in a ratio 1:1 i.e., $Q = 0.5$.

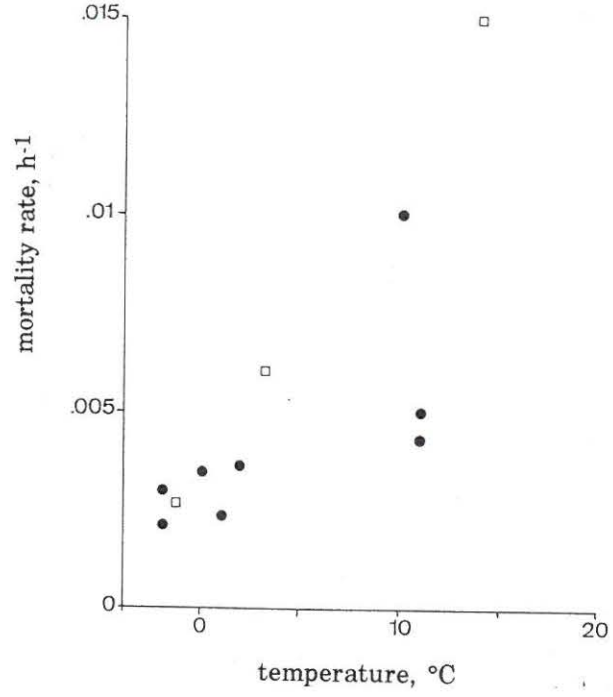

Figure 5.8 : Relationship between the specific mortality rate of bacteria and ambient temperature for natural assemblages. Weddell Sea (●) and Prydz Bay (□).

5.5. The inorganic nitrogen loop

Assumptions : Nitrate and ammonium are the inorganic nutrients considered by the model. Both nutrients, but ammonium preferably, are taken up by phytoplanktonic cells and assimilated into the functional constituents F (other phytoplankton constituents R and S are composed of carbon solely). Ammonium can be occasionally taken up by bacteria according to the nitrogen:carbon ratio of their substrate. Remineralized ammonium is released by bacteria, and bactivorous and herbivorous protozoa as product of their metabolism. The quantitative importance of this regenerating processes is determined by the theoretical nitrogen:carbon ratio of these microorganisms in comparison with the nitrogen:carbon ratio of their respective substrate or food. Nitrification (biological oxidation of ammonium in nitrate), due to the lack of informations on the importance of this microbial process in the Southern Ocean, is neglected.

Mathematical formulation : On this basis, the following equations are used to describe the inorganic nitrogen loop :

$$\frac{dNO_3}{dt} = (-sF\,NC_F)\,(1 - f_{NH_4}) \qquad (19)$$

$$\frac{dNH_4}{dt} = (-sF\,NC_F)\,f_{NH_4} + uptMS\,(NC_{MS} - Y_B\,NC_B) + mB\,(NC_B - Y_{BP}\,NC_{BP}) + (1-J)\,gF\,(NC_F - Y_{HP}\,NC_{HP}) \qquad (20)$$

In these equations :

. NC_F , NC_{MS} , NC_B, NC_{BP}, NC_{HP} are the nitrogen:carbon (w:w) ratios of phytoplankton functional macromolecules, monomeric substrates, bacteria, bactivo –rous and herbivorous protozoa respectively.

. f_{NH_4} is the ratio of phytoplankton ammonium uptake to total inorganic nitrogen uptake.

. Y_B , Y_{HF} , Y_{BP} are the growth efficiencies of bacteria, bactivorous and herbivorous protozoa respectively.

Parameters : All parameters, except the nitrogen:carbon ratio of microorganisms for which theoretical values were chosen, have been determined experimentally :

. Allocation of nitrogen uptake between NO_3 and NH_4 is calculated at any time by the model according to the empirical relationship relating the f_{NH_4} ratio to the relative ambient ammonium concentration (Fig. 5.9). This relationship has been established

from $^{15}NO_3$ and $^{15}NH_4$ uptake data performed during the EPOS expedition (Goeyens *et al.*, 1991a,b) and is mathematically described as follows :

$$f_{NH_4} = \gamma \frac{NH_4}{N_{tot}} + (1-\gamma) \frac{NH_4}{N_{tot}}^{\delta}$$

with $\gamma = -0.21$; $\delta = 0.24$

. Invariable NCF , NCB, NCBP, NCHP ratios of respectively 0.28, 0.25, 0.22 and 0.22 are considered whilst NCMS is calculated at any time by the model.

. The value of 0.38 was estimated for protozoa growth efficiency YBP , YHP on the basis of microcosm experiments conducted under controlled conditions (Björnsen & Kuparinen, 1991).

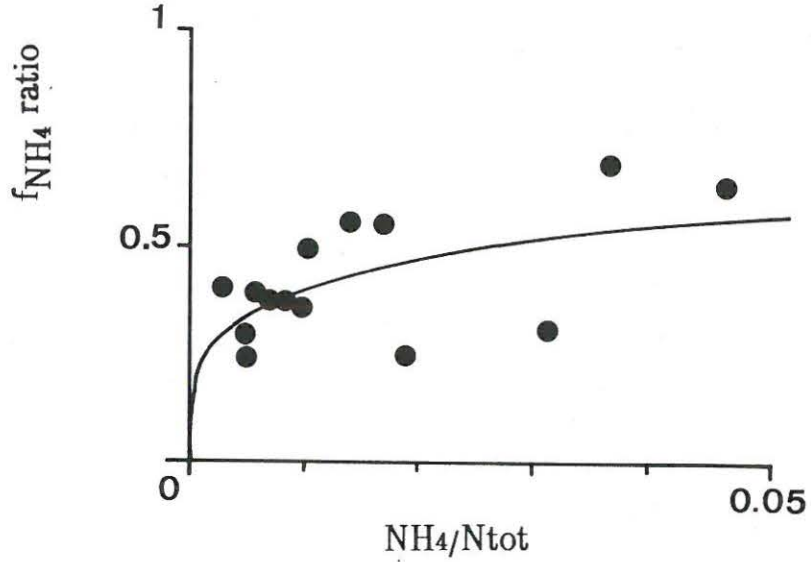

Figure 5.9 : Relationship between relative ammonium uptake by phytoplankton and relative ambient ammonium concentration.

Table 5.II : (part 1) Physiological parameters characterizing ice–edge microbial communities.

Parameters		Units
Phytoplankton :		
Photosynthetic efficiency (α)	0.00065	$h^{-1} (\mu E\ m^{-2}\ sec^{-1})^{-1}$
Optimal specific rate of photosynthesis (k_{max})	0.06	h^{-1}
Index of photoinhibition (β)	0	$h^{-1} (\mu E\ m^{-2}\ sec^{-1})^{-1}$
Maximal specific rate of R synthesis (ρmax)	0.06	h^{-1}
Constant of R catabolism (kR)	0.06	h^{-1}
Maximal specific rate of F synthesis (μF_{max})	0.035	h^{-1}
Half–saturation constant of S assimilation (KS)	0.07	dimensionless
Cst of maintenance of basal metabolism (k_1F)	0.0005	h^{-1}
Energetic costs for F synthesis (ξ) :		
ammonium source :	0.32	dimensionless
nitrate source :	0.70	dimensionless
Constant of motility (k_2F)	0.0006	h^{-1}
Constant of exudation (ϵ)	0.005	h^{-1}
Constant of cell autolysis (kL)	0.002	h^{-1}
Herbivorous protozoa :		
Constant of grazing (kG) temperature (T) dependent : kG = 0.0086 + 0.004 T		h^{-1}
Growth efficiency (YHP)	0.38	dimensionless
Constant of sloppy feeding (J)	0.10	dimensionless

Table 5.II : (part 2) Physiological parameters characterizing ice–edge microbial communities.

Parameters		Units
Microbial loop :		
Maximal specific growth rate of bacteria at optimal temperature (μB_{max})	0.18	h^{-1}
Half–saturation constant of MS uptake (K_{MS})	0.01	mgC l^{-1}
Maximal specific rate of H_1 hydrolyse e_{1max} at optimal temperature ($e_1'_{max}$)	0.75	h^{-1}
Half–saturation constant of H_1 hydrolysis (K_{H_1})	0.1	mgC l^{-1}
Maximal specific rate of H_2 hydrolysis e_{2max} at optimal temperature ($e_2'_{max}$)	0.25	h^{-1}
Half–saturation constant of H_2 hydrolysis (K_{H_2})	2.5	mgC l^{-1}
Constant of bacterial mortality (k_{BM}) temperature dependent : $k_{BM} = 0.0005\ T + 0.0004$		h^{-1}
Growth efficiency of bacteria (Y_B)	0.3	dimensionless
Growth efficiency of bactivorous protozoa (Y_{BP})	0.38	dimensionless

6. MODEL RESULTS

6.1. Validation : the particular case of the northwestern Weddell Sea

6.1.1. Calculation

The ecological model described in the previous section was run for latitudes 57°S to 62°S at meridian 49°W to simulate spring variations of inorganic nitrogen (nitrate and ammonium), phytoplankton, dissolved organic carbon and nitrogen (monomeric and polymeric) and bacteria concentrations in the marginal ice zone of the Scotia/ Weddell Sea area during sea ice retreat 1988. The simulated period covered the EPOS expedition legs 1 & 2.

Local meteorological conditions (wind speed and solar radiation; Fig. 6.1), recorded incident P.A.R. and ice cover observations (van Franeker, 1989) are the forcing variables of the coupled physical–biological model. Initial values of the state variables (Table 6.I) are the concentrations measured at the very beginning of the cruise, i.e. when the ice melting process has not yet started. For phytoplankton, an initial Chl *a* concentration of 0.12 µg l^{-1} was considered, corresponding to the addition of a seeding value of 0.05 µg Chl *a* l^{-1} to a winter water column value of 0.07 (see Fig. 3.4).

Concentrations of the state variables were calculated at each half–degree of latitude in the area between 58 and 62°S during the 70 day–ice retreat period, by integration of equations 1–20 on the variations of light and temperature with time and on the depth up to the depth of the euphotic layer. The light absorption in the water column was assumed to obey the Beer–Lambert's law. The vertical light attenuation coefficient $\mathbf{K_e}$ was calculated by the model from predicted chlorophyll a concentration according to the empirical relationship described in Lancelot *et al.*(1991a) :

$$K_e = 0.054\ \text{Chl}\ a + 0.072$$

A two layer biological model was considered consisting of a homogeneous upper layer in which mixing was instantaneous and a stratified water column. Vertical and temporal step were 0.5m and 1h. Hourly values of the wind mixed layer depth and of temperature are provided by the physical model.

Table 6.I : Modelling the microbial network in the northwestern Weddell Sea : initial concentrations of the state variables.

State variables	Concentrations	Units
Inorganic nitrogen :		
NH_4	0.02	µM
NO_3	31.5	µM
Phytoplankton :		
Chlorophyll *a*	0.12	µg l^{-1}
F	4	µgC l^{-1}
R	0.7	µgC l^{-1}
S	0.3	µgC l^{-1}
Dissolved organic matter :		
MS	2.5	µgC l^{-1}
H_1	5	µgC l^{-1}
H_2	200	µgC l^{-1}
Bacteria :		
B	1	µgC l^{-1}

6.1.2. Temporal variations

As an illustration of the physical, chemical and biological phenomenon operating within the marginal ice zone at the time of ice melting, Fig. 6.1–6.7 show temporal evolution of predicted physical, chemical and biological state variables and associated transformations or processes at latitude 59 30⁰ S during spring 1988. The 70–day simulated period at this latitude covers the whole ice melting process as well as a one–month ice–free period (Fig. 6.1) and thus well illustrates the entire sea ice retreat phenomenon, including the remnant effect of ice melting on the stability of ice–free surface waters (Veth *et al.*, 1992).

As a general trend, reasonable agreement is found between predictions and observations.

Short–term extreme wind fluctuations between 2 and 17 m s^{-1} (as compared to an average value of 8 m s^{-1}) succeeded each other during the studied period at the given latitude (Fig. 6.1c). Solar radiation fluctuated similarly, giving rise to periods of sunny

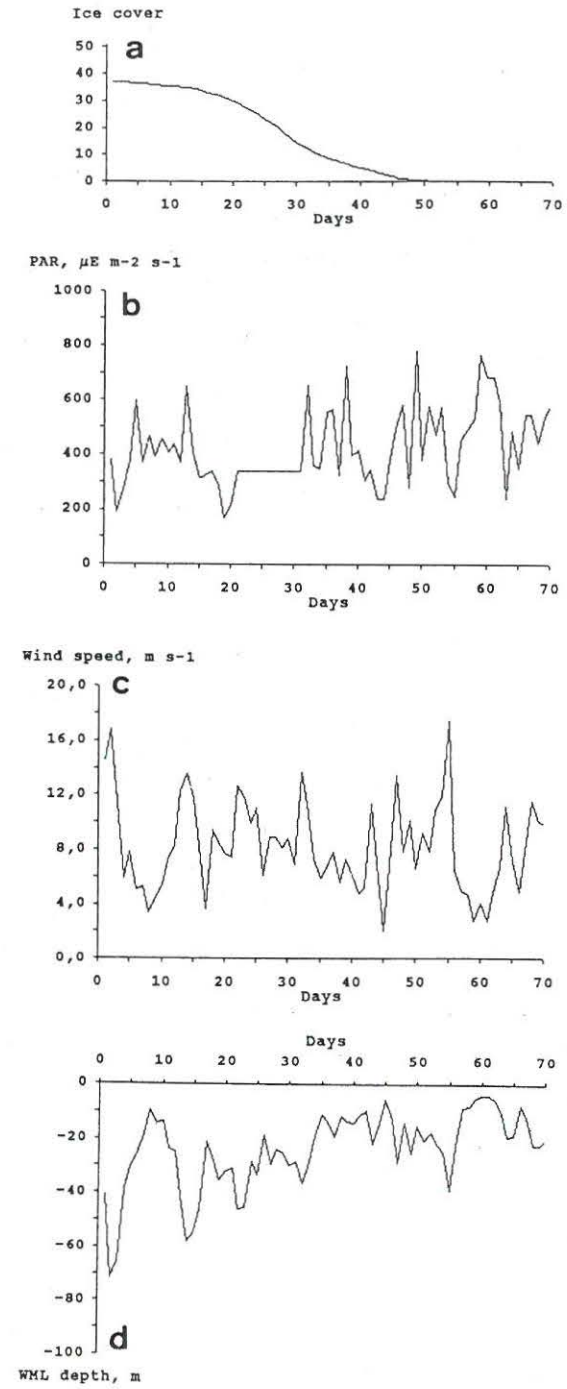

Figure 6.1 : Ice cover (a), global radiation (b), wind speed (c) and predicted upper mixed layer (d) at latitude 59 30⁰ S during spring 1988.

days with low wind, or reversely, cloudy days with high wind. This has dramatical influence on the predicted depth of the upper mixed layer, which directly responds to diurnal fluctuations of wind speed and solar radiation (Fig. 6.1d), by varying between 4 and 70 m. The frequency, duration and strength of mixing events were particularly important during the ice–covered period characterized by an alternance of short–term shallow upper mixed layer (5 to 30 m) and deep vertical mixing (deeper than 50 m). Due to the high–friction coefficient of ice, the layer affected by transient wind events was on an average deeper within the ice covered period (70 m) than after ice melting (38 m), thus reducing to very low level the light available to phytoplankton circulating in upper layers covered by ice.

The key role played by vertical stability and ice cover in the onset of phytoplankton ice–edge development is evidenced by Fig. 6.2 and 6.3. The control of phytoplankton activity by surface light availaibility, on the one hand, is clearly shown on Fig. 6.2 which presents simulations of daily integrated photosynthesis and net primary production (Fig. 6.2b), and nitrate cumulative uptake by phytoplankton (Fig. 6.2c) when ice retreats from 40 % to 0 %. Predicted average net primary production is shown to vary between 200 (range : 50 – 300) and 750 (range : 400 – 1500) mgC m^{-2} d^{-1}, characteristic of high (> 20 %) and weak (< 20 %) ice coverage respectively, in agreement with previous field data in the marginal ice zone of the Weddell Sea (Smith & Nelson, 1986). Accordingly, cumulative nitrate uptake by phytoplankton increases exponentially at ice cover less than 20 % (Fig.6.2c).

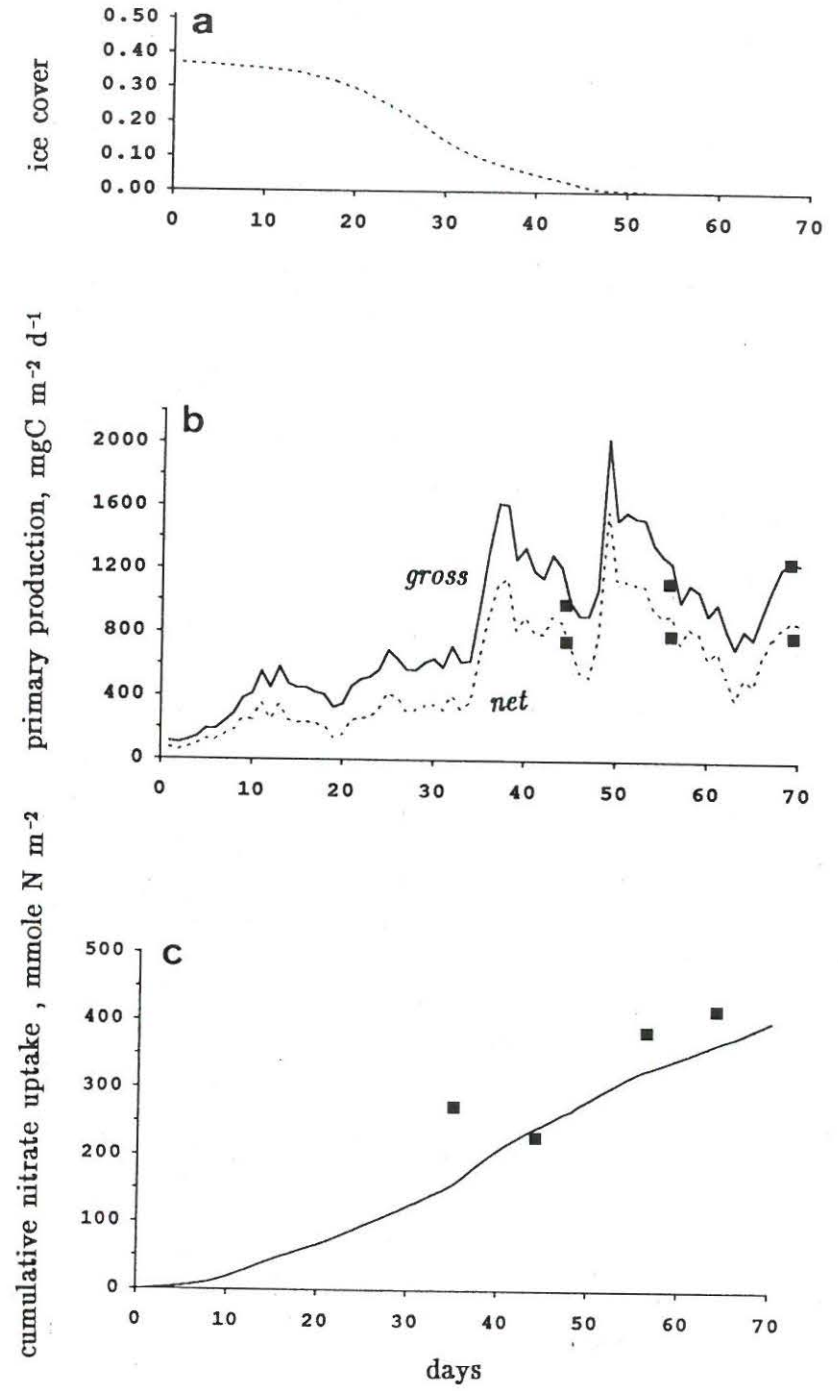

Figure 6.2 : Ice cover (a), predicted (lines) and measured (▪) primary production (b) and cumulative nitrate uptake by phytoplankton (c) at latitude 59 30^0 S during spring 1988.

The additional influence of water column stability, on the other hand, can be seen on Fig. 6.3 showing the calculated variation of chlorophyll *a* concentration in the upper mixed layer during the same period. This simulation clearly suggests that vertical stability and ice cover less than 20 % are the conditions for the onset of an ice–edge phytoplankton bloom.

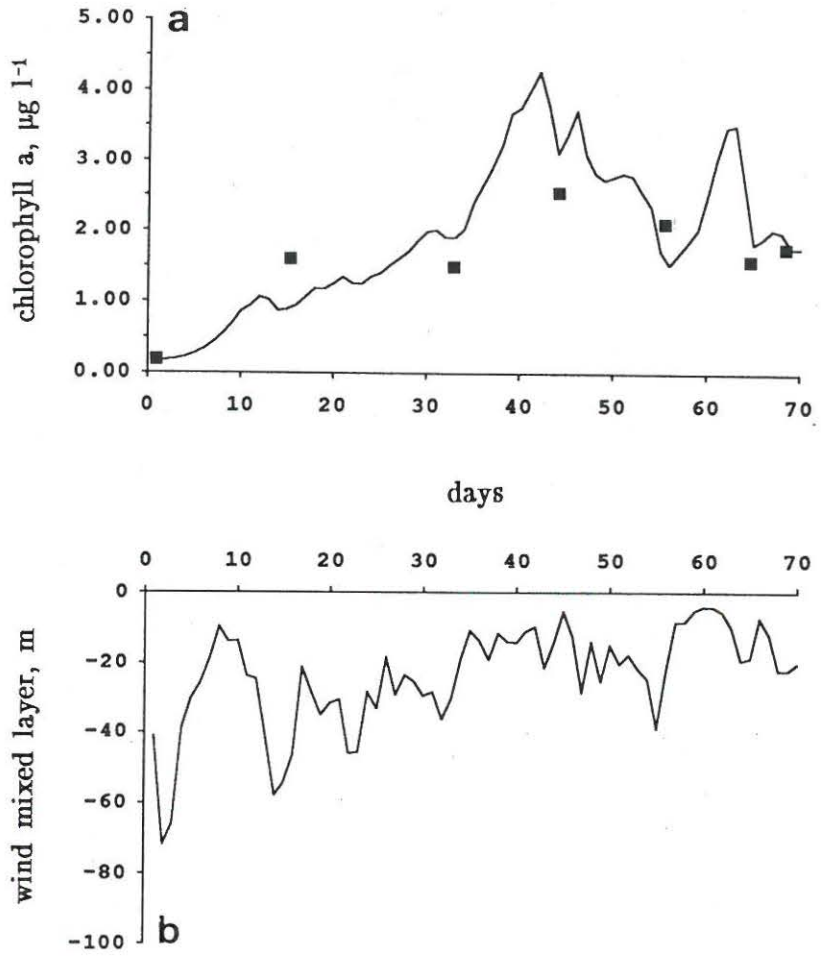

Figure 6.3 : Predicted (line) and observed (▬) chlorophyll *a* concentrations in the upper mixed layer (a), and upper wind mixed layer depth (b) at latitude 59 30⁰ S during spring 1988.

The role played by protozoa grazing pressure on the control of ice–edge bloom magnitude and duration is evidenced by Fig. 6.4 that compares predicted net primary production and grazing pressure by herbivorous protozoa. Due to seawater temperature increase following ice melting and the concomitant increase of food ressources, predicted grazing pressure reaches daily values close to or even higher than phytoplankton growth. In this latter case, an additional food resource supplied by bacteria and bactivorous protozoa is thus required to sustain growth of herbivorous protozoa as shown by experimental data (section 4).

Accordingly, predicted bacterial daily production and biomass (Fig.6.5), whilst remaining at very low levels during the whole ice covered period, reach high values of 120 mgC m^{-2} d^{-1} and 20 µgC l^{-1} respectively after the ice melting process. However, contrasting with grazing pressure of herbivorous protozoa that directly responds to phytoplankton biomass increase (Fig.6.4), a 20 day–delay between the peaks of phytoplankton and bacteria biomass is predicted by the model.

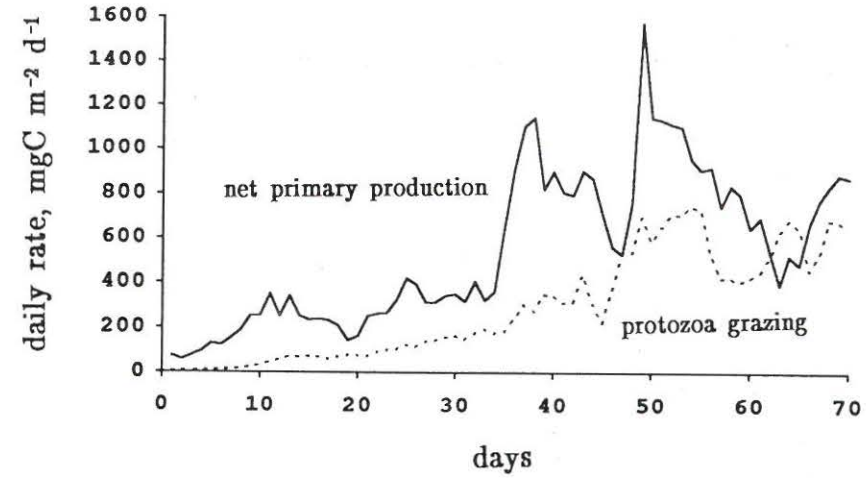

Figure 6.4 : Predicted daily primary production (solid line) and daily rates of protozoan grazing (dashed line) at latitude 59 30⁰ S during spring 1988.

Predicted ammonium concentration (Fig.6.6a), as a result of microheterotrophic activity (bacteria, bactivorous and herbivorous protozoa) (Fig.6.7a), reaches concentrations higher than 1 µM after ice retreat. These elevated ammonium levels significantly reduce nitrate uptake by phytoplankton at the end of the simulated period (Fig.6.2c) as a consequence of phytoplankton preference for ammonium. This has dramatic influence on f_{NO_3} ratio which decreases from 0.90 to 0.44 (Fig.6.6b), consistent with the observation that, in this area, the ice retreat phenomenon is accompanied by a shift from a dominant new production system towards a regenerated one.

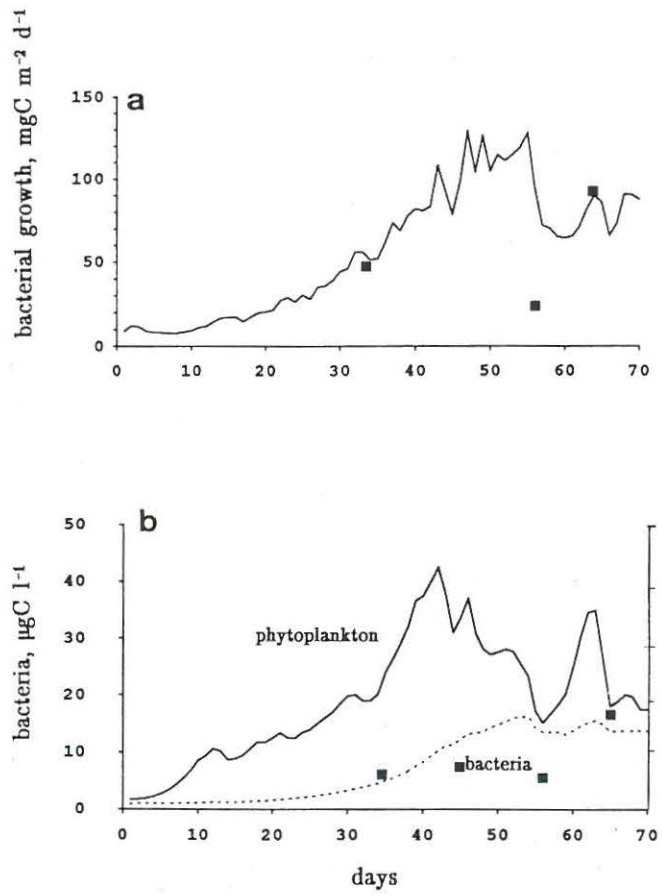

Figure 6.5 : Predicted (solid line) and measured (▪) bacterial production (a), and predicted (dashed line) and measured (▪) bacterial biomass compared with predicted phytoplanktonic biomass (solid line) (b) at latitude 59 30⁰ S during spring 1988.

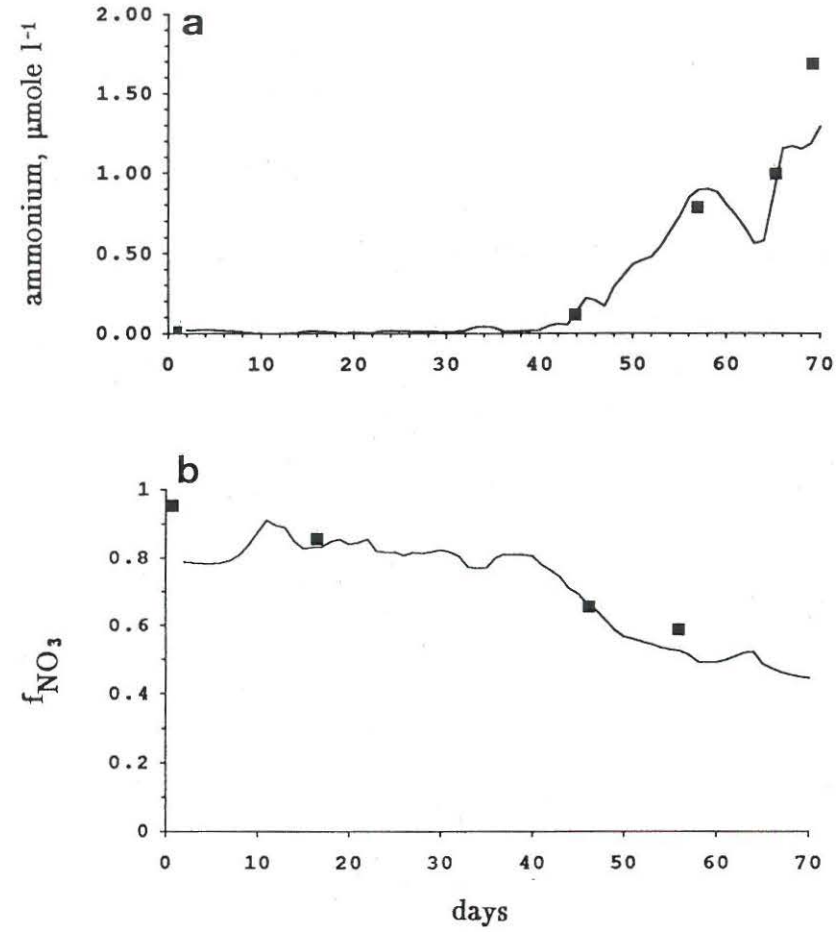

Figure 6.6 : Predicted (solid line) and measured (▪) ammonium concentration (a) and fNO_3 ratio (b) in the upper mixed layer at latitude 59 30⁰ S during spring 1988.

The respective role of herbivorous protozoa and bacteria in regenerating ammonia, illustrated by Fig. 6.7a, evidences the predominance of the former microorganisms during sea ice melting. After this period, however, predicted ammonium regeneration rate by bacteria due to bacterial activity reaches values close to that by herbivorous protozoa. Interestingly, the model predicts that ammonium regeneration through the only herbivorous protozoan activity could sustain almost entirely phytoplankton ammonium demand (Fig.6.7b). Predicted and observed accumulation of ammonium (Fig.6.6a) result therefore from the increase of bacterial activity following the decline of the phytoplankton ice–edge bloom.

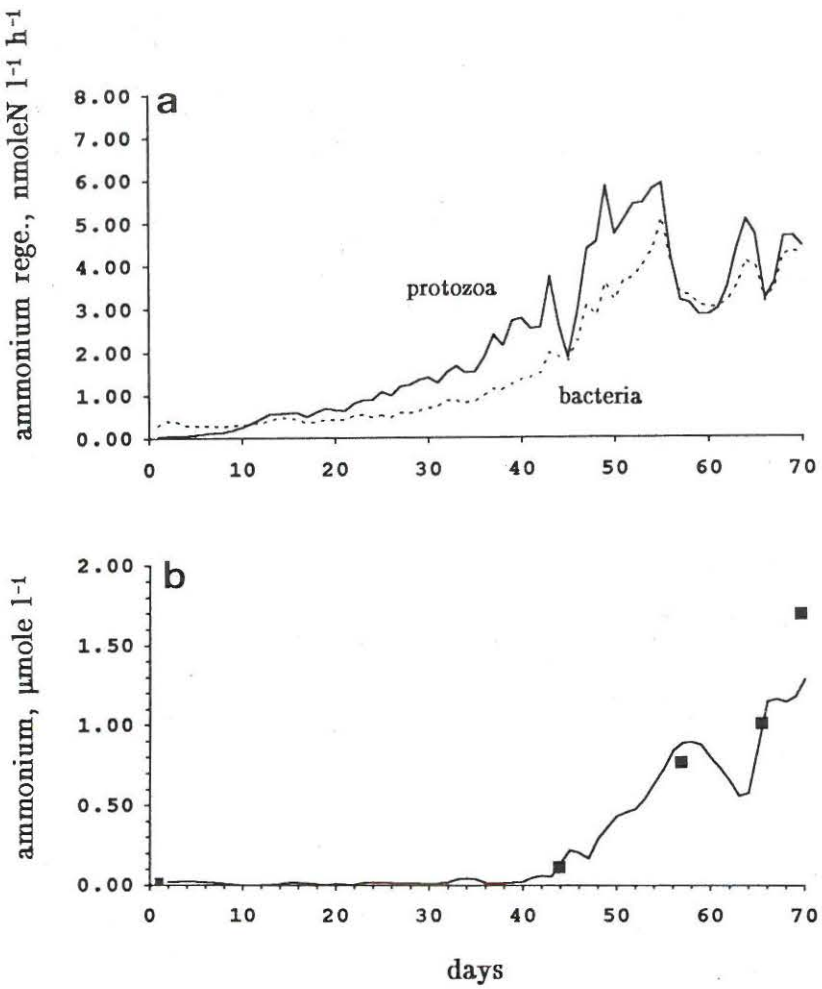

Figure 6.7 : Predicted (lines) and calculated (▪) ammonium regeneration rates through bacterial and herbivorous protozoan activity (a) and ammonium concentration (b) at latitude 59 30⁰ S during spring 1988.

6.1.2. Spatio–temporal variations

The spatio–temporal variation of chlorophyll *a* (Fig.6.8a), bacteria (Fig.6.8b) and ammonium (Fig.6.8c) concentrations and nitrate depletion (Fig.6.8d), predicted during the sea ice retreat was drawn from model runs performed at each half–degree of latitude between 59 and 62⁰ S. Agreement between prediction and observation is reasonably good excepted for bacterial biomass which predicted values in the recently ice–free area are significantly higher than observations.

For other variables, both the magnitude and the location of maxima at the ice–edge position and/or in the 100 km–band seawards from the ice–edge are well simulated. In particular the southward shift of maximum concentrations and biological activities with the receding ice–edge is clearly apparent from model simulations (Fig.6.8).

At one occasion however (Fig.6.8a; lat.60⁰S, 20–24 Dec.), a strong discrepancy exists between predicted and measured chlorophyll *a* which is likely the consequence of a krill passage not taken into account by the model.

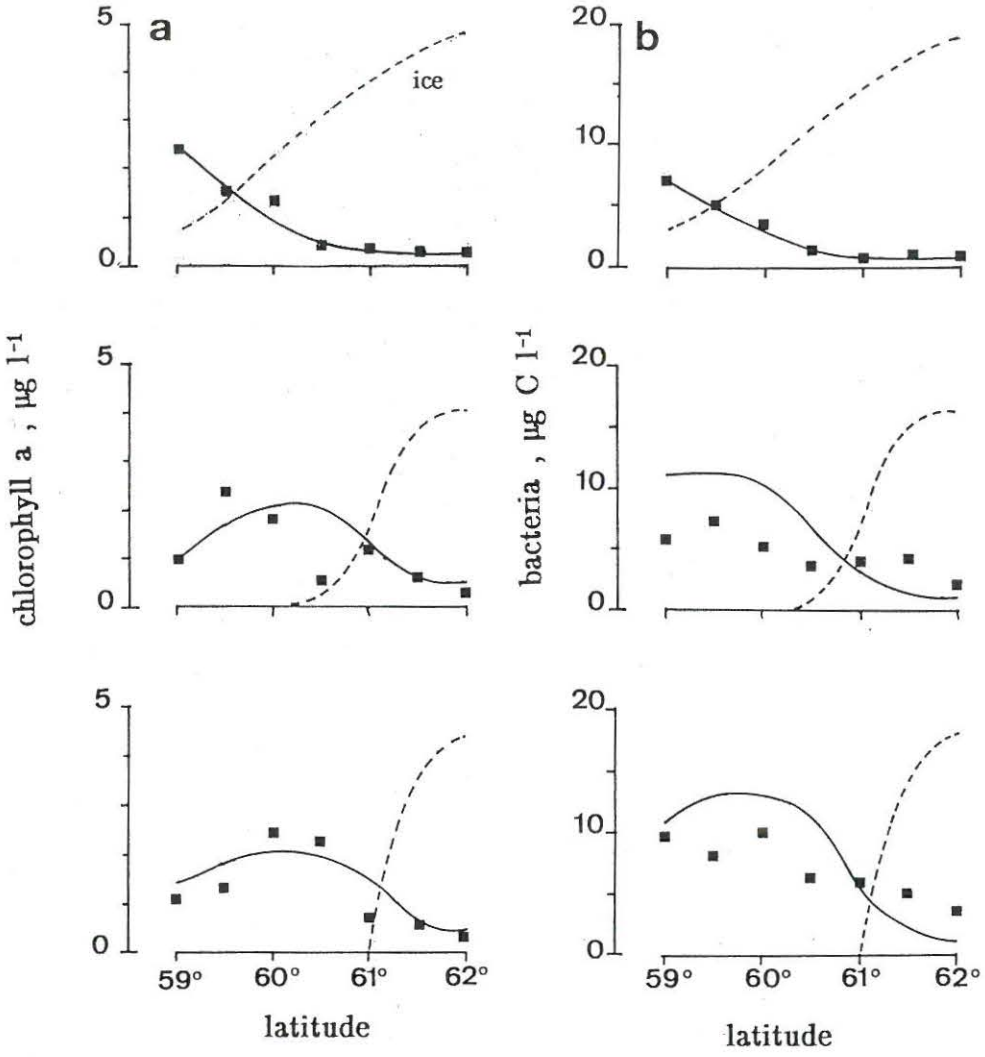

Figure 6.8ab : Predicted (solid line) and observed (▪) spatio–temporal variations of chlorophyll *a* (a) and bacterial (b) concentrations in the upper mixer layer in the northwestern Weddell Sea during sea ice retreat 1988. Ice retreat is represented on each graph as a dashed line.

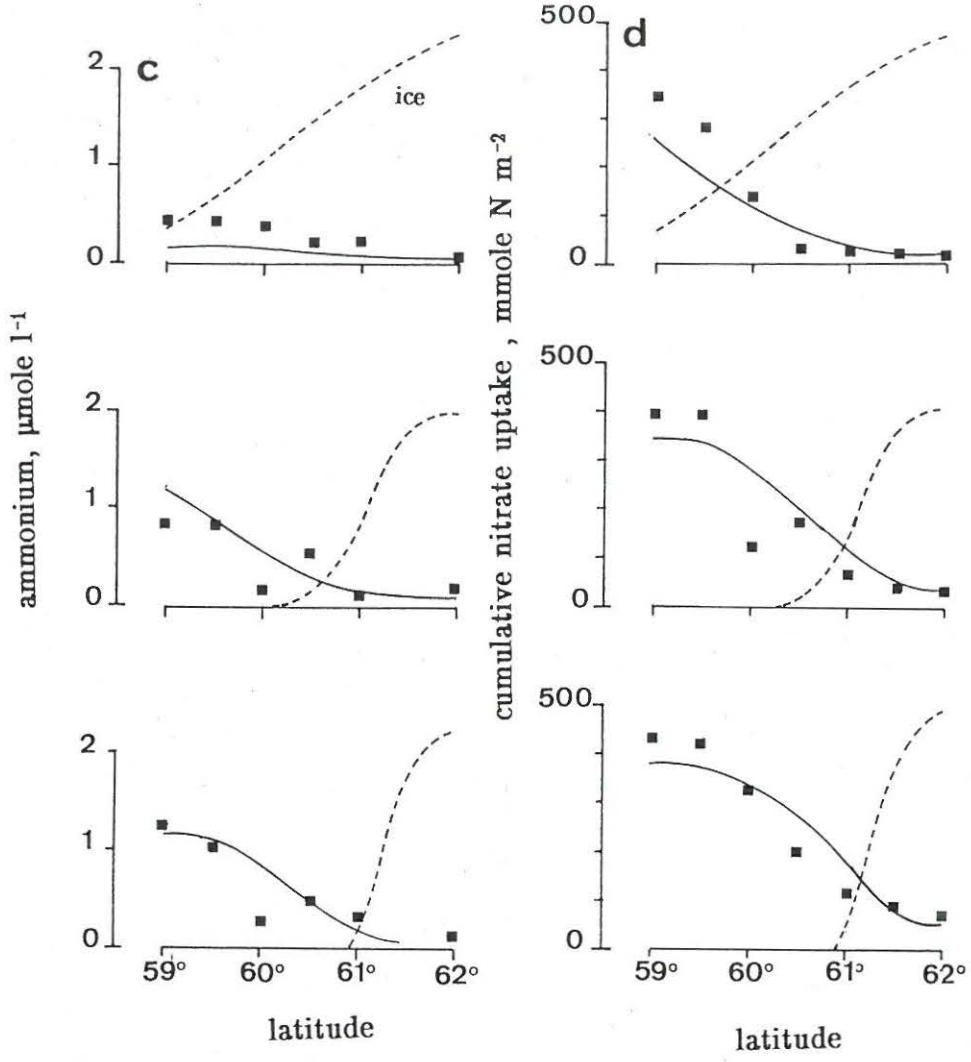

Figure 6.8cd : Predicted (solid line) and observed (▪) spatio–temporal variations of ammonium concentrations in the upper mixed layer (c) and cumulative nitrate uptake by phytoplankton (d) in the northwestern Weddell Sea during sea ice retreat 1988. Ice retreat is represented on each graph as a dashed line.

6.2. Sensitivity analysis : factors controlling phytoplankton ice–edge blooms

The careful analysis of factors controlling phytoplankton bloom development in the marginal ice zone of the northwestern Weddell Sea, through both spatio–temporal examination of observations (sections 3 and 4) and model simulations (§ 6.1.2), suggests that ice–edge bloom initiation is mainly under control of physical processes determining the vertical stability of surface waters. Grazing pressure, on the other hand, actively controls both the magnitude and extent of the bloom, preventing occurrence of massive phytoplankton biomasses in this sector of the circumpolar marginal ice zone. Herbivorous protozoa exert a semi–continuous control on phytoplankton development whilst the role of krill is more episodical, owing to its life history. Krill acts on the height of the phytoplankton ice–edge bloom by determining sea ice algae seeding concentration of the water column and on the bloom development by grazing on phytoplankton patches during their migrations. The successive action of physical and biological factors limiting primary production might well explain the geographical location of phytoplankton blooms close to the retreating ice–edge . However, it is evident that these factors are not always exclusive, as shown for instance by the additional role played by physical processes like deep mixing on phytoplankton bloom magnitude through the vertical dilution of phytoplankton concentrations. To which extent physical and biological factors interact in generating and controlling phytoplankton blooms in the circumpolar marginal ice zone of the Southern Ocean was investigated through a sensitivity analysis of the coupled physical–biological model described here above applied at latitude 59 30^0 S within the marginal ice zone of the northwestern Weddell Sea during spring.

Meteorological conditions : Highly fluctuating weather conditions occurring at a scale sometimes less than one week are typical of the Southern Ocean (Deacon 1984). Accordingly, short–term extreme wind fluctuations between 2 and 17 m s^{-1} around an average value of 8 m s^{-1} succeeded to each other during the studied period at the given latitude (Fig. 6.1c). To which extent these episodic wind events affect sea ice–associated phytoplankton bloom development is depicted in Figs. 6.9. and 6.10. which compare the evolution of surface layer phytoplankton predicted for different weather scenarii. Comparison of simulations generated by local weather conditions and those averaged over the 70–day simulated period strongly suggests that during the ice–covered period, when light penetration is considerably reduced by sea ice albedo, current shallow upper layer events were insufficient for counterbalancing deep

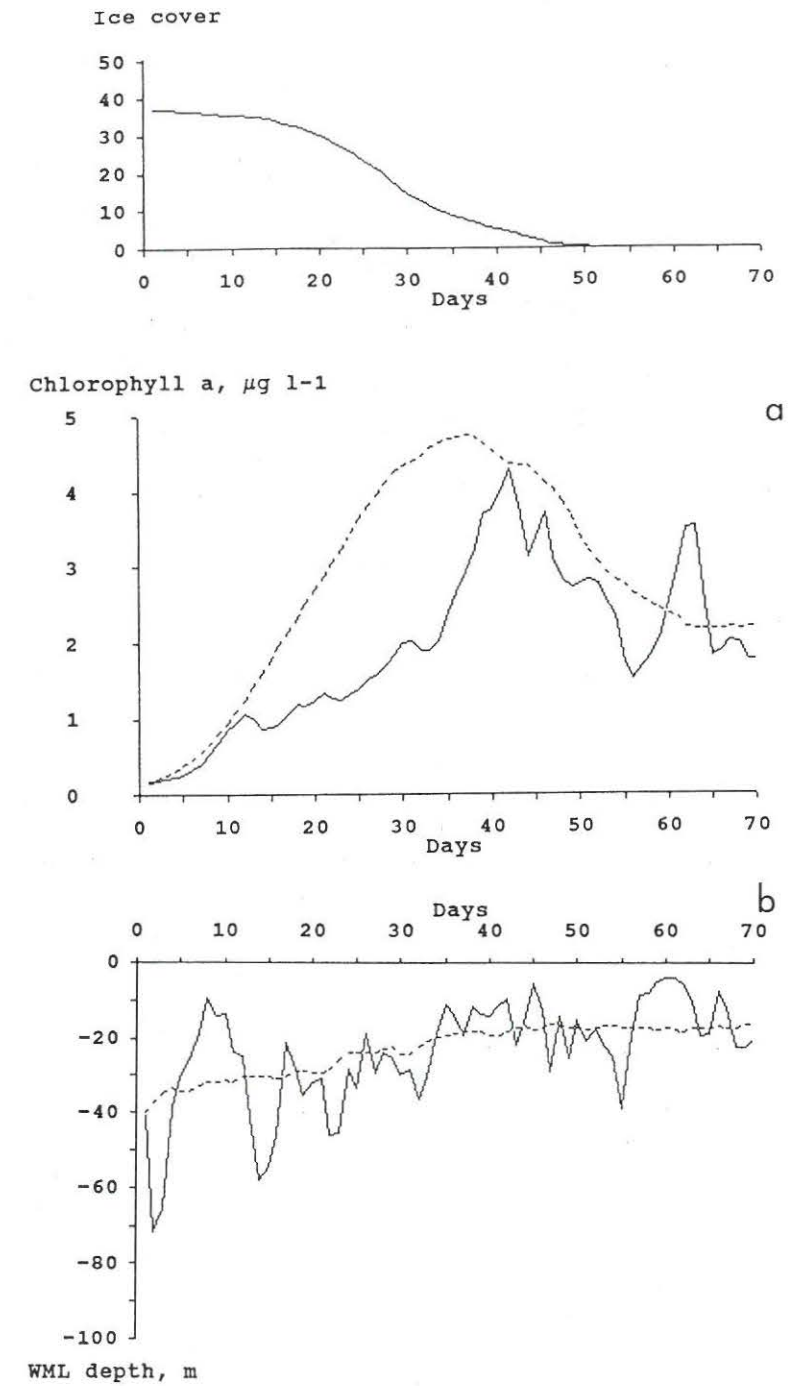

Figure 6.9 : Predicted chlorophyll *a* concentration (a) and upper mixed layer depth (b) at latitude 59 30^0 S during the ice melting period under local (solid line) and averaged (dashed line) meteorological conditions.

mixing which dilutes phytoplankton concentration in a lower mean irradiance environment. This is the consequence of the assymetrical behavior of the wind mixed layer regarding deepening and shallowing. Indeed whilst phytoplankton dilution accompanies deep mixing, no concentration takes place during shallowing, with the result that a single deep mixing event has major consequence for phytoplankton bloom initiation. During EPOS expedition, in particular, the successive wind mixing events occurring during the ice–covered period considerably delays the exponential development of phytoplankton as well as its maximum level with respect to that predicted under constant averaged wind conditions (Fig. 6.9). On the other hand, very similar maximum chlorophyll *a* concentration of about 4.5 μg l^{-1} are predicted by both scenarios (Fig. 6.9).

The role of wind velocity on phytoplankton ice–edge bloom development and magnitude is evidenced by Fig. 6.10, which compares chlorophyll *a* concentrations predicted under various constant wind climates. These simulations show that, according to the wind speed, the phytoplankton peak appearance shifts with respect to ice cover,occurring between 0 and 20 % of this latter. More spectacular is the range of maximum phytoplankton concentration predicted, varying between 1.5 and 11 μg Chl $a\,l^{-1}$ (Fig. 6.10). Under constant wind of 14 m s^{-1}, however, no significant phytoplankton bloom is predicted.

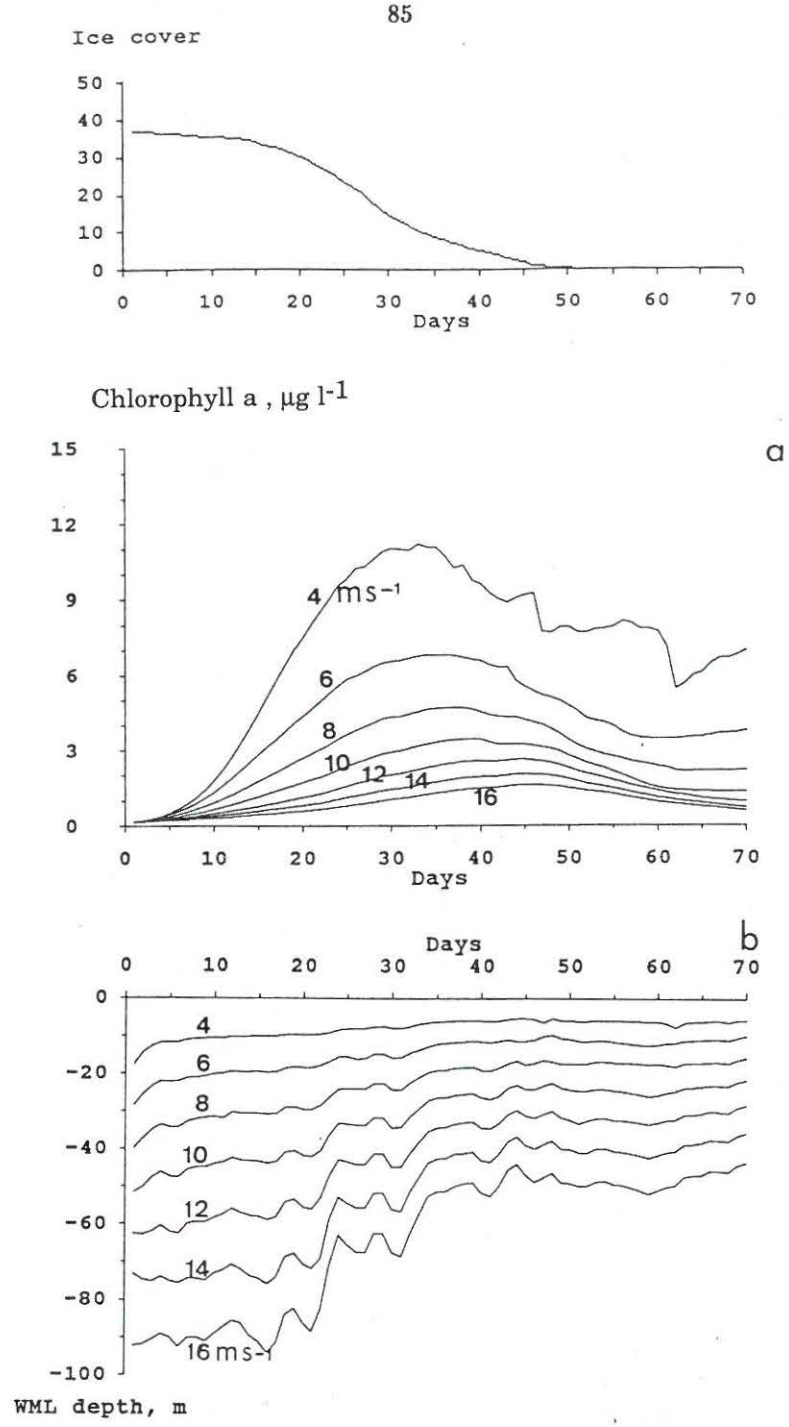

Figure 6.10 : Predicted chlorophyll *a* concentration (a) and upper mixed layer depth (b) at latitude 59 30⁰ S during the ice melting period under various constant wind speed.

Seeding : The role of seeding in generating phytoplankton ice–edge bloom was approached by comparing simulation runs with various initial concentrations of phytoplankton corresponding to realistic seeding concentrations. These latter were calculated from chlorophyll *a* concentrations measured in sea ice floes (Garrison *et al.*, 1986) diluted within the upper mixed layer at initial conditions, assuming an ice floe average diameter of 20 m at the time of melting (van Franeker, pers. com.) and a preferential peripherical distribution of sea ice communities. Simulations (Fig. 6.11) clearly show that seeding acts solely on the early development of phytoplankton during the ice covered period by allowing occurrence of sporadic minor blooms, the importance of which is related to weather conditions, without however affecting peak appearance and maxima reached by the ice–edge bloom.

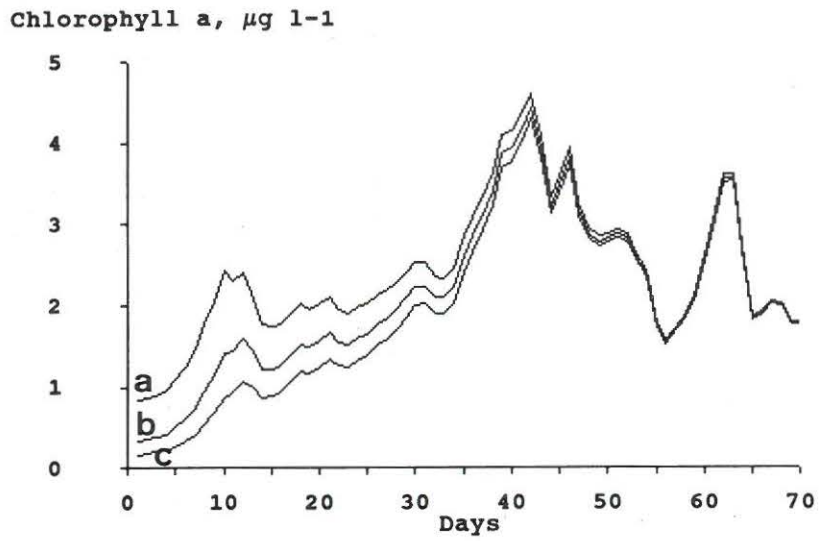

Figure 6.11 : Predicted chlorophyll *a* concentration at latitude 59 30⁰ S during the ice melting period for various seeding scenarios of 0.8 (a), 0.4 (b), and 0.1 (c) µg Chl *a* l^{-1}.

Grazing pressure : The role of protozoan grazing pressure in determining the level and magnitude of the ice–edge phytoplankton bloom on the other hand is outlined by analysing, especially after the ice melting period, predictions resulting from elimination of protozoan grazing pressure (Fig. 6.12). Whilst unsignificant in the early development of phytoplankton, grazing pressure actively determines the maximum concentration of 7.5 µg Chl *a* l^{-1} reached by the sea ice associated bloom which is 70 % up on eliminating grazing pressure (Fig. 6.12). Hence this concentration represents the maximum ice–edge phytoplankton biomass to be reached under local meteorological conditions. The ice–edge bloom extent on the other hand is clearly determined by the balance beween phytoplankton losses due to grazing pressure and the persistence of optimal light conditions due to favorable wind conditions. Phytoplankton ice–edge decline is predicted under observed grazing pressure whilst bloom development persists when grazing is eliminated (Fig. 6.12).

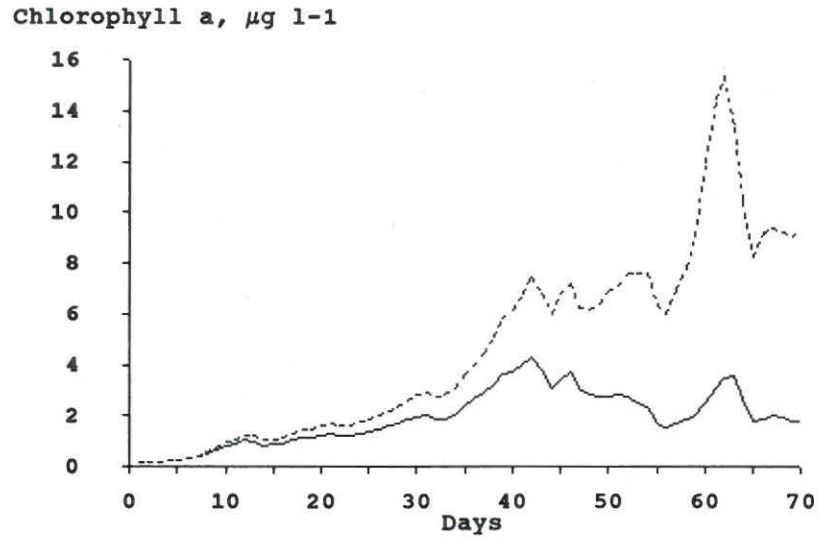

Figure 6.12 : Predicted chlorophyll *a* concentration at latitude 59 30⁰ S during the ice melting period under *in situ* grazing pressure by protozoa (solid line) and after protozoa elimination (dashed line).

Most scenarios predict a summer steady state phytoplankton concentration, the value of which greatly depending on weather conditions (Fig. 6.9 & 6.10) and grazing pressure (Fig. 6.12). The occurrence of secondary phytoplankton peaks during the ice–free period as predicted around day 20 by local weather conditions (Fig. 6.12) on the other hand, is clearly related to the amplitude and duration of wind mixing events. Indeed no summer development is predicted by constant wind scenarii (Fig. 6.10). The height of these secondary phytoplankton blooms is determined by both the grazing pressure and the persistence of vertical stability providing favorable light conditions to phytoplankton whilst their decline is mostly due to vertical dilution of phytoplankton into a lower mean irradiance field (Fig. 6.9).

Krill: The impact of krill passage on the development of sea ice associated phytoplankton bloom is determined by its occurrence with respect to phytoplankton development stage (Fig. 6.13). A single krill event occurring under the ice (Fig. 6.13a) has little influence on chlorophyll *a* bloom prediction associated to the ice melting process, reducing it to a mean value of 70 %, and no effect on secondary blooms resulting from stable wind mixing events. Reversely, a krill passage at the blooming stage eliminates the bloom and controls the magnitude of secondary summer peaks (Fig. 6.13b).

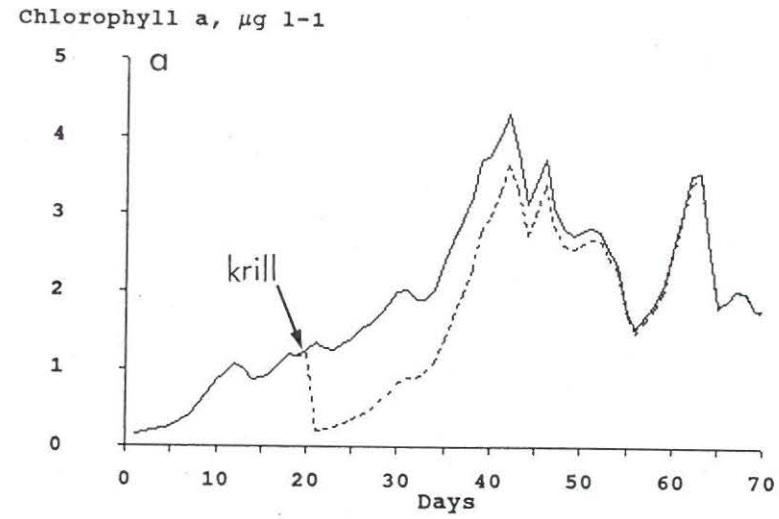

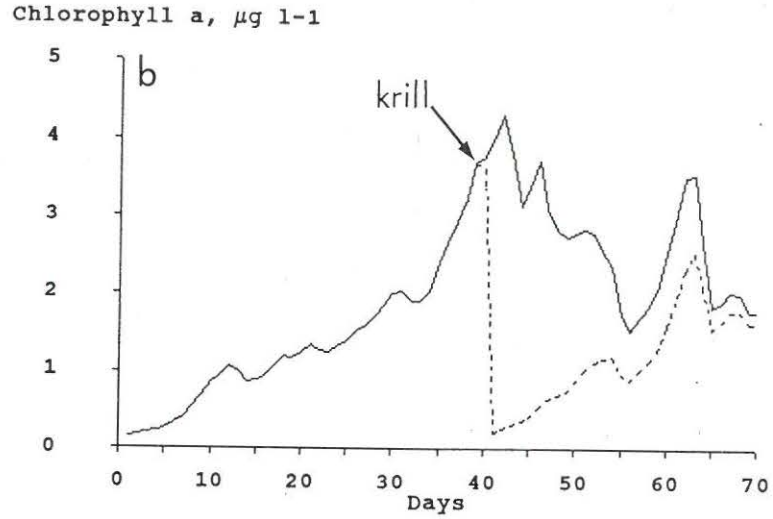

Figure 6.13 : Predicted chlorophyll *a* concentration at latitude 59 30⁰ S during the ice melting period after krill passage at the initial (a) and blooming (b) stage of phytoplankton development.

6.3. Applications

6.3.1. Carbon and nitrogen budget of microbial activities during sea ice retreat : the particular case of the northwestern Weddell Sea

The budget of carbon and nitrogen cycling through the microbial network characteristic of the Weddell Sea marginal ice zone around the 49° W meridian has been calculated by integration over the ice–retreat period of biological activities predicted by the ecological model, in the area extended from latitude 58 30° S to 61° S. Results of these calculations expressed in gC m^{-2} and gN m^{-2} for the ice–retreat period (Table 6.II) are shown on Fig. 6.14.

This budget calculation indicates that a total of 33 gC m^{-2} is produced by phytoplankton (net primary production) whilst 31 % (16 gC m^{-2}) of the total photoassimilated C or gross primary production (50 gC m^{-2}) is lost by respiration and 2 % (1 gC m^{-2}) by exudation. 88 % of net primary production (29 gC m^{-2}) is assimilated in the microbial food–web composed of bacterioplankton, bactivorous and herbivorous protozoa. Total net microbial food–web secondary production amounts 8 gC m^{-2} which represents an efficiency of about 25 %. This quantity added to the part of phytoplankton production not accounted by microbial loop consumption (4 gC m^{-2}) gives a total amount of 12 gC m^{-2}. This amount represents the maximum predicted food resources available for krill and other zooplankton, provided by the marginal ice zone. This value fits reasonably well with local mesozooplankton demand estimated by Fransz (pers. com.) at this period.

Organic production supported by nitrate represents 67 % (22 gC m^{-2} or 5.2 gN m^{-2}) of total net primary production (33 gC m^{-2} or 7.6 gN m^{-2}). This corresponds to a mean NO_3–based primary production or new production of 315 mgC m^{-2} d^{-1}. This value is highly comparable to that of 400 mgC m^{-2} d^{-1} estimated in that part of the marginal ice zone of the Weddell Sea between meridian 41 and 37° W during spring 1983 by Smith & Nelson (1990) from scattered measurements of vertical profiles of $^{15}NO_3$ uptake multiplied by the Redfield carbon:nitrogen ratio. Ammonium production through herbivorous protozoan metabolism amounts 2.2 gN m^{-2} which represents 61 % of total ammonium released by the microbial loop (3.6 gN m^{-2}) and is almost balanced by phytoplankton ammonium demand (2.4 gN m^{-2}). Total ammonium regenerated through the microbial loop is by far superior to ammonium uptake by phytoplankton, giving rise, in the absence of nitrification, to ammonium accumulation of 1.2 µM.

Table 6.II : Spring budget of microbial activities in the Scotia/Weddell Sea sector of the Southern Ocean.

Processes	Marginal ice zone MIZ	Adjacent permanently Open Sea POOZ	Permanently ice–covered PICZ
PHYTOPLANKTON :			
photosynthesis (gC m^{-2})	50	37	7
excretion	1	0.8	0.3
respiration	16	10.5	2.1
net primary prod. :			
total (gC m^{-2})	33	25	4.2
NO_3–based.(gC m^{-2})	22	14	3.2
NH_4–based (gC m^{-2})	11	11	1
fNO_3 ratio	0.66(0.39–0.79)	0.57(0.46–0.78)	0.75(0.69–0.79)
autolysis (gC m^{-2})	9	4.5	2
MICROHETEROTROPHS :			
herbivorous protozoa (HP) grazing (gC m^{-2})	20	19.5	0.6
bactivorous protozoa (BP) grazing (gC m^{-2})	1	0.5	0.2
HP growth	8	7.5	0.3
DOC bacterial assimilation	12	7.7	2.3
bacterial growth	3.5	2.3	0.7
total NH_4 regeneration (gN m^{-2})	3.6	2	0.5
HP regeneration (gN m^{-2})	2.2	1.9	0.1
Bact. & BP regeneration (gN m^{-2})	1.4	1.1	0.4
MAXIMUM FOOD AVAILABLE FOR KRILL AND ZOOPLANKTON			
from phytoplankton (gC m^{-2})	4	1	1.5
from microbial loop	8	7.5	0.3

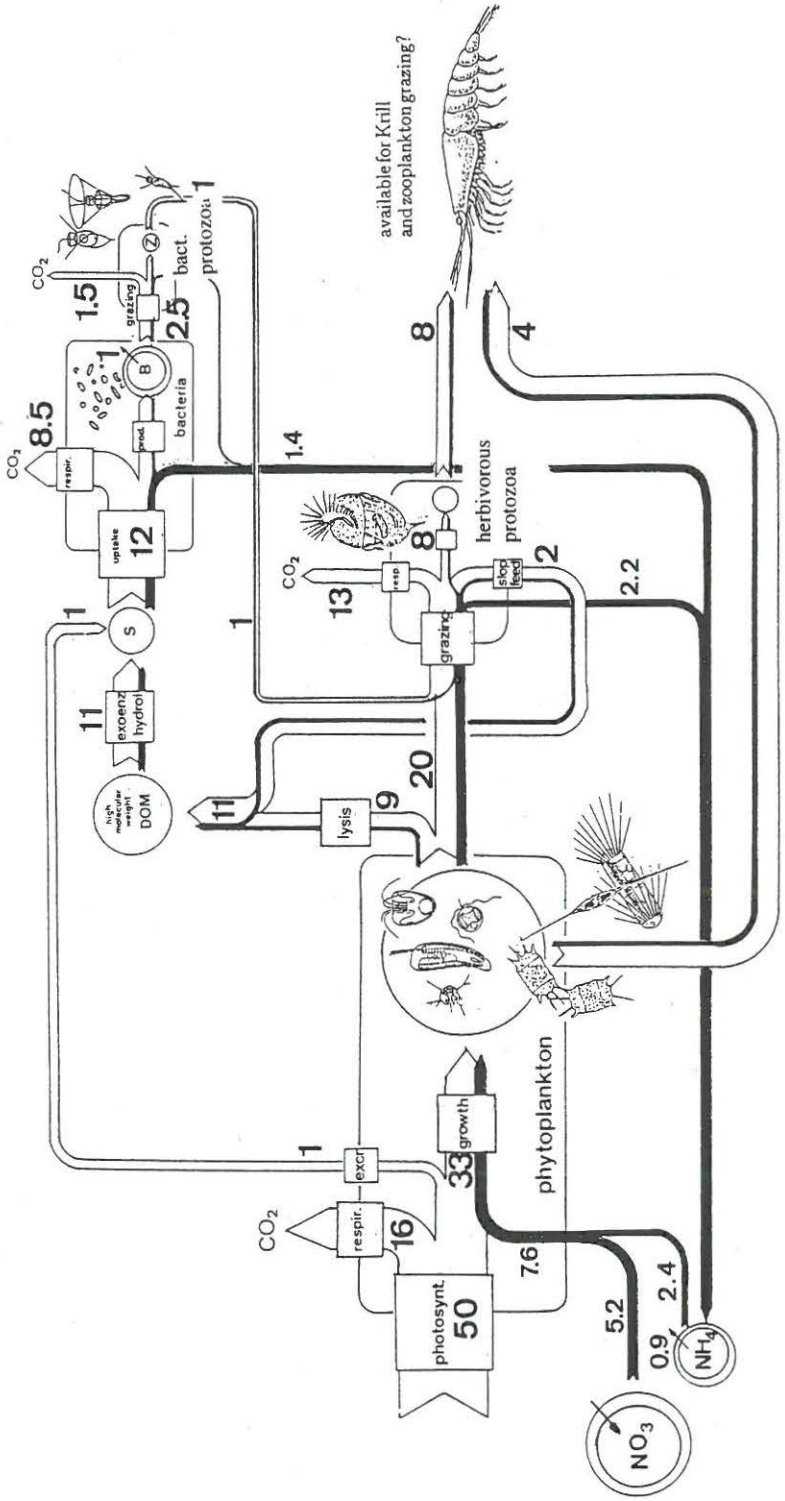

gC/m².ice retreat period

Figure 6.14 : Budget of C and N cycling through the microbial network of the northern Weddell Sea during ice retreat 1988.

Comparing these results with similar calculations conducted in the adjacent permanently open (latitude 58° S) and ice–covered (latitude 62° S) zone as summarized on Table V1.2 well demonstrates that the marginal ice zone is a region of enhanced phytoplankton development at the time of ice melting. Net primary production associated with the process of ice retreat is about one order of magnitude and one third higher than in ice–covered areas limited by light availability and in the adjacent permanently ice–free area respectively. In this latter environment, however, model prediction indicates that high phytoplankton development is not so much prevented by light limitation mediated by deeper turbulent mixing (Lancelot *et al.*,1993; Veth *et al.*, 1992), as often reported (Sullivan *et al.*, 1988), but rather by grazing pressure of herbivorous protozoa that increases with the advance of the season. As much as 94 % of primary production is indeed taken up by heterotrophic microorganisms, herbivorous protozoa for 78 %, leaving only 1 gC m^{-2} to zooplankton and krill. 94 % (7.5 gC m^{-2}) of food resources available to these latter (8.5 gC m^{-2}) is then provided by microbial loop secondary production.

Comparing nitrogen budgets shows in addition that the ice–edge effect is even greater when new production is considered, indicating that substantially greater amounts of material are available for export from the marginal ice zone than from other Southern Ocean surface waters.

6.3.2. Ice–edge primary production of the Weddell Sea

Primary production associated to the receding ice–edge in the Weddell Sea has been estimated from extrapolation of the above budget to the region of the Weddell Sea area concerned by ice retreat. This calculation assumes that the food–web structure illustrated by Fig. 6.14 is representative of the marginal ice zone of the whole Weddell Sea, as supported by observations in other regions of the Weddell Sea (Hewes *et al.*, 1985, 1990; Garrison & Buck, 1989a, b). A mean surperficie of 5.8 10^6 km^2 was considered for the seasonal sea ice zone of the Weddell Sea (Smith & Nelson, 1986). This calculation yields a net ice–edge primary production of 192 10^{12} gC, i.e. almost twice higher than the value estimated by Smith & Nelson (1986) from field primary productions and above sea ice zone superficie.

The geographical boundaries of the marginal ice zone, however, largely vary from year to year due to the variability in ice cover and concentration (Zwally *et al.*, 1983; Comiso & Zwally, 1989). During the period 1979–1986 in particular, the area of the

Weddell Sea concerned by ice retreat varied from 4.2 to 5.9 10^6 km^2 (Comiso & Zwally, 1989). On this basis, interannual variation of ice–edge associated primary production have been calculated for the Weddell Sea and are illustrated by Fig. 6.15. It shows that realistic interannual variation of sea ice extent in this sector of the Southern Ocean has a significant impact on ice–edge primary production.

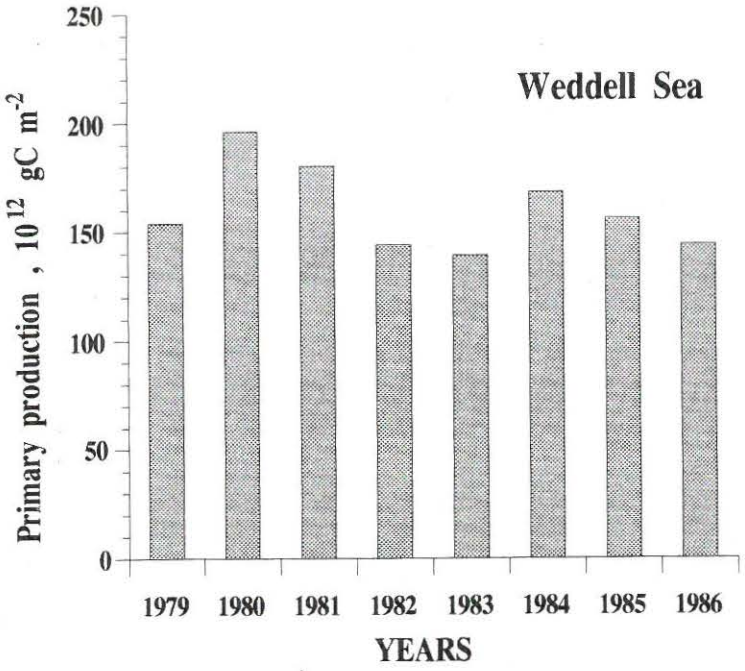

Figure 6.15 : Interannual variations of ice–edge primary production in the Weddell Sea for the period 1979–1986.

6.3.3. Annual primary production of the Southern Ocean

The presence in the Southern Ocean of seasonal sea ice which forms and melt according to the seasonal cycle strongly determines the pattern of primary production, making questionable any estimate of global primary production based on scattered local measurements as often reported in other oceanic areas. Application along the course of a seasonal cycle of the idealized ecological model developed in the previous section at the different latitudes of the Southern Ocean would allow realistic estimate of annual primary production in the Southern Ocean.

Providing the introduction of krill in the model, this is indeed the first model describing explicitely the interaction between the dynamics of sea ice retreat and the physiology of phytoplankton growth and mortality. Model runs over a seasonal cycle are actually prevented by lack of availability of meteorological data (the forcing variables of the model) time series and the inadequacy of existing meteorological models.

As an alternative, annual primary production of the Southern Ocean has been estimated by considering three different phytoplankton habitats, the permanently open ocean zone **POOZ**, the marginal ice zone **MIZ** and the permanently ice coverered zone **PICZ**, the geographical limits and production of which vary according to the seasonal cycle. Total superficie of 38.1 10^6 km^2 has been considered for the whole Southern Ocean, bordered by the Antarctic Convergence. Seasonal variation of phytoplankton habitat superficie has been calculated from monthly ice concentration contours established for the period 79–86 by Comiso & Zwally (1989) on the basis of polar microwave brightness temperature data collected by Nimbus–7 SMMR. For each sub–area, a monthly mean primary production has been considered (Table 6.III). Daily primary production typical of the growing season are those calculated by the model whilst autumn and winter values originated from a careful analysis of existing data (Mathot *et al.*, 1992). Result of this calculation, summarized on table 6.IV, evaluates to 1.85 GT the annual production of the Southern Ocean, increasing by a factor 3 the previous estimate by El Sayed (1984). Within this extreme environment, sea ice associated systems contribute for 30 % of the global primary production. Note that the calculations assume that the high protozoan grazing pressure observed in the Weddell Sea also applies in the whole circumpolar marginal ice zone. Recent data reporting occasional elevated phytoplankton biomass in the Ross Sea (Smith & Nelson, 1985; Tréguer *et al.*, 1991) and the Prydz Bay (Dehairs, pers. com.) contradict

however the above conclusion. On the other hand, grazing pressure by pelagic krill is not taken into account in the ice–free areas owing to the scarce knowlegde on krill distribution. Contribution of sea ice associated areas to annual primary production as determined in the present report (Table 6.IV) constitutes thus a minimum estimate.

Table 6.III : Mean daily primary production in different areas of the Southern Ocean.

Season	POOZ (1)	MIZ <15% IC (1)	MIZ 15–85% IC (1)	PICZ 85–100% IC (1)	References
Growing season					
October	180	160	85	30	This model
November, December January, February	300	470	300	60	This model
Autumn					
March	130		130	30	Smith & Nelson, 1990 Cota *et al.*, 1991
April, May	100		100	20	Cota *et al.*, 1991
Winter					
June, July	10			2	Brightman & Smith, 1989

(1) $mgC\ m^{-2}\ d^{-1}$
IC = ice cover

Table 6.IV : Annual primary production in the Southern Ocean.

Area	Primary production 10^{12}gC		
Open ocean	1,293		
Marginal ice zone	507		
Ice–covered area	48		
Total :	1,850	or	**1.85 GT**

7. CONCLUSIONS AND PERSPECTIVES

The comprehensive analysis of the physical and chemical transformations and biological processes occurring in the marginal ice zone of the northwestern Weddell Sea at the time of ice retreat evidences the key role played by sea ice in determining the structure and functioning of the planktonic food web at the receding ice–edge. This role is twofold : (i) its structural characteristics provides a habitat for microorganisms and a refuge for overwintering krill and other mesozooplankton; (ii) the dynamics of its retreat and formation strongly influences the light conditions experienced by phytoplanktonic cells.

As a matter of evidence, the physical processes associated with ice retreat enhance the development of phytoplankton blooms at the receding ice–edge by providing phytoplankton cells with optimal light conditions owing to the formation of shallow vertically stable surface layer as a result of meltwater production.

The magnitude of the phytoplanktonic bloom is then regulated by the combined action of grazing pressure by protozoa, mesozooplankton and krill and meteorological conditions, these latter determining the vertical stability of surface waters. The relative importance of micro– and mesograzers in controlling phytoplankton ice–edge blooms, and hence the structure of the planktonic food–web, is determined both by the composition of sea–ice assemblages at the time of ice melting and the presence beneath the ice of overwintering krill and mesozooplankton. The former depends on the initial composition of sea–ice assemblages originating from planktonic and benthic auto– and heterotrophic microorganisms scavenged at the time of ice formation, the physico–chemical characteristics of the ice habitat and the environmental light conditions of early spring. Overwintering herbivorous underneath the ice, by grazing selectively on large phytoplankton like some diatoms and *Phaeocystis* colonies or their aggregates strongly determine the species composition of the seeded microbial population and hence the structure of the planktonic food–web developing at the receding ice–edge. In the presence of krill, a very efficient microbial network composed of nano–sized auto– and heterotrophs thus predominates and moderate phytoplankton ice–edge blooms are expected. On the contrary, in the absence of overwintering krill, large blooms dominated by micro–sized phytoplanktonic species should prevail.

The extent of the bloom in ice–free area is determined by local meteorological conditions, in particular the frequence and intensity of wind mixing events, and by passage of krill swarms. The impact of these latter on the structure of the planktonic food–web, whilst episodic, is drammatic as these grazers litteraly clear the water from phytoplankton, heterotrophic microorganisms and copepods. Only bacterial activity is enhanced after a krill event, owing to the release of organic matter resulting from the feeding activity of these grazers.

Thus, although the enhancement of ice–edge blooms by the physics associated to the process of ice melting is a general feature in the circumpolar marginal ice zone of the Southern Ocean, regional differences in the magnitude and extent of these blooms are however to be expected, depending on the geographical distribution of overwintering and pelagic krill. Our field experience as well as our litterature knowledge suggest that large diatoms and *Phaeocystis* occur occasionally in the Ross Sea and Prydz Bay area whilst moderate ice–edge blooms of nanophytoplankton prevail in the Weddell Sea. In particular, our investigations in the marginal ice zone of the northwestern Weddell Sea revealed the existence in this area of a very efficient complex microbial network, with nano–sized protozoa grazing on phytoplankton and bacteria. Application in this area of a coupled hydrodynamical–biological model established on the basis of physical and biological processes measurements carried out during the EPOS cruise stress the quantitative importance of protozoa as regulator of ice–edge phytoplankton blooms, as link between krill and microorganisms and as important ammonium regenerator, inducing a shift from a nitrate– to a ammonium–based primary production system.

Taking all this into consideration, it becomes clear that the contribution of ice–edge blooms to the overall annual production of the Southern Ocean will be appraised by developing coupled hydrodynamical–biological models along the course of a seasonal cycle in different sub–regions of the circumpolar marginal ice zone of the Southern Ocean, chosen according to the physical characteristics and krill distribution. The general structure of this ecological model is illustrated by Fig. 7.1 that shows the seasonal cycle of sea ice and the coupling between the sea ice community (**SIMCO**) and planktonic (**SWAMCO**) biological model occurring in early spring and autumn. The former constitute the initial conditions of the SWAMCO model at the time of ice melting whilst the latter constitute the initial conditions of the SIMCO model at the time of ice formation. The ecological model of the microbial network developed in the

marginal ice zone constitutes a first step in this direction. Some limitation still prevents its successful application in every sub–region of the circumpolar marginal ice zone of the Southern Ocean. These limitations lie for instance in the inadequacy of the mathematical description of the grazing function, the consideration of one single phytoplankton compartment, and the lack of taking into account of krill. Further development of our research in the Southern Ocean will include the improvment of the existing model, with the development of two additional sub–models, describing respectively the metabolism of large phytoplankton species and protozooplankton and the consideration of the role of overwintering and pelagic krill.

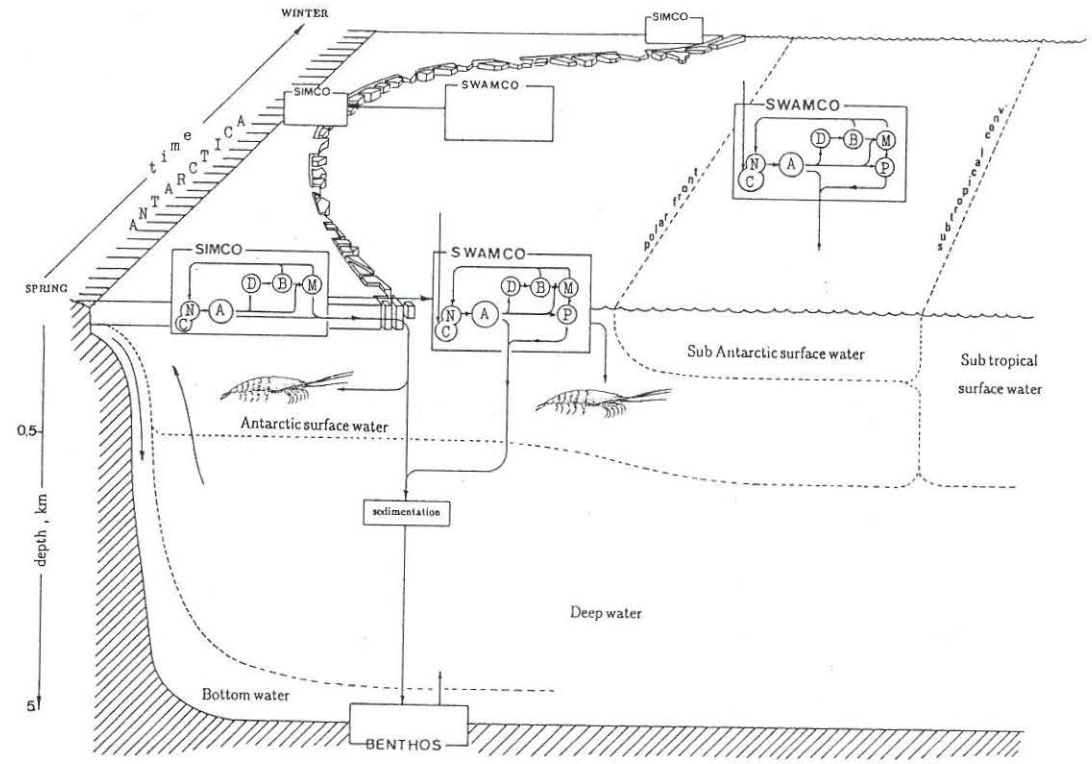

Figure 7.1 : Diagrammatic representation of the ecological model applied to the whole Southern Ocean along the course of a seasonal cycle.
SIMCO : model of sea ice microbial communities; **SWAMCO**: model of sea water microbial community. **C** : CO_2; **N** : inorganic nutrients; **A** : microalgae; **D** : dissolved organic matter; **B** : bacteria **M** : micrograzers; **P** : particulate organic matter.

8. ACKNOWLEDGMENTS

This work is part of the Belgian Scientific Research Programme on Antarctica, funded by the Science Policy Office (Brussels, Belgium), under contract ANTAR/05.

ANTAR II/05

All the data presented in this report were collected during the European venture EPOS on board of the German vessel RV POLARSTERN.

We take this opportunity to express our gratitude to the European Science Foundation and the Alfred Wegener Institut for allowing participation in EPOS and to thank the Captain and the crew of RV POLARSTERN for their helpful assistance during the work. We are especially grateful to Victor Smetacek and Kees Veth, respectively the Chief Scientist and Scientific Advisor of the Leg 2. The bright ideas and delighful personality of Victor, the organisations skill and comradeship of Kees contribute to the large success of this expedition.

The scientific concepts and ecological models we develop here are not only the fruit of the knowledge we gained from other studies in temperate aquatic environments, but mostly originate from scientific collaborations and discussions we had on board and during the different workshops and symposium that followed the expedition. We are especially grateful to Victor Smetacek. His impressive knowledge of polar biology, and his enthusiasm, greatly stimulated our understanding of the Antarctic pelagic ecosystem and the key role of krill. Also we thank Kees Veth for the physical development of the model and for the "credit" he gave to biological demands.

Our gratefulness to Peter Björnsen and Jorma Kuparinen who contributed to our knowledge of the protozoan grazing function and to Hein de Baar who puts some light on the iron problem.

Special thanks to our Belgian colleagues, Frank Dehairs and Leo Goeyens who took an active part in the formulation of the inorganic nitrogen loop.

Finally, all our thanks to our friends and colleagues of the EPOS Leg 2 expedition, each contributed in their individual unique way to the success of this expedition.

Last but not least, we thank Janine D'haenens for her assistance in the edition of this report.

9. REFERENCES

Ackley, S.F., Buck, K.R. & Taguchi, S., 1979. Standing crop of algae in the sea ice of the Weddell Sea region. *Deep Sea Res.*, 26A : 269–282.

Ackley, S.G., 1981. A review of sea–ice weather relationships in the Southern Hemisphere. In : *Sea level, ice and climate change*, Proceedings of the Canberra Symposium, IAHS Publ., 136 : 127–159.

Becquevort, S., Mathot, S. & Lancelot, C., 1992. Interaction in the microbial community of the marginal ice zone of the northwestern Weddell Sea through size distribution analysis, *Polar Biol.*, 12 : 211–218.

Beers, J.R. & Stewart, G.L., 1970. Numerical abundance and estimated biomass of microzooplankton. In : J.D.H. Strickland, ed., *The Ecology of the plankton of La Jolla, California, in the period April through September* 1967. Bull Scripps Inst. Oceanogr., 17 : 67–87.

Bergström, B., Hempel, G., Hempel, I., Marschall, H.P., North, A., Siegel, B. & Strömberg, J.O., 1989. Antarctic krill (*Euphausia superba).* In : *The expedition Antarktis VII/1 and 2 (EPOS Leg 1) of RV "Polarstern" in 1988/1989. Reports on Polar Research*, Hempel I., ed., pp. 149–156.

Bergström, B.I., Hempel, G., Marschall, H.P., North, A.W., Siegel V. & Strömberg, J.O., 1990. Spring distribution, size composition and behaviour of krill *Euphausia superba* in the western Weddell Sea. *Polar Rec.*, 26 : 85–89.

Billen, G. & Fontigny, A., 1987. Dynamics of *Phaeocystis*–dominated spring bloom in Belgian coastal waters. II. Bacterioplankton dynamics. *Mar. Ecol. Progr. Ser.*, 37 : 249–257.

Billen, G. & Servais, P., 1989. Modélisation des processus de dégradation de la matière organique en milieu aquatique. In : *Micro–organismes dans les écosystèmes océaniques.* Bianchi, M. et al., ed., pp 219–245, Masson, Paris.

Billen, G., 1990. Delayed development of bacterioplankton with respect to phytoplankton : a clue for understanding their trophic relationships. *Arch. Hydbiol. Beih .Ergebn. Limnol.*, 114 : 415–429.

Billen, G., 1991. Protein degradation in Aquatic Environments. In : *Microbial Enzymes in Aquatic Environments*, R. Chrost, ed., Springer Verlag, 7 : 123–143.

Billen, G. & Becquevort, S., 1991. Phytoplankton–bacteria relationship in the Antarctic marine ecosystem. *Polar Res.* 10 : 245–253.

Björnsen, P.K. & Kuparinen, J., 1991. Growth and herbivory by heterotrophic dinoflagellates in the Southern Ocean studied by microcosm experiments. *Mar. Biol.*, 109 : 397–405.

Bölter, M. & Dawson, R., 1982. Heterotrophic utilization of biochemical compounds in Antarctic waters. *Neth.J.Sea Res.*, 16 : 315–332.

Brightman, R.I. & Smith, W.O., Jr. 1989. Photosynthesis–irradiance relationships of Antarctic phytoplankton during austral winter. *Mar. Ecol. Progr. Ser.*, 53 : 143–151.

Buma, A.G.J., de Baar, H., Nolting, R.F. & van Bennekom, A.J., 1991. Metal enrichment experiments in the Weddell–Scotia Seas : Effects of iron and manganese on various plankton communities, *Limnol. Oceanogr.*, 36 : 1865–1878.

Cederlöf, U., Ober, S., Schmidt, R., Svansson, A. & Veth, C., 1989. Physics and chemistry : Hydrography. In : Hempel, I., Schalk, P.H. & Smetacek, V., ed. *Reports on Polar Research – The expedition ANTARKTIS VII/3 (EPOS Leg 2) of the RV "Polarstern" in 1988/89*, pp. 14–19.

Coale, K.H., 1991. The effects of iron, manganese, copper and zinc enrichments on productivity and biomass in the Subarctic Pacific, *Limnol. Oceanogr.*, 36 : 1851–1864.

Cohen, D. & Parnas, H., 1976. An optimal policy for the metabolism of storage materials in unicellular algae, *J. Theor.Biol.*, 56 : 1–18.

Comiso, J.C. & Zwally, H.J., 1984. Concentration gradients and growth and decay characteristics of the seasonal sea ice cover, *J. Geophys. Res.*, 89 : 8081–8103.

Comiso, J.C. & Zwally, H.J., 1989. Polar Microwave Brightness Temperatures from Nimbus–7 SMMR, *NASA Reference Publication* 1223, 82 p.

Comiso, J.C., Maynard, N.G., Smith, W.O. & Sullivan, C.W., 1990. Satellite ocean color studies of Antarctic ice edges in summer and autumn, *J. Geophys. Res.*, C6 : 9481–9496.

Cota, G.F., Kottmeier, S.T., Robinson, D.H., Smith, W.O.Jr & Sullivan, C.W., 1991. Bacterioplankton in the marginal ice zone of the Weddell Sea : biomass, production and metabolic activities during austral autumn. *Deep–Sea Res.*, 37(7) : 1145–1167.

Cuzin–Roudy, J. & Schalk, P.H., 1989. Macrozooplankton – Biomass, development and activity. In : *The Expedition Antarktis VII/3 (EPOS LEG 2) of RV "Polarstern" in 1988/89, Reports on Polar Research*, Hempel, I., Schalk, P.H. & Smetacek, V., ed., pp. 146–159.

Deacon, G., 1984. The Antarctic circumpolar ocean, *Studies in Polar Research*, Cambridge University Press, 180 p.

de Baar, H., Buma, A.G.J., Nolting, R.F., Cadée, G.C., Jacques, G. & Tréguer, P., 1990. On iron limitation of the Southern Ocean : Experimental observations in the Weddell and Scotia Sea. *Mar. Ecol. Progr. Ser.*, 65 : 105–122.

Denman, K.L., 1973. A time–dependent model of the upper ocean. *J. Phys. Ocean*, 3 : 173–184.

Dorsey, T.E., Mc Donald, P. & Roels, O.R., 1978. Measurements of phytoplankton protein content with the heated biuret–folin assay. *J. Phycol.*, 14 : 167–171.

Dugdale, R.C. & Wilkerson, F.P., 1990. Iron addition experiments in the Antarctic, *Global Biochem. Cycles*, 4(1) : 13–19.

Edler, L., 1979. Recommendations for marine biological studies in the Baltic Sea – Phytoplankton and Chlorophyll, *Baltic Marine Biologist*, 5 : 1–38.

Eicken, H., Lange, M.A. & Dieckmann, G.S., 1991. Spatial variability of sea–ice properties in the northwestern Weddell Sea. *J. Geophys. Res.*, 96(C6) : 10603–10615.

El–Sayed, S.Z., 1984. Productivity of the Antarctic waters : a reappraisal. In : *Marine Phytoplankton and productivity*, Holm–Hansen, O., Bolis, L. & Gilles, R., ed., Springer, Berlin, pp. 73–91.

EPOS–Leg 2 (1991). Data report – Hydrography, Part 1 (second edition), NIOZ, Texel, The Netherlands.

Eppley, R.W. & Peterson, B.J., 1979. Particulate organic flux and planktonic new production in the deep ocean, *Nature*, Lond., 282 : 677–680.

Fontigny A., Billen G. & Vives Rego J., 1987. Some kinetics characteristics of exoproteolytic activity in coastal sea water. *Est.Coast.Mar.Sci.*, 25 : 127–134.

Fransz, H.G., 1988. Vernal abundance, structure and development of epipelagic copepod populations of the Eastern Weddell Sea (Antarctica). *Polar Biol.*, 9 : 107–114.

Fransz, H.G. & Gonzales, S.R., 1992. The spring–summer distribution, development and production of epipelagic copepod populations in the Weddell–Scotia Confluence, *EPOS Symposium Abstracts*, 103 pp.

Fuhrman, J.A. & Azam, F., 1982. Thymidine incorporation area measure of hetero–trophic bacterioplankton evaluation in marine surface waters : evaluation and field result. *Mar.Biol.*,66 : 109–120.

Garrison, D.L., Ackley, S.F. & Buck, K.R., 1983. A physical mechanism for establishing algal populations in frazil ice, *Nature*, Lond., 306 : 363–365.

Garrison, D.L. & Buck, K.R., 1985. Sea–ice algal communities in the Weddell Sea : Species composition in ice and plankton assemblages, *Marine Biology of Polar Regions and Effects of Stress on Marine Organisms*, J.S. Gray & E. Christiansen, ed., J. Wiley & Sons Ltd.

Garrison, D.L., Sullivan, C.W. & Ackley, S.F., 1986. Sea ice communities in Antarctica. *BioScience*, 36 : 243–249.

Garrison, D.L., Buck, K.R. & Fryxell, G.A., 1987. Algal assemblages in Antarctic pack ice and in ice–edge plankton, *J. Phycol.*, 23 : 564–572.

Garrison, D.L. & Buck, K.R., 1989a. Protozooplankton in the Weddell sea, Antarctica : Abundance and distribution in the ice–edge zone, *Polar Biol.*, 9 : 341–351.

Garrison, D.L. & Buck, K.R., 1989b. The biota of antarctic pack ice in the Weddell Sea and Antarctic Peninsula regions, *Polar Biol.*, 10 : 211–219.

Garrison, D.L. & Gowing, M.M., 1993. Protozooplankton. In : *Antarctic Microbiology* Friedmann, E.I., ed., in press.

Goeyens, L., Sörensson, F., Tréguer, P., Morvan, J., Panouse, M. & Dehairs, F., 1991a. Spatiotemporal variability of inorganic nitrogen stocks and uptake fluxes in the Scotia–Weddell Confluence area during November and December 1988, *Mar. Ecol. Progr. Ser.*, 77(1) : 7–19.

Goeyens, L., Tréguer, P., Lancelot, C., Mathot, S., Becquevort, S., Morvan, J., Dehairs, F. & Baeyens, W., 1991b. Ammonium regeneration in the Scotia–Weddell Confluence area during spring 1988. *Mar. Ecol. Progr. Ser.*, 78 : 241–252.

Gordon, A.L., 1967. Structure of Antarctic waters between 20⁰ W and 170⁰ W. *Antarctic Map Folio Series*, Folio 6, V.C. Bushnell, ed., Amer. Georgr. Soc. pp 10.

Hayes, P.K., Whitakker, T.M. & Fogg, G.E., 1984. The distribution and nutrient status of phytoplankton in the Southern Ocean between 20⁰ and 70⁰ W, *Polar Biol.* 3 : 153–165.

Hempel, G., 1985. Antarctic marine food webs. In : *Antarctic Nutrient Cycles and Food Webs*, Siegfried, W.R., Condy, P.R. & Laws, R.M., ed., Springer Berlin Heidelberg New York, pp 266–270.

Hewes, C.D., Holm–Hansen, O. & Sakshaug, R., 1985. Alternate carbon pathways at lower trophic levels in the Antarctic food web. In : *Antarctic nutrient cycles and food webs*, Siegried, W.R., Condy, P.R. & Laws, R.M., ed., pp. 237–283.

Hewes, C.D., Sakshaug, E., Reid, F.M. & Holm–Hansen, O., 1990. Microbial autotrophic and heterotrophic eucaryotes in Antarctic waters : Relationships between biomass and chlorophyll, adenosize triphosphate and particulate organic carbon, *Mar. Ecol. Progr. Ser.*, 63 : 27–35.

Horner, R.A., 1985. Ecology of sea ice microalgae. In : *Sea Ice Biota*, Horner, R.A., ed., CRC Press, Boca Raton, pp. 83–103.

Horner, R.A., Syvertsen, E.E., Thomas, D.P. & Lange, C., 1988. Proposed terminology and reporting units for sea ice algal assemblages. *Polar Biol.*, 8 : 249–253.

Jacques, G. & Panouse, M., 1991. Biomass and composition of size fractionated phytoplankton in the Weddell Sea Confluence area, *Polar Biol.*, 11 : 315–328.

Koroleff, F., 1969. Direct determination of ammonia in natural waters as indophenol blue. *Comm. Meet. int. Counc. Explor. Sea*, C.M.–ICES/C : 19–22.

Koroleff, F., 1976. Determination of ammonia. In : Grasshof, K., ed., *Methods of seawater analysis*. Verlage Chemie, Weinheim, p. 126–133.

Kottmeier, S.T. & Sullivan, C.W., 1987. Late winter primary production and bacterial production in sea ice and seawater west of the Antarctic Peninsula. *Mar. Ecol. Prog. Ser.* 36 : 287–298.

Lancelot, C. & Mathot, S., 1985. Biochemical fractionation of primary production by phytoplankton in Belgian coastal waters during short– and long–term incubations with ^{14}C–bicarbonate. I. Mixed diatom population. *Mar.Biol.*, 86(3) : 219–226.

Lancelot, C., Billen, G. & Mathot, S., 1989. Ecophysiology of phytoplankton and bacterioplankton growth in the Southern Ocean. In : *Belgian Scientific Research Programme on Antarctica. Scientific Results of Phase One (Oct.85 – Jan.89).* Vol.1 : *Plankton Ecology*, pp. 1–97.

Lancelot, C., Veth, C. & Mathot, S., 1991a. Modelling ice–edge phytoplankton bloom in the Scotia–Weddell sea sector of the Southern Ocean during spring 1988. *J. Mar. Syst.*, 2 : 333–346.

Lancelot, C., Billen, G., Veth, C., Becquevort, S. & Mathot, S., 1991b. Modelling carbon cycling through phytoplankton and microbes in the Scotia–Weddell Sea area during sea ice retreat; *Marine Chemistry*, 35(1–4) : 305–324.

Lancelot, C., Mathot, S., Veth, C. & de Baar, H., 1993. Factors controlling phytoplankton ice–edge blooms in the marginal ice zone of the northwestern Weddell Sea during sea ice retreat 1988: field observations and mathematical modelling, *Polar Biol.*, 13 : 000–000.

Lange, M.A. & Eicken, H., 1989. Sea ice conditions. In : *The Expedition Antarktis VII 1 and 2 (Epos I) of RV "Polarstern" in 1988/1989. Berichte zur Polarforschung*, Hempel, I., ed., pp. 55–63.

Larsson, A.M., 1990. Hydrological, chemical and biological observations during EPOS 1. Distributed by Department of Oceanography, University of Gothenburg, Box 4038, S–400 40 Gothenburg, Sweden.

Lorenzen, C.J., 1967. Determination of chlorophyll and phaeopigments: spectrophotometric equations, *Limnol. Oceanogr.*, 12 : 343–346.

Magas, B. & Svansson, A., 1989. Optics. In : *The expedition Antarktis VII/3 (EPOS Leg 2) of RV "Polarstern" in 1988/1989, Berichte zur Polarforschung*, Hempel, I., Schalk, P.H. & Smetacek, V., ed., pp. 20–24.

Marr, J.W.S., 1962. The natural history and geography of the Antarctic krill (*Euphausia superba* Dana). Discovery Rep. 32:33–464.

Marschall, H.P., 1988. The overwintering strategy of Antarctic krill under the pack–ice of the Weddell Sea, *Polar Biol.*, 9 : 129–135.

Martin, J.H. & Fitzwater, S.E., 1988. Iron deficiency limits phytoplankton growth in the north–east Pacific Subarctic, *Nature*, 331 : 341–343.

Martin, J.H., Gordon, R.M. & Fitzwater, S.E., 1990a. Iron in Antarctic waters, *Nature*, 345 : 156–158.

Martin, J.H., Fitzwater, S.E. & Gordon, R.M., 1990b. Iron deficiency limits phytoplankton growth in Antarctic waters, *Global Biogeochemical Cycles*, 4 : 5–12.

Mathot, S., Becquevort, S. & Lancelot, C., 1991. Microbial communities from the sea ice and adjacent water column at the time of ice melting in the northwestern part of the Weddell Sea. *Polar Res.* 10 : 267–2755

Mathot, S., Dandois, J.M. & Lancelot, C., 1992. Gross and net primary production in the Scotia–Weddell Sea sector of the Southern Ocean during spring 1988, *Polar Biol.*, 12 : 321–332.

Mitchell, B.G. & Holm–Hansen, O., 1991. Observations and modelling of the Antarctic phytoplankton crop in relationship to mixing depth, *Deep Sea Res.*, 38(8/9A) : 981–1008.

Neveux, J.& Panouse, M., 1987. Spectrofluometric determination of chlorophylls and phaeophitines, *Arch. für Hydrobiol.*, 109 : 567–581.

Nolting, R.F., de Baar, H.J.W., van Bennekom, A.J. & Masson, A., 1991. Cadmium, copper and iron in the Scotia Sea, Weddell Sea and Weddell/Scotia Confluence (Antarctica), *Marine Chemistry*, 35 : 219–243.

Palmisano, A.C. & Sullivan, C.W., 1983. Sea ice microbial communities (SIMCO). I. Distribution, abundance, and primary production of ice microalgae in Mc Murdo Sound, Antarctica in 1980, *Polar Biol.*, 2 : 171–177.

Parsons, T.R. & Strickland, J.D.H., 1962. On the production of particulate organic carbon by heterotrophic processes in seawater, *Deep Sea Research*, 8 : 211–222.

Platt, T., Gallegos, L.L. & Harrison, W.G., 1980. Photoinhibition of photosynthesis in natural assemblages of marine phytoplankton. *J. Mar. Res.*, 38 : 687–701.

Porter, K.G. & Feig, Y.S., 1980. The use of DAPI for identifying and counting aquatic microflora. *Limnol.Oceanogr.*, 25(5) : 943–948.

Riebesell, U., Schloss, I. & Smetacek, V., 1991. Aggregation of algae released from melting sea ice : Implication for seeding and sedimentation, *Polar Biol.*, 11 : 239–248.

Riemann, B., Björnsen, P.K., Newell, S.Y. & Fallon, R.D., 1987. Calculation of bacterioplankton production from measurements of ^{3}H–Thymidine incorporation. *Limn.Oceanogr.* 32 : 471–476.

Schalk, P.H., 1990. Biology activity in the Antarctic zooplankton community, *Polar Biol.*, 10 : 405–411.

Schnack, S.B., Smetacek, V.S., von Bodungen, B. & Stegmann, P., 1985. Utilization of phytoplankton by copepods in Antarctic Waters during spring. In : *Marine Biology of Polar Regions and Effects of Stress on Marine Organisms*, Gray, J.S. & Christiansen, M.E., ed., John Wiley & Sons Ltd, pp. 65–81.

Servais, P., Billen, G. & Vives–Rego, J., 1985. Rate of bacterial mortality in aquatic environments. *Appl.Environ.Microbiol.* 49 : 1448–1455.

Servais, P., 1986. Etude de la dégradation de la matière organique par les bactéries hétérotrophes en rivière. Développement d'une démarche méthodologique et application à la Meuse belge. Université Libre de Bruxelles. Faculté des Sciences. Thèse, 271 pp.

Servais, P., Billen, G. & Hascoët, M.C., 1987. Determination of the biodegradable fraction of dissolved organic matters in waters, *Water Res.*, 21 : 445–450.

Servais, P., Billen, G., Martinez, J. & Vives–Rego, J., 1989. Estimating bacterial mortality by the disappearance of ^{3}H–labelled intracellular DNA. Technical validation and field measurements. *FEMS Microbiol. Ecology.*, 62 : 119–126.

Shuter, B., 1979. A model of physiological adaptation in unicellular algae. *J. Theor. Biol.*, 78 : 519–552.

Siegel, V., Bergström, B., Strömberg, J.O. & Schalk, P.H., 1990. Distribution, size frequencies and maturity stages of krill, *Euphausia superba*, in relation to sea–ice in the northern Weddell Sea. *Polar Biol.*, 10 : 549–557.

Simon, M. & Azam, F., 1989. Protein content and protein synthesis rates of planktonic marine bacteria. *Mar. Ecol. Progr. Ser.*, 51 : 201–213.

Smetacek, V., Scharek, R. & Nöthig, E.–M., 1990. Seasonal and regional variation in the pelagial and its relationship to the life history cycle of krill. In : *Antarctic Ecosystems : Ecological change and conservations*, Kerny, R. & Hempel, G., ed., Springer Verlag, Berlin Heidelberg, p.103–114.

Smith, W.O.Jr & Nelson, D.M., 1985. Phytoplankton bloom produced by a receding ice–edge in the Ross Sea : Spatial coherence with the density field, *Science*, 227 : 163–165.

Smith, W.O.Jr & Nelson, D.M., 1986. Importance of ice–edge phytoplankton blooms in the Southern Ocean., *Bioscience*, 36 : 251–257.

Smith, W.O.Jr & Nelson, D.M., 1990. Phytoplankton growth and new production in the Weddell Sea marginal ice zone in the austral spring and autumn. *Limnol. Oceanogr.*, 35(4) : 809–821.

Somville, M. & Billen, G., 1983. A method for determining exoproteolytic activity in natural waters. *Limnol.Oceanogr.*, 28 : 190–193.

Somville, M., 1984. Measurement and study of substrate specificity of exoglucosidase activity in eutrophic water. *Appl.Environ.Microbiol.*, 48 : 1181–1185.

Stretch, J.J., Hamner, P.P., Hamner, W.M., Michel, W.C., Cook, J. & Sullivan, C.W., 1988. Foraging behavior of Antarctic krill *Euphausia superba* on sea ice microalgae, *Mar. Ecol. Progr. Ser.*, 44 : 131–139.

Sullivan, C.W., 1985. Sea ice bacteria : reciprocal interactions of the organisms and their environment. In : *Sea Ice Biota*, Horner, R.A., ed., CRC Press, Boca Raton, pp. 159–171.

Sullivan, C.W., McClain, C.R., Comiso, J.C. & Smith, W.O.Jr, 1988. Phytoplankton standing crops within an Antarctic ice–edge assessed by satellite remote sensing. *J. Geophys. Res.*, 93(C10) : 12487–12498.

Tilzer, M.M., Elbrächter, M., Gieskes, W.W. & Beese, B., 1986. Light–temperature interactions in the control of photosynthesis in Antarctic phytoplankton. *Polar Biol.* 5 : 105–111.

Tilzer, M.M. & Dubinsky, Z., 1987. Effects of temperature and day length on the mass balance of Antarctic phytoplankton. *Polar Biol.*, 7 : 35–42.

Tréguer, P. & Le Corre, P., 1975. Manuel d'analyses automatiques des sels nutritifs par Auto Analyser II Technicon, Université de Bretagne Occidentale, Brest.

Utermöhl, H., 1958. Zur Vervollkommnung der quantitativen Phytoplankton – Methodik. *Mitt. int. Verein theor. angew. Limnol.*, 9 : 1–38.

Van Aken, H.M., 1984. A one dimensional mixed–layer model for stratified Shelf Seas with tide and wind–induced mixing. *Dt.Hydrogr.Z.*, 37 : 1–27.

van Bennekom, J., Estrada, M., Goeyens, L., Magas, B., Masson, A., Morvan, J., Tréguer, P., Svansson, A. & Veth, C., 1989. Distribution of nutrients in surface, subsurface and deep layers. In : *The Expedition Antarktis VII/3 (EPOS Leg 2) of RV "Polarstern" in 1988/1989*, Hempel, I., Schalk, P.H. & Smetacek, V., ed., *Ber. Polarforsch.*, pp 47–56.

van Franeker, J.A., 1989. Sea ice conditions. In : *The Expedition Antarktis VII/3 (EPOS Leg 2) of RV "Polarstern" in 1988/89*, Hempel, I., Schalk, P.H. & Smetacek, V., ed., *Berichte Polarforschung*, pp. 10–13.

Veth, C., 1991. The evolution of the upper water layer in the marginal ice zone, austral spring 1988, Scotia–Weddell Sea, *J. Mar. Syst.*, 2 : 451–464.

Veth, C., Lancelot, C. & Ober, S., 1992. On processes determining the vertical stability of surface waters in the marginal ice zone of the north–western Weddell Sea and their relationship with phytoplankton bloom development. *Polar Biol.*, 12 : 237–243.

von Bodungen, B., Smetacek, V.S., Tilzer, M.M. & Zeitzschel, B., 1986. Primary production and sedimentation during spring in the Antarctic Peninsula region, *Deep Sea Res.*, 33 : 177–194.

Weber, L.H. & El–Sayed, S.Z., 1987. Contributions of the net, nano– and picoplankton to the phytoplankton standing crop and primary productivity in the Southern Ocean. *J. Plankton Res.*, 9(5) : 973–994.

Westerlund, S. & Öhman, P., 1991. Iron in the water column of the Weddell Sea, *Marine Chemistry*, 35:199–217.

Whitaker, T.M., 1977. Sea ice habitats of Signy Island (South Orkneys) and their primary productivity. In : Llano, G.A., ed., *Adaptations within Antarctic ecosystems.* Gulf Publ. Co., Houston, Texas, p. 75–82.

Wright, R.T. & Hobbie, J.E., 1965. The uptake of organic solutes in lake water. *Limnol. Oceanogr.*, 10 : 22–28.

Zwally, H.J., Parkinson, C.L. & Comiso, J.C., 1983. Variability of Antarctic sea ice and changes in carbon dioxide. *Science*, 220 : 1005–1012.